USGS
science for a changing world

DOE/ID-22227

Prepared in cooperation with the U.S. Department of Energy

Geochemistry of Groundwater in the Beaver and Camas Creek Drainage Basins, Eastern Idaho

Scientific Investigations Report 2013–5226

U.S. Department of the Interior
U.S. Geological Survey

Cover: Photograph of Camas Creek near site 99 with flow backed up by diversion to canal on Camas National Wildlife Refuge, eastern Idaho. Centennial Mountains in background. (Photograph taken by Chris Mebane, U.S. Geological Survey.)

Inset left: Photograph of pH, specific conductivity, dissolved oxygen, and water temperature measurements being taken with a Hydrolab Quanta® multiparameter water-quality sonde from groundwater flowing through irrigation pipe at site 18, Camas National Wildlife Refuge, eastern Idaho. (Photograph taken by Chris Mebane, U.S. Geological Survey.)

Inset center: Photograph of thin section prepared from basalt sample B1 under cross-polarized light and with 20x magnification. Minerals include (in order of abundance) plagioclase, olivine (with rim alteration to iddingsite), pyroxene, opaques, quartz, and calcite. (Photograph taken by Michael Ginsbach, Idaho State University.)

Inset right: Photograph of collection of groundwater-quality samples by Michael Ginsbach at site 11, eastern Idaho. (Photograph taken by Chris Mebane, U.S. Geological Survey.)

Geochemistry of Groundwater in the Beaver and Camas Creek Drainage Basins, Eastern Idaho

By Gordon W. Rattray and Michael L. Ginsbach

DOE/ID-22227
Prepared in cooperation with the U.S. Department of Energy

Scientific Investigations Report 2013–5226

U.S. Department of the Interior
U.S. Geological Survey

U.S. Department of the Interior
SALLY JEWELL, Secretary

U.S. Geological Survey
Suzette M. Kimball, Acting Director

U.S. Geological Survey, Reston, Virginia: 2014

Suggested citation:
Rattray, G.W., and Ginsbach, M.L, 2014, Geochemistry of groundwater in the Beaver and Camas Creek drainage basins, eastern Idaho: U.S. Geological Survey Scientific Investigations Report 2013–5226 (DOE/ID-22227), 70 p., *http://dx.doi.org/10.3133/sir20135226*.

ISSN -2328-0328 (online)

Contents

Contents—Continued

Figures

Tables

Conversion Factors, Datums, and Abbreviations and Acronyms

Conversion Factors

Inch/Pound to SI

Multiply	By	To obtain
	Length	
inch (in.)	2.54	centimeter (cm)
inch (in.)	25.4	millimeter (mm)
foot (ft)	0.3048	meter (m)
mile (mi)	1.609	kilometer (km)
	Area	
square mile (mi^2)	2.590	square kilometer (km^2)
	Volume	
quart (qt)	0.9464	liter (L)
gallon (gal)	3.785	liter (L)
	Flow rate	
cubic foot per second (ft^3/s)	0.02832	cubic meter per second (m^3/s)
	Mass	
ounce, avoirdupois (oz)	28.35	gram (g)
pound, avoirdupois (lb)	0.4536	kilogram (kg)
	Radioactivity	
picocurie per liter (pCi/L)	0.037	becquerel per liter (Bq/L)
	Hydraulic conductivity	
foot per day (ft/d)	0.3048	meter per day (m/d)
	Hydraulic gradient	
foot per mile (ft/mi)	0.1894	meter per kilometer (m/km)

Temperature in degrees Celsius (°C) may be converted to degrees Fahrenheit (°F) as follows:

$$°F=(1.8×°C)+32.$$

Specific conductance is given in microsiemens per centimeter at 25 degrees Celsius (µS/cm at 25 °C).

Concentrations of chemical constituents in water are given in milligrams per liter (mg/L), micrograms per liter (µg/L), millimoles per liter (mmol/L), micromoles per kilogram (µmol/kg), and milliequivalents per liter (meq/L).

Conversion Factors, Datums, and Abbreviations and Acronyms—Continued

Datums

Horizontal coordinate information is referenced to the North American Datum of 1927.

Vertical coordinate information is referenced to the National Geodetic Vertical Datum of 1929 (NGVD29).

Altitude, as used in this report, refers to distance above the vertical datum.

Abbreviations and Acronyms

BLS	Below land surface
CNWR	Camas National Wildlife Refuge
CO_2	Carbon dioxide
CSU	Combined standard uncertainty
DO	Dissolved oxygen
DOC	Dissolved organic carbon
ESRP	Eastern Snake River Plain
INL	U.S. Department of Energy Idaho National Laboratory
LRL	Laboratory reporting level
LT-MDL	Long-term method detection level
MRL	Minimum reporting level
NAD	Normalized absolute difference
NWIS	U.S. Geological Survey National Water Information System
NWQL	U.S. Geological Survey National Water Quality Laboratory
QA	Quality assurance
RSD	Relative standard deviation
RSIL	U.S. Geological Survey Reston Stable Isotope Laboratory
SITL	U.S. Geological Survey Menlo Park Stable Isotope and Tritium Labs
USGS	U.S. Geological Survey

Geochemistry of Groundwater in the Beaver and Camas Creek Drainage Basins, Eastern Idaho

By Gordon W. Rattray[1] and Michael L. Ginsbach[2]

Abstract

The U.S. Geological Survey (USGS), in cooperation with the U.S. Department of Energy, is studying the fate and transport of waste solutes in the eastern Snake River Plain (ESRP) aquifer at the Idaho National Laboratory (INL) in eastern Idaho. This effort requires an understanding of the natural and anthropogenic geochemistry of groundwater at the INL and of the important physical and chemical processes controlling the geochemistry. In this study, the USGS applied geochemical modeling to investigate the geochemistry of groundwater in the Beaver and Camas Creek drainage basins, which provide groundwater recharge to the ESRP aquifer underlying the northeastern part of the INL.

Data used in this study include petrology and mineralogy from 2 sediment and 3 rock samples, and water-quality analyses from 4 surface-water and 18 groundwater samples. The mineralogy of the sediment and rock samples was analyzed with X-ray diffraction, and the mineralogy and petrology of the rock samples were examined in thin sections. The water samples were analyzed for field parameters, major ions, silica, nutrients, dissolved organic carbon, trace elements, tritium, and the stable isotope ratios of hydrogen, oxygen, carbon, sulfur, and nitrogen.

Groundwater geochemistry was influenced by reactions with rocks of the geologic terranes—carbonate rocks, rhyolite, basalt, evaporite deposits, and sediment comprised of all of these rocks. Agricultural practices near and south of Dubois and application of road anti-icing liquids on U.S. Interstate Highway 15 were likely sources of nitrate, chloride, calcium, and magnesium to groundwater.

Groundwater geochemistry was successfully modeled in the alluvial aquifer in Camas Meadows and the ESRP fractured basalt aquifer using the geochemical modeling code PHREEQC. The primary geochemical processes appear to be precipitation or dissolution of calcite and dissolution of silicate minerals. Dissolution of evaporite minerals, associated with Pleistocene Lake Terreton, is an important contributor of solutes in the Mud Lake-Dubois area. Oxidation-reduction reactions are important influences on the chemistry of groundwater at Camas Meadows and the Camas National Wildlife Refuge. In addition, mixing of different groundwaters or surface water with groundwater appears to be an important physical process influencing groundwater geochemistry in much of the study area, and evaporation may be an important physical process influencing the groundwater geochemistry of the Camas National Wildlife Refuge. The mass-balance modeling results from this study provide an explanation of the natural geochemistry of groundwater in the ESRP aquifer northeast of the INL, and thus provide a starting point for evaluating the natural and anthropogenic geochemistry of groundwater at the INL.

Introduction

The U.S. Geological Survey (USGS), in cooperation with the U.S. Department of Energy, has collected extensive geohydrologic, hydraulic, geochemical, and radiochemical data to understand the fate and transport of waste solutes in the eastern Snake River Plain (ESRP) aquifer at and near the Idaho National Laboratory (INL) in eastern Idaho. These data are used in interpretive studies (Olmstead, 1962; Robertson and others, 1974; Busenberg and others, 2001) to describe the temporal and spatial distribution of chemical-and radioactive-waste solutes, and to identify the physical and chemical processes that control their concentration and migration rates, which include advection, dispersion, mixing, evaporation, dilution, adsorption, radioactive decay, and chemical and biological reactions. Chemical and radiochemical constituents in groundwater at the INL are derived from natural and anthropogenic sources. These constituents undergo chemical reactions between the gaseous, aqueous, and solid phases, and these reactions are an important control on the fate and mobility of waste solutes in the unsaturated zone and aquifer. Consequently, a better understanding of the natural geochemistry of groundwater at the INL, and the physical and chemical processes controlling the geochemistry, will improve our understanding of the fate and transport of waste solutes.

[1]U.S. Geological Survey.

[2]Idaho State University.

Studies undertaken to understand the natural geochemistry of the ESRP aquifer at the INL have included an evaluation of the geochemistry of groundwater in surface-water drainage basins that recharge the ESRP aquifer at and near the INL (Carkeet and others, 2001; Swanson and others, 2002, 2003; Ginsbach, 2013). The focus of the current study is to describe the groundwater geochemistry, and to identify the important physical and chemical processes that control the groundwater geochemistry, of the Beaver and Camas Creek drainage basins. Groundwater in these drainage basins, which mostly originates in the Beaverhead and Centennial Mountains northeast of the INL, provides a source of groundwater to the ESRP aquifer underlying the INL (fig. 1). Groundwater in the drainage basins has a unique geochemical character because of the source and location of recharge and the physical and chemical processes that take place during the migration of groundwater. An understanding of the geochemistry and physical and chemical processes controlling the geochemistry of these drainage basins will provide information about the natural geochemistry of groundwater in the ESRP aquifer at the INL.

Previous Investigations

The chemistry of groundwater at the INL was described by Olmstead (1962), Robertson and others (1974), and Busenberg and others (2001). Knobel and others (1997) described plausible natural geochemical reactions, based on the mineralogy, water chemistry, and thermodynamic state of the groundwater that may occur in the ESRP aquifer beneath the INL. McLing (1994) developed geochemical mass-balance models of the pre-anthropogenic evolution of groundwater at the INL. Schramke and others (1996) developed geochemical mass-balance models of the northern part of the INL to identify possible groundwater sources of recharge to the area, and Busenberg and others (2001) developed a geochemical mass-balance model of the southeastern part of the INL to aid in determination of the young fraction of water in groundwater from this area. The geochemistry of the Big Lost River, Little Lost River, Birch Creek, and Medicine Lodge Creek drainage basins, all of which provide recharge to the INL, were described in Carkeet and others (2001), Swanson and others (2002, 2003), and Ginsbach (2013).

The Beaver and Camas Creek drainage basins encompass the northeastern extent of the ESRP, and are therefore included in regional studies of the ESRP. The earliest study that included the Beaver and Camas Creek drainage basins was a study of the geology and water resources of the ESRP by Russell (1902). Other studies of the ESRP were an investigation of groundwater used for irrigation (Mundorff and others, 1964), a reconnaissance of groundwater quality (Parliman, 1983), and studies of volcanism in the ESRP and Yellowstone Plateau (Christiansen, 1982; Embree and others, 1982; Morgan and others, 1984; Kuntz and others, 1992; Morgan, 1992; Lanphere and others, 2002; Morgan and McIntosh, 2005; Iwahashi, 2010). The most comprehensive investigation of the ESRP aquifer was the Regional Aquifer-System Analysis (RASA) of the Snake River Plain aquifer conducted by the USGS (Lindholm, 1996). The RASA investigation included descriptions of the geohydrology of the ESRP (Whitehead, 1992), water use on the ESRP (Goodell, 1988), and the solute geochemistry and plausible geochemical reactions in the ESRP (Wood and Low, 1988).

The Beaver and Camas Creek drainage basins are a small part of the upper Snake River basin, and are therefore included in regional studies of the upper Snake River basin. The USGS conducted investigations of the water quality of surface water and groundwater in the upper Snake River basin as part of the National Water-Quality Assessment (NAWQA) Program. The results of the NAWQA investigations were presented by Clark (1994), Rupert (1994, 1996), and Maupin (1995). Benjamin and others (2004) developed a local meteoric water line for the stable isotopes of hydrogen and oxygen for an area that includes the northern and eastern parts of the upper Snake River basin.

The Beaver and Camas Creek drainage basins include parts of the Beaverhead and Centennial Mountains. Investigations of these mountains include a geologic reconnaissance of the Lost River, Lemhi, Beaverhead, and Centennial Mountains (Kirkham, 1927) and geologic studies of the Centennial Mountains (Witkind, 1975, 1980, 1982).

Studies of the Mud Lake area, which includes the southwestern part of the Beaver and Camas Creek drainage basins, include an assessment of geology and water resources (Stearns and others, 1939), an analysis of water-level changes (Ralston and Chapman, 1969), a description of stratigraphic and water-level relations (Crosthwaite, 1973), a study of groundwater flow characteristics (Luttrell, 1982), groundwater flow models (Johnson and others, 1984), an investigation of the geohydrology and a groundwater flow simulation (Spinazola and others, 1992; Spinazola, 1994), and a presentation of groundwater quality monitoring results (Carlson and others, 2002).

Studies encompassing just the Beaver and Camas Creek drainage basins include a water resources and data management model (Brockway and other, 1988) and an assessment of the water quality and total maximum daily load for streams in the basins (Thompson, 2005).

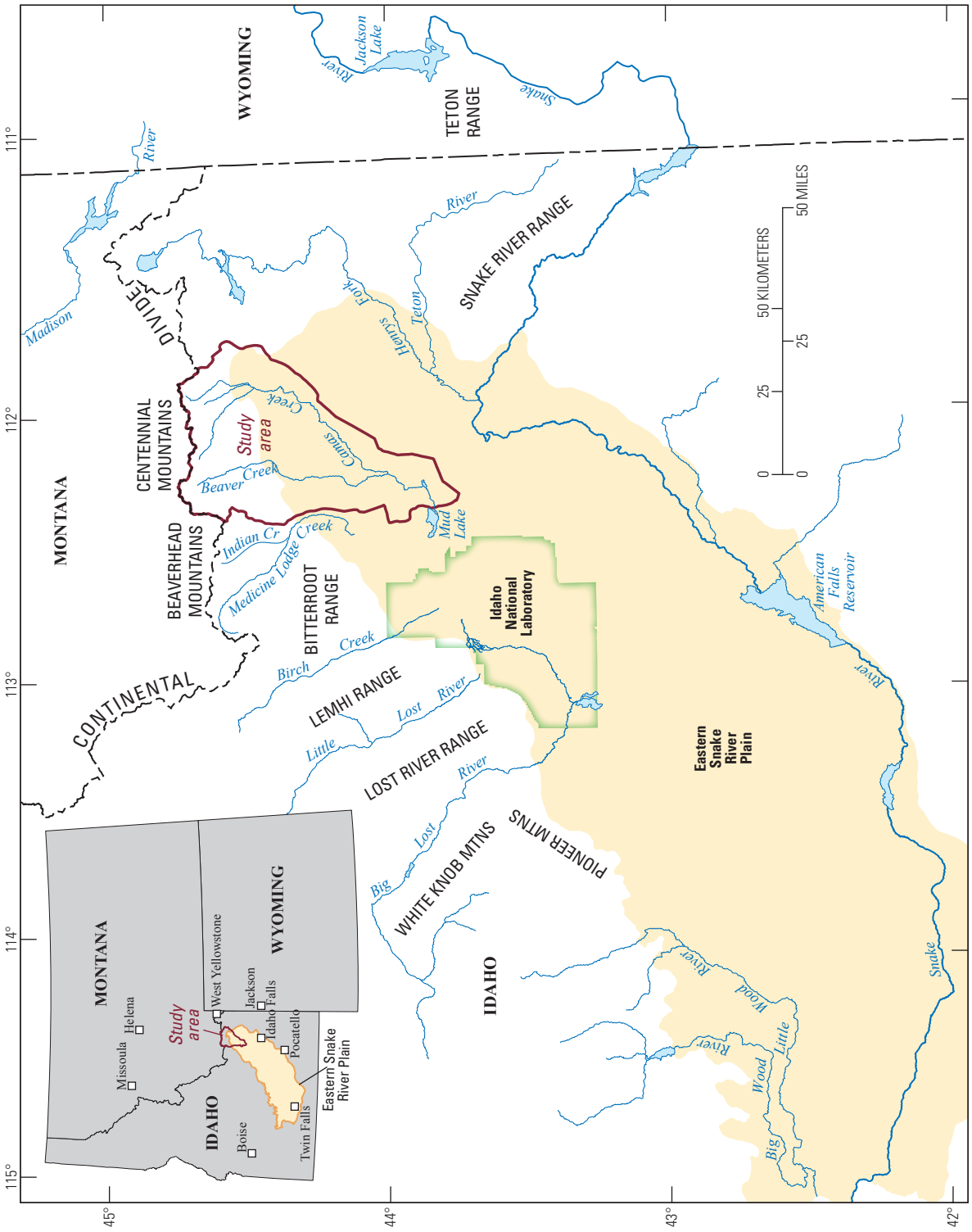

Figure 1. Location of the study area, Idaho National Laboratory, and eastern Snake River Plain, Beaver and Camas Creek drainage basins, eastern Idaho. Modified from Benjamin and others (2004, fig. 1).

Purpose and Scope

The purpose of this report is to characterize the geochemistry and to understand the physical and chemical processes controlling the geochemistry of groundwater in the Beaver and Camas Creek drainage basins. This information will improve the understanding of the natural chemistry of groundwater in the ESRP aquifer at the INL.

Two sediment and three rock samples were collected in October 2010 and analyzed for petrology and mineralogy. Water-quality samples collected (fig. 2) (during August 2011) for this study include 2 surface-water and 11 groundwater samples. Other water-quality samples used in this study include 2 surface-water and 9 groundwater samples; these samples were collected between 1981 and 2011 for other studies. All water-quality samples were analyzed for field parameters, major ions, silica, selected nutrients, and selected trace elements. Some of the water-quality samples were analyzed for dissolved organic carbon (DOC), tritium, and the stable isotope ratios of hydrogen, oxygen, carbon, sulfur, and nitrogen.

Solid-phase mineralogy was compiled from literature and analysis of rock and sediment samples. The distribution of chemical species (dissolved gases, solutes, and isotopes) in groundwater was determined from water-chemistry data; the composition and distribution of major ions was presented graphically in a trilinear diagram and in bar charts on maps of the study area. The sources of groundwater in the drainage basins were determined from hydrologic conditions, water temperature, water chemistry, and the hydrogen and oxygen stable isotope ratios of groundwater. The sources of chemical species were interpreted from the hydrology, geology, mineralogy, land cover and use, and surface-water and groundwater chemistry of the drainage basins. A set of hypothesized chemical reactions between the gaseous, aqueous, and solid phases in the groundwater system was formulated to account for changes in water chemistry taking place in the aquifer. The thermodynamic conditions of groundwater was evaluated using the computer code PHREEQC (Parkhurst and Appelo, 2013) to determine if the hypothesized chemical reactions were plausible, and the set of plausible geochemical reactions was used in a series of geochemical mass-balance models using the inverse (mass balance) modeling capability of PHREEQC.

Description of Study Area

The Beaver and Camas Creek drainage basins in eastern Idaho are adjacent to Montana and northeast of the INL (fig. 1). The southern part of the study area includes about 700 mi^2 of the northeastern extent of the ESRP, and the northern part of the study area includes about 160 mi^2 of the southeastern corner of the Beaverhead Mountains and 270 mi^2 of the southwestern part of the Centennial Mountains. Elevation in the study area ranges from 4,780 ft at Mud Lake in the southwestern corner of the study area to 9,889 ft in the Centennial Mountains.

Climate

The study area has a desert to semi-desert type climate in the southern part of the drainage basins, and a continental type in the northern part. A desert to semi-desert type climate is typified by annual precipitation of less than 10 or less than 20 in., respectively, such as seen near Hamer (8.7 in.) and Dubois (11.9 in.) (table 1 and figs. 3–4). A continental climate is typified by large seasonal changes in temperature, which occurs throughout the study area.

Table 1. Site name, number, location, altitude, period of record, mean maximum temperature for January and July, mean annual temperature, precipitation, and snowfall, Beaver and Camas Creek drainage basins, eastern Idaho.

[Location of sites are shown in figure 3. Hamer, Dubois, and Kilgore data are from the National Oceanic and Atmospheric Administration (2012). Crab Creek data are from U.S. Department of Agriculture (2012). Latitude and longitude are shown in degrees (dd) and minutes (mm). **Abbreviations:** NGVD 29, National Geodetic Vertical Datum of 1929; ºC, degrees Celsius; in., inch; nd, not determined]

Site name	Site No.	Latitude (ddmm)	Longitude (ddmm)	Altitude (feet above NGVD 29)	Period of record	Mean maximum daily temperature (ºC)		Mean annual		
						January	July	Temperature (ºC)	Precipitation (in.)	Snowfall (in.)
Hamer, 4 NW	50	43°58′	112°16′	4,790	1948–2011	-2.1	31.0	5.8	8.7	26.8
Dubois Experiment Station	51	44°15′	112°12′	5,445	1925–2011	-2.7	29.7	6.2	11.9	47.7
Kilgore	52	44°24′	111°53′	6,160	1961–1977	-4.6	25.3	2.0	21.0	131.6
Crab Creek	53	44°26′	112°00′	6,860	[1]1982–2011	nd	nd	nd	29.0	nd

[1]Water years.

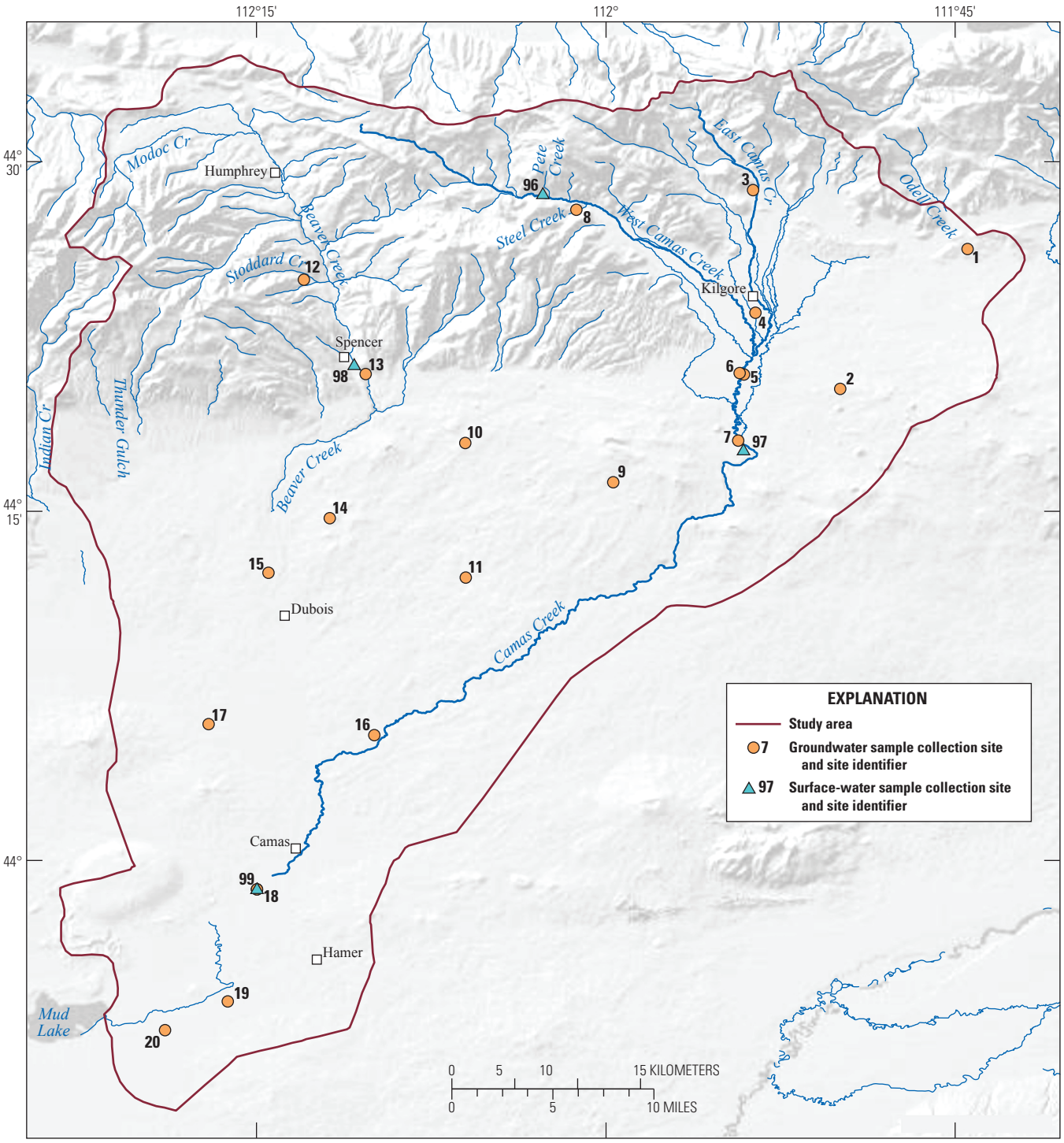

Base from U.S. Geological Survey digital data, 1:24,000 and 1:100,000. Coordinate system and datum: NAD 1927 (definition 1976).

Figure 2. Location of water-quality sample collection sites, Beaver and Camas Creek drainage basins, eastern Idaho.

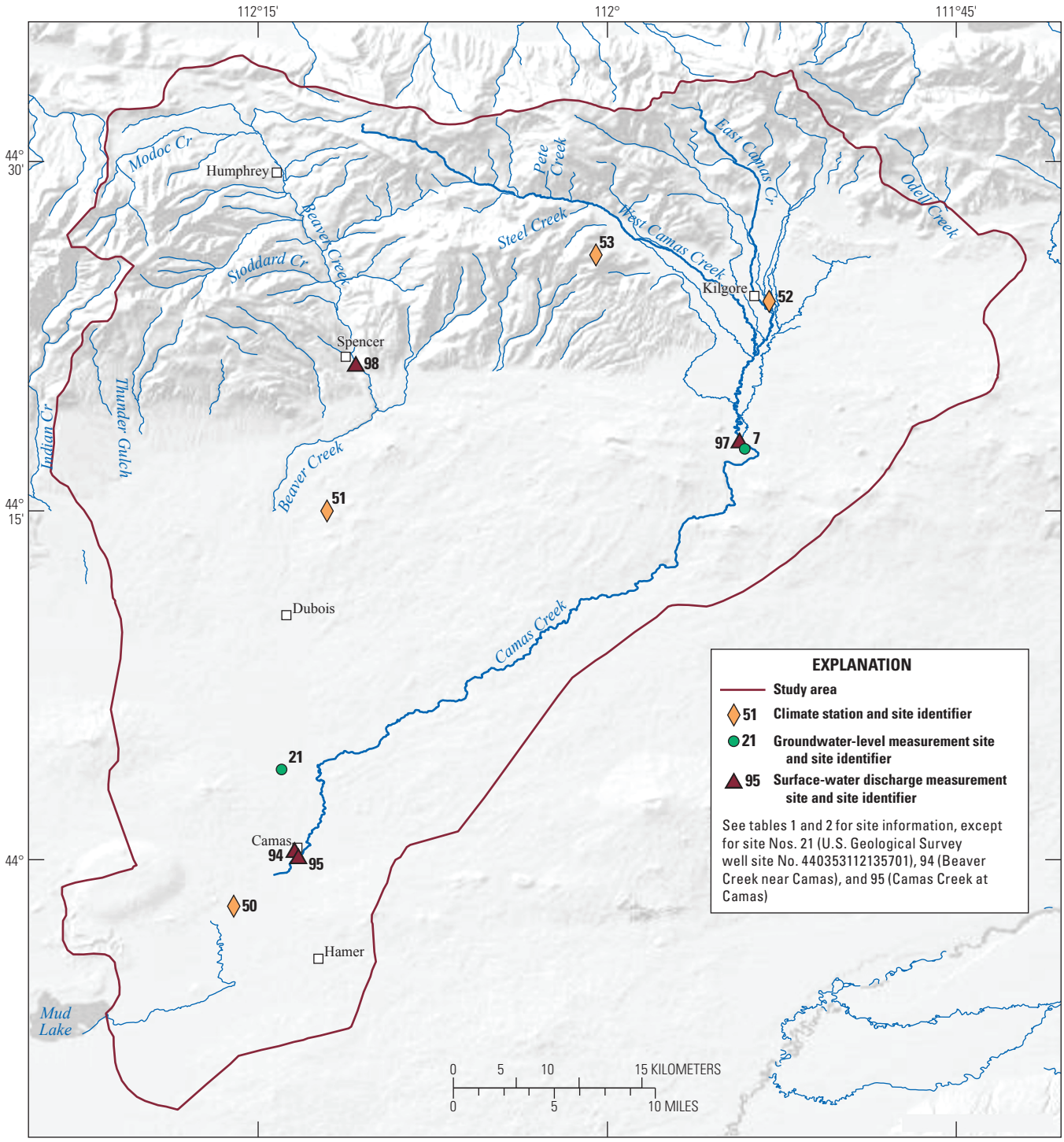

Base from U.S. Geological Survey digital data, 1:24,000 and 1:100,000. Coordinate system and datum: NAD 1927 (definition 1976).

Figure 3. Location of climate stations, and surface-water discharge and groundwater-level measurement sites, Beaver and Camas Creek drainage basins, eastern Idaho.

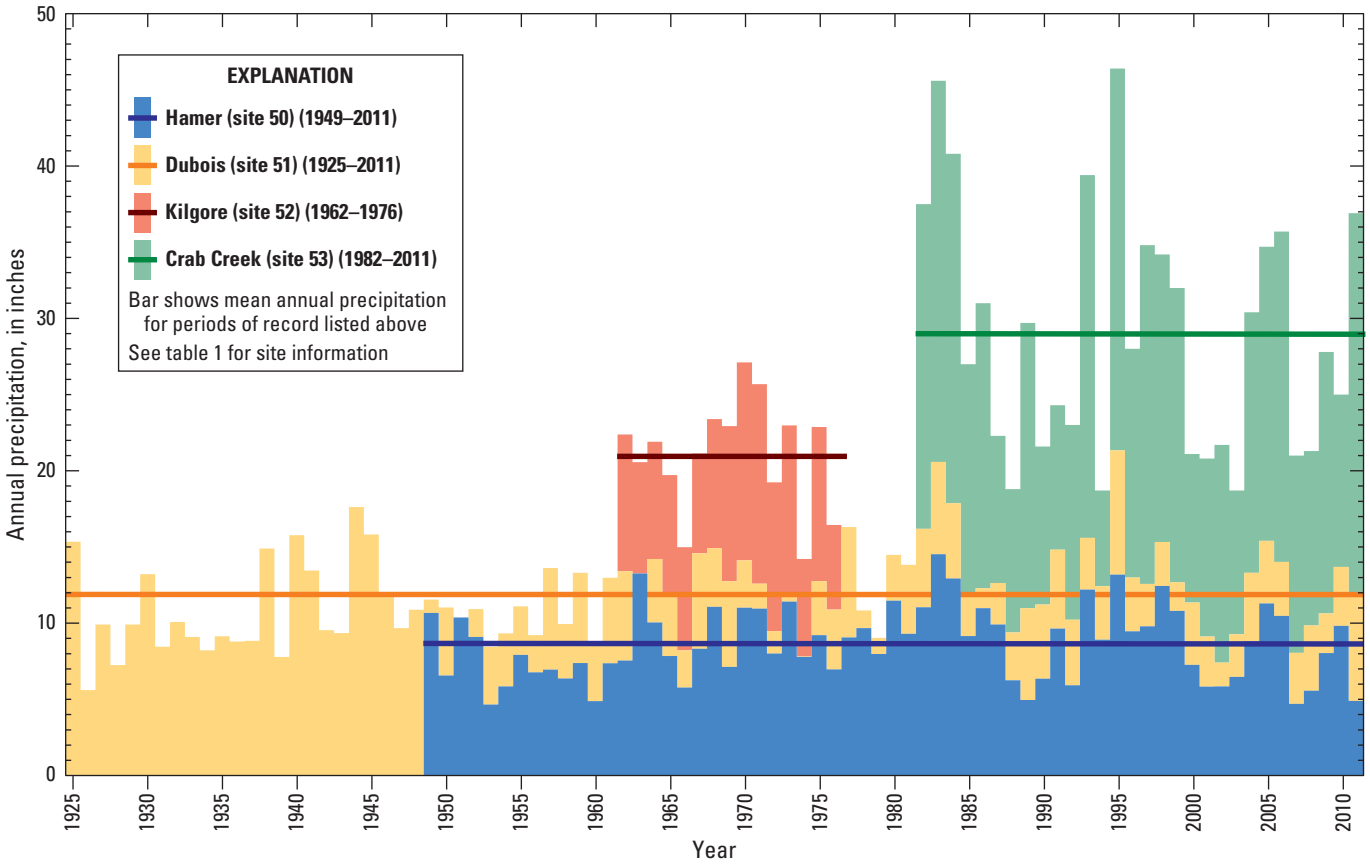

Figure 4. Annual and mean annual precipitation at or near Hamer, Dubois, Kilgore, and Crab Creek, Beaver and Camas Creek drainage basins, eastern Idaho.

The difference in climate type is due to topographic relief in the study area. The elevations in the mountainous, northern part of the study area are higher than in the relatively flat ESRP that comprises the southern part of the study area. This large topographic relief results in orographic precipitation at the higher elevations from Pacific Ocean air masses moving eastward and northeastward. For example, climate data from climate stations at or near Hamer, Dubois, Kilgore, and Crab Creek, at altitudes of 4,790, 5,445, 6,160, and 6,860 ft, respectively, show that temperature decreases and precipitation increases with elevation (table 1). Mean annual precipitation increases from 8.7 in. near Hamer to 29.0 in. at Crab Creek, and is estimated to be more than 40 in. in the highest parts of the study area (Idaho Department of Environmental Quality, 2005, p. 4). Snowfall increases from 26.8 in. near Hamer to 131.6 in. at Kilgore. At Crab Creek, the mean annual cumulative snow water equivalent is 16.8 in., or about 58 percent of the mean annual precipitation (U.S. Department of Agriculture, 2012).

Geology

The upper reaches of the Beaver and Camas Creek drainage basins are in the Beaverhead and Centennial Mountains, which are part of the northern Basin and Range Province. The drainage basins extend onto the ESRP, which is part of the Snake River Plain-Yellowstone Plateau volcanic province (Morgan and McIntosh, 2005, p. 289; Iwahashi, 2010, p. 9–10). Sediment in the drainage basins consists of surficial and interbedded sediments; surficial sediments overlie much of the bedrock, and interbedded sediments are present in basalt interflow zones.

Beaverhead and Centennial Mountains

The majority of rocks in the mountains are Paleozoic, Mesozoic, and Cenozoic sedimentary rocks; Pliocene volcanic rocks; and Quaternary surficial sediments (fig. 5) (Stearns and others, 1939, p. 18–20; Witkind, 1975, 1980, 1982; Rember and Bennett, 1979). The sedimentary rocks include shale, claystone, siltstone, sandstone, limestone, dolomite, conglomerate, seams of Paleozoic age carbonaceous shales, and Cretaceous-age coal found along the crest of the Centennial Mountains and around Humphrey (Kirkham, 1927, p. 40–41; Witkind, 1980, p. 13). The volcanic rocks include ESRP rhyolite (in the foothills of the mountains), basalt, and andesite. The groundmass of the basalt and andesite is composed of augite, olivine, plagioclase, glass, and magnetite with phenocrysts of labradorite, augite, olivine, opaques, hypersthene, biotite, and hornblende. Opal is present in some lava flows as vesicle fillings and coatings on joint surfaces (Witkind, 1980).

Eastern Snake River Plain

The ESRP is a bimodal volcanic province in which voluminous eruptions of high-silica rhyolites were followed by basalt eruptions. In the study area, which includes the northeastern extent of the ESRP, Miocene to Pliocene rhyolites are overlain by a thick accumulation of numerous Quaternary olivine basalt flows plus surficial and interbedded Quaternary sediments.

ESRP rhyolites include ash-flow tuffs, lava flows, and dikes, and are primarily from regional, caldera-forming ignimbrites of the Kilgore Tuff of the Heise Group and the Huckleberry Ridge Tuff of the Yellowstone Group (Witkind, 1980; Christiansen, 1982, p. 348; Morgan, 1992, p. 216–222; Lanphere and others, 2002, p. 560; Morgan and McIntosh, 2005, p. 289–291). The thickness of the rhyolite is spatially variable, but near Kilgore the thickness appears to be at least several hundreds of feet (Embree and others, 1982, p. 341; Morgan and others, 1984, p. 8,667–8,668). The rhyolites contain vitrophyric, lithophysal, and devitrified zones with phenocrysts generally less than or equal to 10 percent in the Kilgore Tuff (Morgan and McIntosh, 2005, p. 299) and ranging from phenocryst-poor to phenocryst-rich in the Huckleberry Ridge Tuff (Christiansen, 1982, p. 351). Groundmass in the rhyolites is composed of glass, quartz, feldspar, and minor biotite and magnetite and phenocrysts consist of plagioclase (An_{10-35} in the Kilgore Tuff), quartz, sanidine, augite to ferroaugite, magnetite, zircon and, rarely, biotite, apatite, fayalite, hedenbergite, and chevkinite (Witkind, 1975, 1980, 1982; Christiansen, 1982, p. 351; Embree and others, 1982, p. 341; Morgan and others, 1984, p. 8,670; Morgan and McIntosh, 2005, p. 299).

Most of the basalt in the study area originated from the Spencer-High Point volcanic field (Kuntz and others, 1992; Iwahashi, 2010). The total thickness of the basalt flows varies over hundreds of feet with a maximum thickness of about 1,000 ft in the southwestern part of the study area (Crosthwaite, 1973, p. 25–26; Spinazola and others, 1992, p. 18–24; Whitehead, 1992, pl. 3). Basalts in the ESRP are typically olivine basalts to more evolved basalts (Kuntz, 1992, p. 251; Iwahashi, 2010, p. 68). The basalts include up to 10 percent glass (with evidence of secondary hydration), phenocrysts of plagioclase and olivine that comprise up to 1 to 25 percent of the rock, and a groundmass composed of 90 to 95 percent plagioclase with lesser amounts of olivine, glass, augite, and opaques (McLing, 1994, p. 16; Iwahashi, 2010, p. 58–62). In basalt within or near the study area, abundant caliche and occasional pyrite were observed in vesicles, and olivine was observed to alter to iddingsite (Stearns and others, 1939, p. 26; Crosthwaite, 1973, p. 31). Kuntz and others (1992, p. 250–251), reviewing the petrography of a variety of basaltic rocks from the ESRP, reported that olivine basalts typically consisted of olivine (Fo_{80-90}), augite to ferroaugite, plagioclase (An_{50-70}), titanomagnetite, ilmenite, and glass.

Sediment

The source areas for surficial and interbedded sediments in the Beaver and Camas Creek drainage basins are eolian transport of outwash from mountains to the west of the drainage basins (Phillips, 2012) and outwash from the Beaverhead and Centennial Mountains. The sediments were derived from glacial, fluvial, eolian, and lacustrine processes and consist of clay, silt, sand, and gravel (Stearns and others, 1939, p. 37–41; Crosthwaite, 1973, p. 11; Luttrell, 1982, p. 17–21; Spinazola, 1994, p. 10–13; Iwahashi, 2010, p. 54). The total thickness of surficial and interbedded sediment ranges from less than 10 ft in the eastern part of the study area to 100–500 ft in the southern part (Luttrell, 1982, fig. 5; Whitehead, 1992, pl. 5) where Pleistocene lacustrine deposits from former Lake Terreton were deposited (Stearns, 1939, p. 37; Kuntz and others, 1994; Gianniny and others, 2002).

The mineralogy of surficial sediments in the drainage basins was discussed by Stearns and others (1939, p. 37–41) and Gianniny and others (2002, p. 82–84), and the composition of interbedded sediments in the southern part, south of, and southwest of the drainage basins was investigated in several reports (Crosthwaite, 1973, p. 22–43; Robertson and others, 1974, p. 57–58; Barraclough and others, 1976, p. 123–124; Rightmire, 1984, p. 17–18; Rightmire and Lewis, 1987, p. 35; Bartholomay, 1990b, table 2; Reed and Bartholomay, 1994). The surficial sediment in the drainage basins includes sedimentary rocks, rhyolite, and basalt in alluvial fans extending southward from the mountain

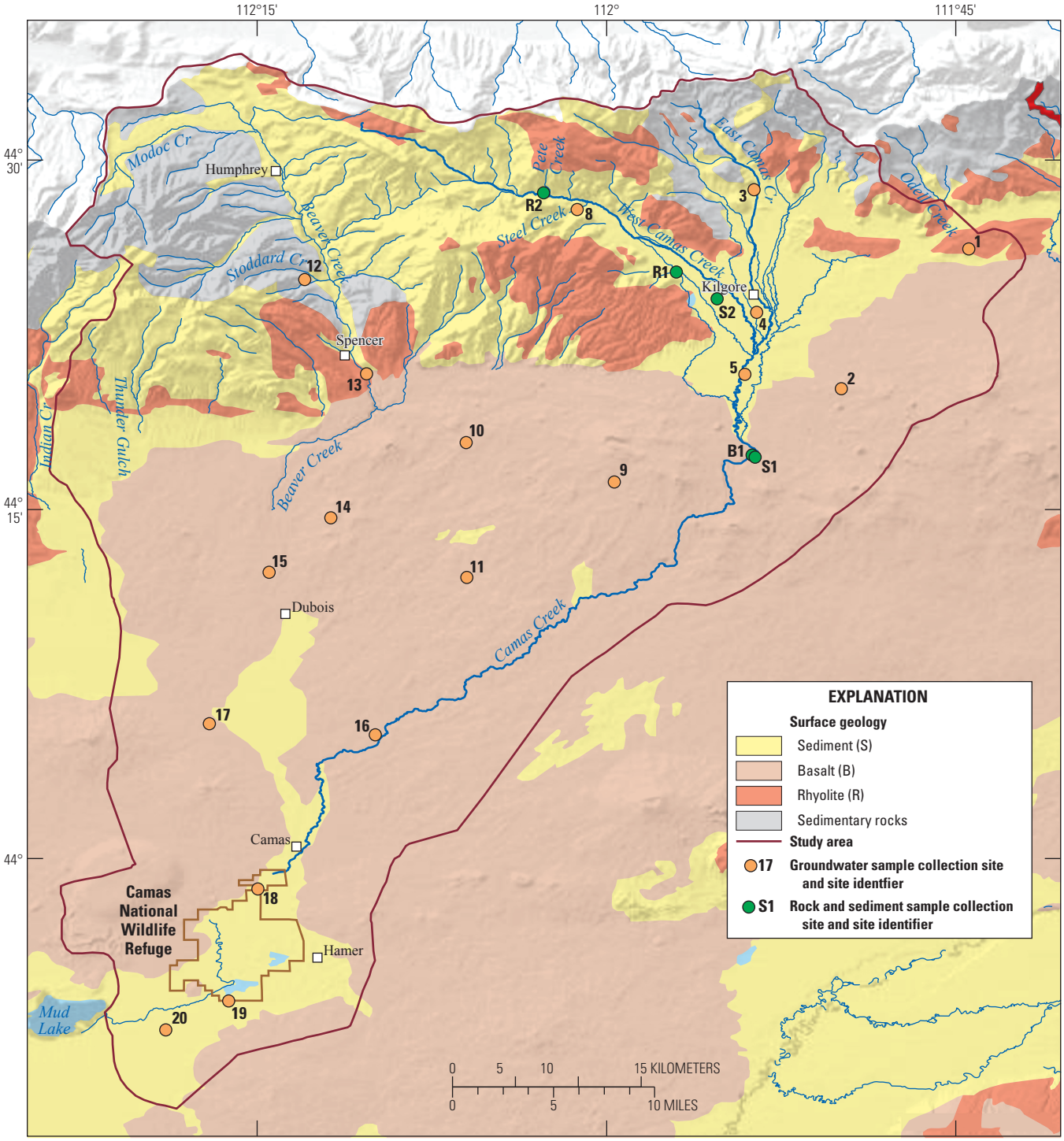

Base from U.S. Geological Survey digital data, 1:24,000 and 1:100,000. Coordinate system and datum: NAD 1927 (definition 1976).

Geologic information and map from U.S. Geological Survey (2005).

Figure 5. Surface geology, groundwater-quality sample collection sites, and rock and sediment sample collection sites, Beaver and Camas Creek drainage basins, eastern Idaho.

fronts; glacial outwash of sand, gravel, and clay in the small sedimentary basin surrounding Kilgore; clay, silt, sand, gravel, and ostracods of lacustrine, fluvial, and eolian origin near Mud Lake; and eolian-derived quartz in sand dunes on the ESRP (Stearns and others, 1939, p. 37–41; Luttrell, 1982, p. 17–21). Interbedded sediments, which are located in basalt interflow zones that consist of the highly fractured basalt and rubble derived from the top of one basalt flow and the base of the overlying basalt flow (Whitehead, 1992, p. 26), were composed of rock fragments of rhyolite and basalt; the minerals quartz, plagioclase, potassium feldspar, calcite, smectite, kaolinite, and illite; and lesser amounts of pyroxene, dolomite, chlorite, caliche, biotite and olivine. Gypsum was identified in subsurface sediments southwest of the study area, and indicated the presence of evaporative depositional conditions (Geslin and others, 2002, p. 13) during the Pleistocene as lake levels in Lake Terreton fluctuated in response to changing climate conditions (Gianniny and others, 2002, p. 78).

Land Cover and Use

Land cover in the study area consists primarily of forest in the mountains, shrub and grassland in the ESRP north and east of Dubois, irrigated acreage in the area surrounding Kilgore and in the ESRP at and south of Dubois, and wetlands in the area surrounding Kilgore (hereafter referred to as Camas Meadows) and the Camas National Wildlife Refuge (CNWR) (fig. 6). Much of the shrub and grassland is used for grazing about 9,000 head of cattle (U.S. Department of Agriculture, 2009, p. 319) and about 3,000 head of sheep (U.S. Department of Agriculture, 2013). Dryland agriculture occurs north of Dubois along Beaver Creek and at the base of the Beaverhead Mountains (Lindholm and Goodell, 1986).

Hydrology

There are numerous perennial streams in the study area that originate in the Beaverhead and Centennial Mountains, and almost all of these streams provide flow to either Beaver or Camas Creek. Streams that do not flow into Beaver or Camas Creek terminate on the ESRP. Several of the streams originating in the Centennial Mountains converge south of Kilgore to form Camas Creek, and this confluence of streams forms the wetlands at Camas Meadows. Beaver and Camas Creeks are perennial streams until reaching the Snake River Plain, after which both streams are ephemeral due to streamflow infiltration into the porous alluvium and basalt on the plain, evapotranspiration, and diversions for agricultural purposes (Stearns and others, 1939, p. 44–45, 73–75; Mundorff and others, 1964, p. 131; Spinazola, 1994, p. 16; Thompson, 2005, p. 27–28). Surface-water diversions for agriculture occur in the vicinity of Kilgore and south of Dubois, although most of the land south of Dubois is irrigated with groundwater (Lindholm and Goodell, 1986; Spinazola, 1994, p. 31). Flow in the streams generally reaches Camas only during spring runoff, which usually occurs during April, May, and June (fig. 7). Beaver Creek, when flowing as far south as Camas, joins Camas Creek near Camas. When Camas Creek does not flow south of Camas, groundwater is pumped into the dry creek bed and the water is transported downstream for irrigation and for maintaining wetlands, ponds, and lakes on the CNWR (fig. 6). When Camas Creek does flow south of Camas, any water remaining in Camas Creek after irrigation and wildlife refuge diversions enters and sustains Mud Lake (Spinazola, 1994, p. 16; Thompson, 2005, p. 28).

Aquifers in the study area include the regional ESRP aquifer and several local, unnamed aquifers. The layers of basalt and interbedded sediment in the ESRP (fig. 5) comprise a regional, continuous aquifer that underlies the 10,800 mi^2 ESRP (Lindholm, 1996). The ESRP aquifer is estimated to be several thousand feet thick in some locations (Garabedian, 1992, p. 43). Local aquifers include the sedimentary and volcanic rocks in the mountains, alluvium in the mountain valleys, alluvial fans along the mountain fronts, and lacustrine and stream sediments at Camas Meadows. Rapid percolation of diverted surface water or pumped groundwater at ponds and lakes at the CNWR (Brian Wehausen, manager of the CNWR, oral commun., May 2013) indicate that groundwater in lacustrine and stream sediments south of Dubois are connected to the ESRP aquifer. Most groundwater in the study area is unconfined; however, some impermeable units may produce locally confined groundwater at Sheridan Ridge and Camas Meadows. For example, the water level rose about 500 ft during drilling of the well at site 1 on Sheridan Ridge, and the well at site 4 at Kilgore was a flowing well when it was drilled (table 2).

The thickness of the unsaturated zone above the ESRP aquifer ranges from less than 20 ft at the CNWR west of Hamer (site 18, table 2 and fig. 8) to about 1,000 ft in the ESRP southwest of Kilgore (site 9, table 2 and fig. 8). A shallow, perched aquifer may be present at Camas Meadows (Stearns and others, 1939, p. 57–59).

Groundwater in the alluvium of the mountain valleys probably moves horizontally in a direction aligned with the orientation of the valley, and groundwater in the alluvium in Camas Meadows and the ESRP basalt aquifer probably moves horizontally in a downgradient direction perpendicular to the contours of the potentiometric surface (Spinazola, 1994, p. 29). The transition of groundwater from the mountains and Camas Meadows to the ESRP is not well understood. In the ESRP aquifer, groundwater probably moves preferentially through porous rubble- and sediment-filled interflow zones instead of through the dense basalt matrix (Whitehead, 1992, p. 26).

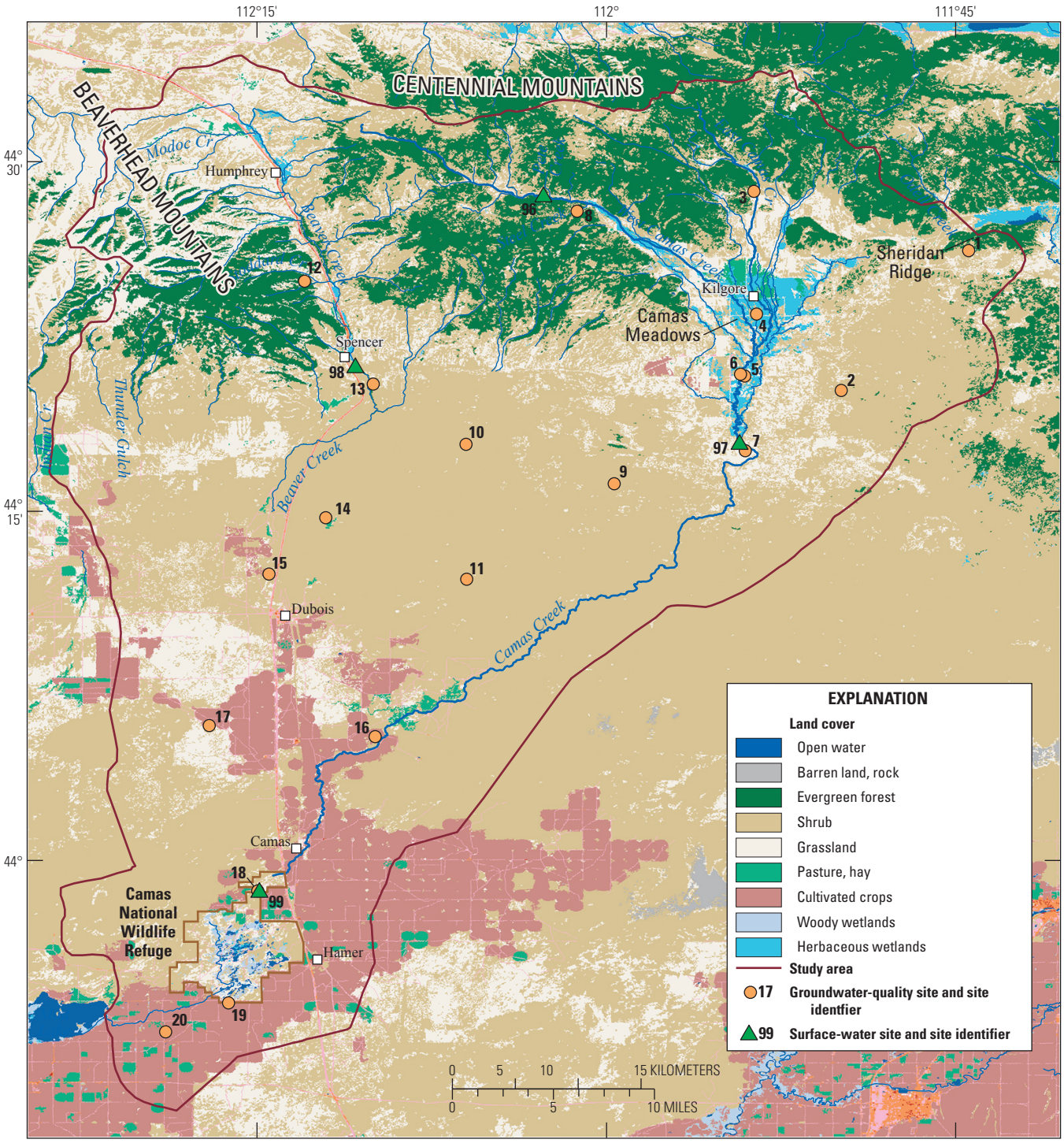

Base from U.S. Geological Survey digital data, 1:24,000 and 1:100,000. Coordinate system and datum: NAD 1927 (definition 1976).

Land cover information and map from U.S. Geological Survey (2007)

Figure 6. Land cover and use, surface-water and groundwater sample collection sites, and locations of the Camas National Wildlife Refuge, Camas Meadows, and Sheridan Ridge, Beaver and Camas Creek drainage basins, eastern Idaho.

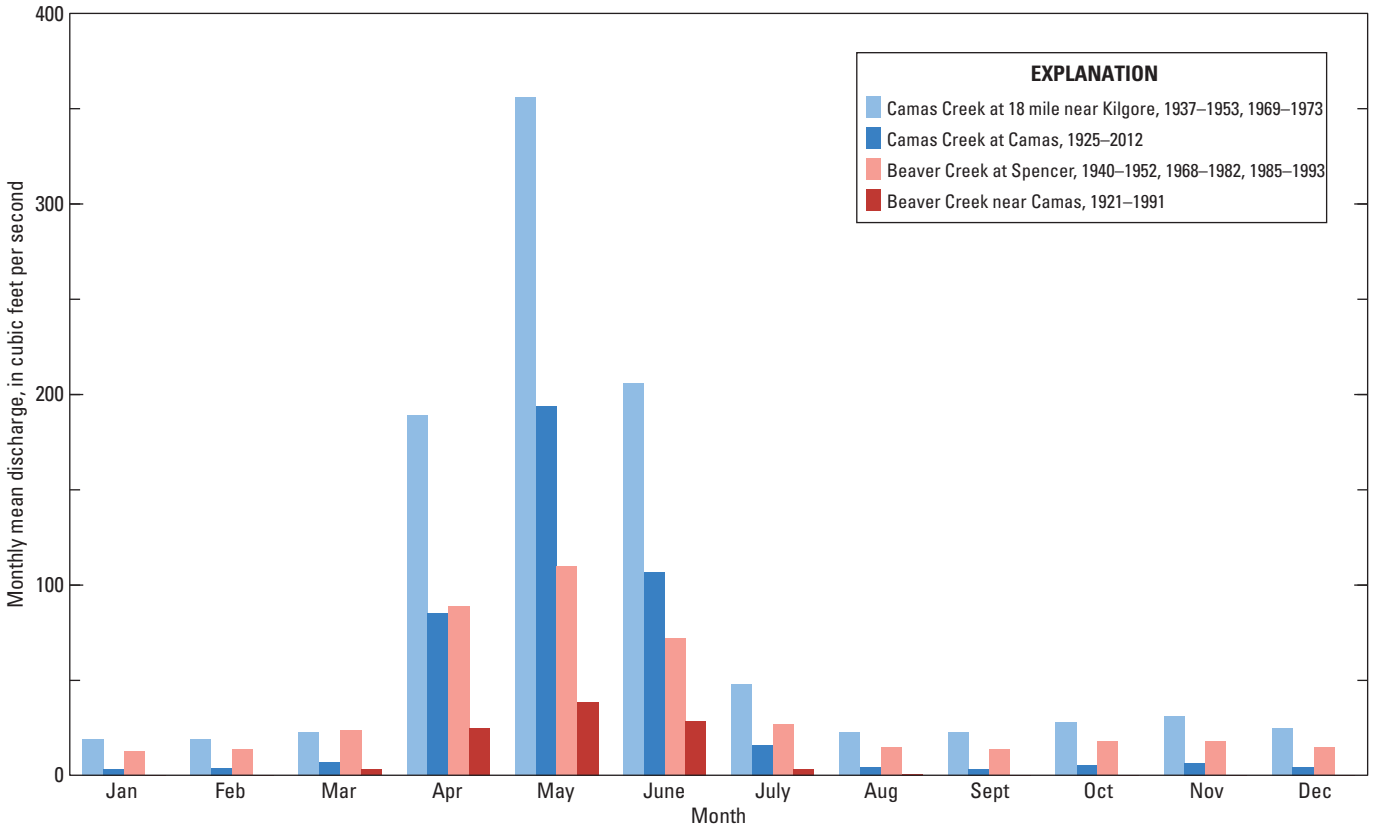

Figure 7. Monthly mean discharge at U.S. Geological Survey streamgages on Beaver and Camas Creeks, Beaver and Camas Creek drainage basins, eastern Idaho. Locations of surface-water measurement sites are shown in figure 3.

The approximate water table in and near the study area (fig. 9) was interpolated, using the natural neighbor technique (Sibson, 1981), from 237 water-level measurements. Two-hundred twenty-two of the measurements were made between March and August of 1989 [USGS well site numbers and date of water-level measurement are listed in table A2, in appendix A; all water-level measurements are from the USGS National Water Information System (NWIS) database (U.S. Geological Survey, 2013a)]. The measurements are primarily from the area around Dubois, include 15 measurements south and east of Kilgore, and 12 water-level measurements (made between 1957 and 2002) that were used to provide control for interpolation of water-table contours on the ESRP between Kilgore and Dubois. This skewed spatial distribution of water levels means that the water-table contours are only well defined in the area south and east of Kilgore and south of Dubois. However, based on these approximate water table contours, horizontal groundwater movement in the ESRP appears to be south between Spencer and Camas and southwest between Kilgore and Camas. Water-table maps of the Mud Lake area for 1980 (Garabedian, 1992, pl. 4; Spinazola, 1994, p. 28) indicate similar flow directions.

Hydraulic gradients in the ESRP aquifer were estimated from water-table contours. The hydraulic gradient was about 100 ft/mi (calculated between the 4,900 and 6,100 contour intervals and using an approximate distance between these contour intervals of 12 mi) north and east of Dubois, and the hydraulic gradient was about 7 ft/mi (calculated between the 4,900 and 4,700 contour intervals and using an approximate distance between these contour intervals of 28 mi) south of Dubois. This wide range of hydraulic gradients is similar to those observed at and near the INL (1–60 ft/mi, Ackerman and others, 2006, p. 39). If the hydraulic conductivities and effective porosities are similar between the ESRP aquifer at and near the INL and the ESRP aquifer in the Beaver and Camas Creek drainage basins, which is a reasonable

Table 2. Water-quality sample site number and type, site location and altitude, well depth and open interval, approximate depth to water, approximate depth of open interval below water table, and aquifer material, Beaver and Camas Creek drainage basins, eastern Idaho.

[Location of sites are shown in figure 2. Latitude and longitude are shown in degrees (dd), minutes (mm), and seconds (ss). **Abbreviations:** NGVD 29, National Geodetic Vertical Datum of 1929; na, not applicable; unk, unknown; ft, foot; bls, below land surface]

Site No.	Site type	Latitude (ddmmss)	Longitude (ddmmss)	Altitude (ft above NGVD 29)	Well depth (ft bls)	Well open interval (ft bls)	Approximate depth to water (ft bls)	Approximate depth of open interval below water table (ft)	Aquifer material
1	Stock well	442615	1114425	6,544	700	176–700	[1]200	0–500	Rhyolite
2	Stock well	442015	1114956	6,421	690	215–690	507	0–183	Basalt
3	Domestic well	442847	1115341	6,630	145	115–125	107	8–18	Sedimentary rock
4	Irrigation well	442331	1115334	6,312	212	180–208	[2]4	176–204	Alluvium
5	Domestic well	442051	1115404	6,270	120	77–120	83	0–37	Basalt
6	Domestic well	442056	1115415	6,274	160	57–160	140	0–20	Basalt
7	Monitoring well	441740	1115405	6,244	758	0–754	549	0–205	Basalt
8	Recreation well	442756	1120116	6,681	200	120–180	100	20–80	Sedimentary rock
9	Stock well	441614	1115941	6,145	1,115	203–1,115	1,011	0–104	Basalt
10	Stock well	441756	1120602	5,955	856	800–856	731	69–125	Basalt
11	Stock well	441208	1120601	5,439	750	90–750	653	0–97	Basalt
12	Recreation well	442456	1121258	6,370	280	279–280	192	87–88	Sedimentary rock
13	Domestic well	442053	1121019	5,870	120	20–120	58	0–62	Basalt
14	Stock well	441442	1121151	5,500	765	unk	671	unk	Basalt
15	Stock well	441222	1121430	5,240	580	20–580	450	0–130	Basalt
16	Irrigation well	440523	1120956	5,010	233	20–233	213	0–20	Basalt
17	Irrigation well	440552	1121704	4,921	250	120–250	135	0–115	Basalt
18	Irrigation well	435846	1121459	4,805	255	53–255	16	37–239	Basalt
19	Irrigation well	435357	1121614	4,793	100	70–100	41	29–59	Basalt
20	Domestic well	435243	1121856	4,785	218	167–218	189	0–29	Basalt
96	West Camas Creek	442840	1120243	6,650	na	na	na	na	na
97	Camas Creek	441802	1115419	6,260	na	na	na	na	na
98	Beaver Creek	442119	1121048	5,850	na	na	na	na	na
99	Camas Creek	435849	1121459	4,829	na	na	na	na	na

[1]Water was reached at a depth of 700 ft bls, at which point the water level rose 500 ft (Jim Hagenbarth, oral commun., August 2011).

[2]Drillers' log recorded this as a flowing well (Idaho Department of Water Resources, 2012).

assumption given the similar aquifer materials and stratigraphy, then the average linear groundwater velocities between the two areas should be similar or slightly larger for the Beaver and Camas Creek drainage basins. Average linear groundwater velocities were estimated to range from 2 to 20 ft/d in the ESRP aquifer at and near the INL (Ackerman and others, 2006, p. 46–47), and similar or slightly larger velocities may be expected in the ESRP aquifer in the Beaver and Camas Creek drainage basins.

Temporal changes in groundwater levels in the ESRP were observed to respond to short-term climate cycles and irrigation withdrawals (fig. 10). [For a discussion of groundwater response in the ESRP aquifer to wet and dry climate cycles, see Ackerman and others (2006, p. 43).] Water levels began to rise or decline within a year or two of the onset of a wet or dry climate cycle, respectively, indicating that water levels in the ESRP respond fairly rapidly to recharge from precipitation. Water levels in the ESRP did not change seasonally in response to vertical infiltration of snowmelt, which indicates that infiltration of snowmelt in the ESRP is limited.

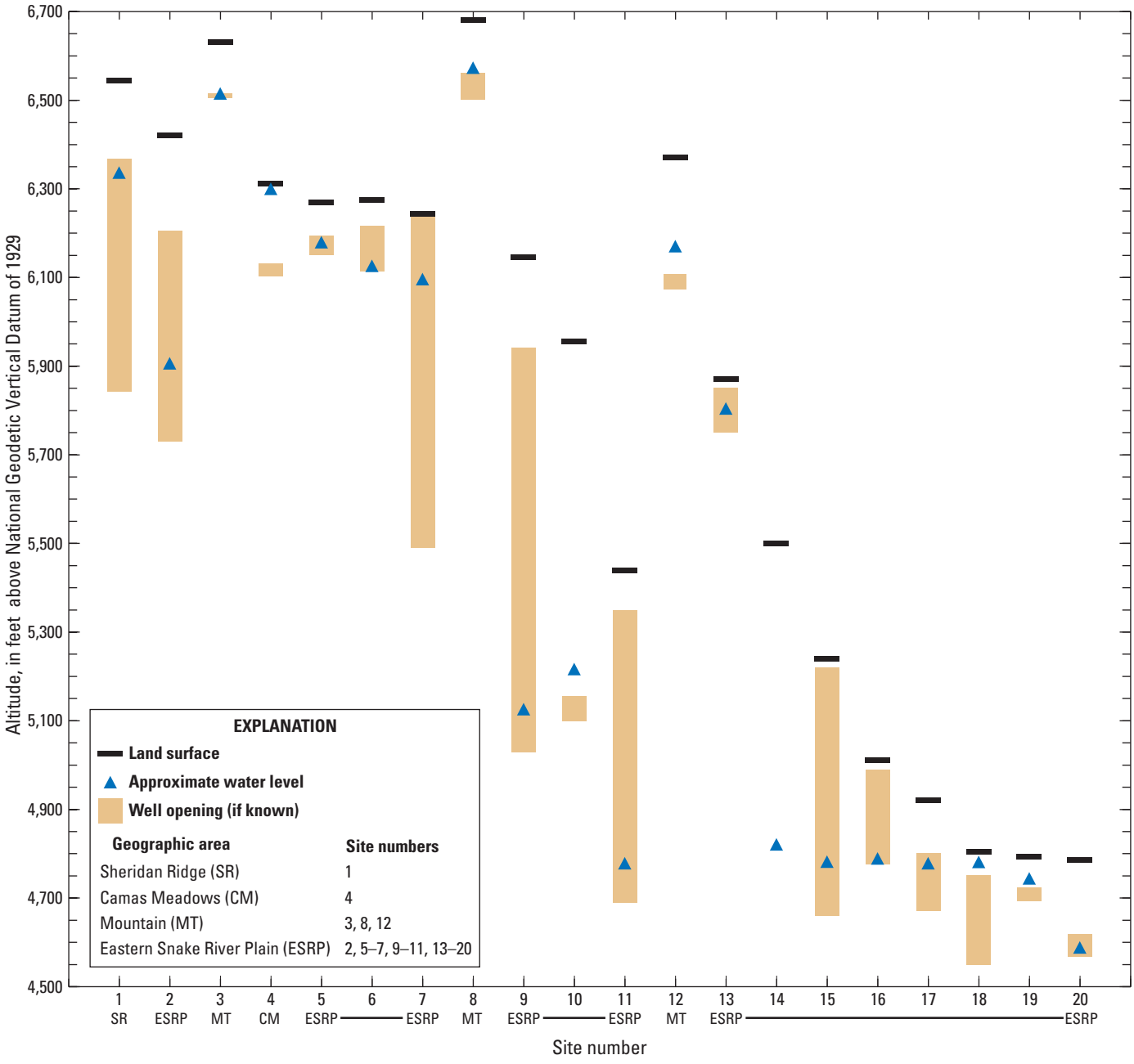

Figure 8. Altitude of the land surface, water level, and well opening for groundwater sampling sites, Beaver and Camas Creek drainage basins, eastern Idaho.

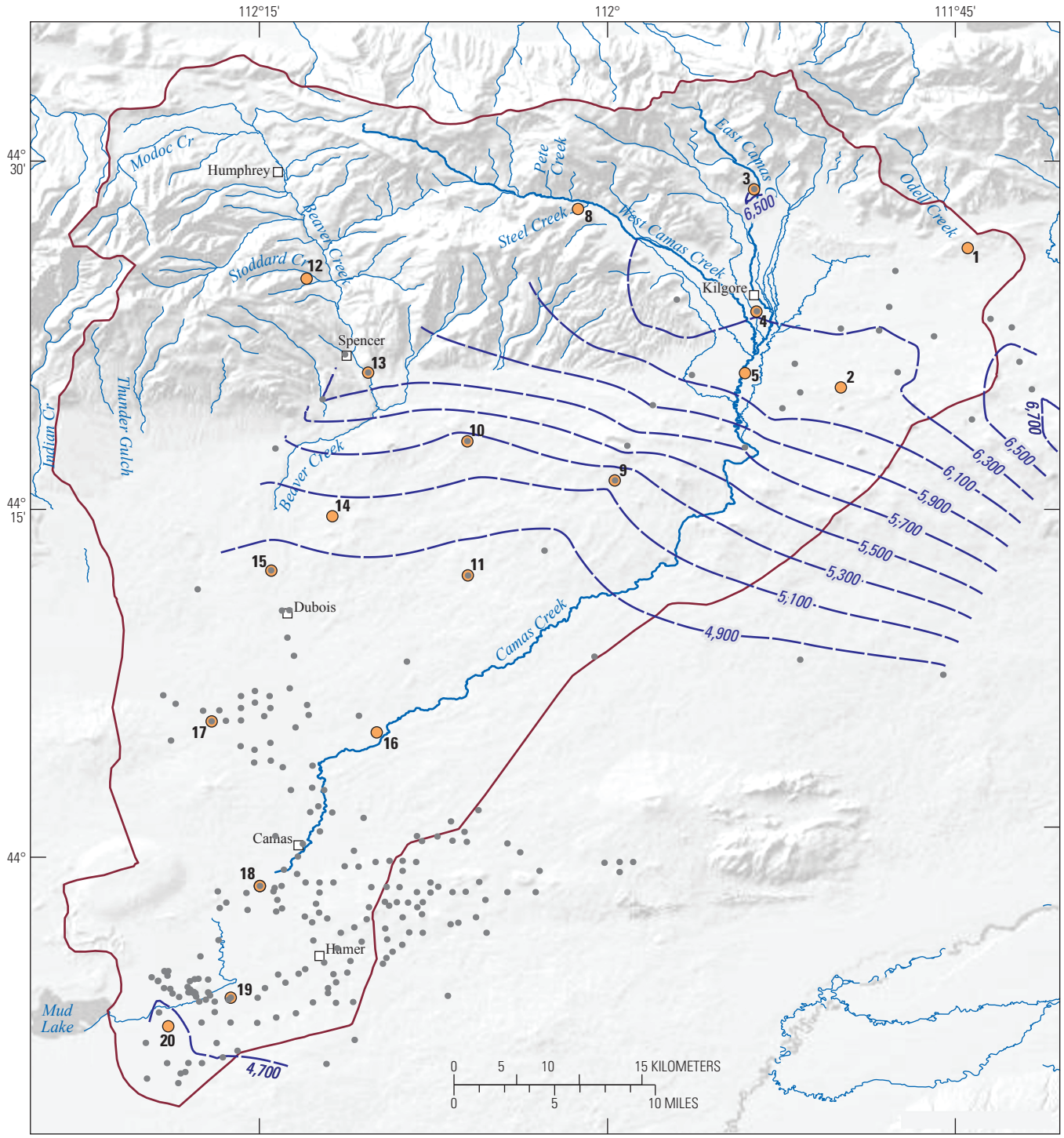

Base from U.S. Geological Survey digital data, 1:24,000 and 1:100,000. Coordinate system and datum: NAD 1927 (definition 1976).

EXPLANATION

- **Study area**
- 6,500 **Water-table contour**—Shows approximate altitude of water table, 1989. Contour interval, 200 feet. Datum is National Geodetic Vertical Datum of 1929.
- 5 **Groundwater sample-collection site and site identifier**
- **Well with water-level measurement**

Figure 9. Water-table contours and locations of wells with water-level measurements used to generate the contours, Beaver and Camas Creek drainage basins, eastern Idaho.

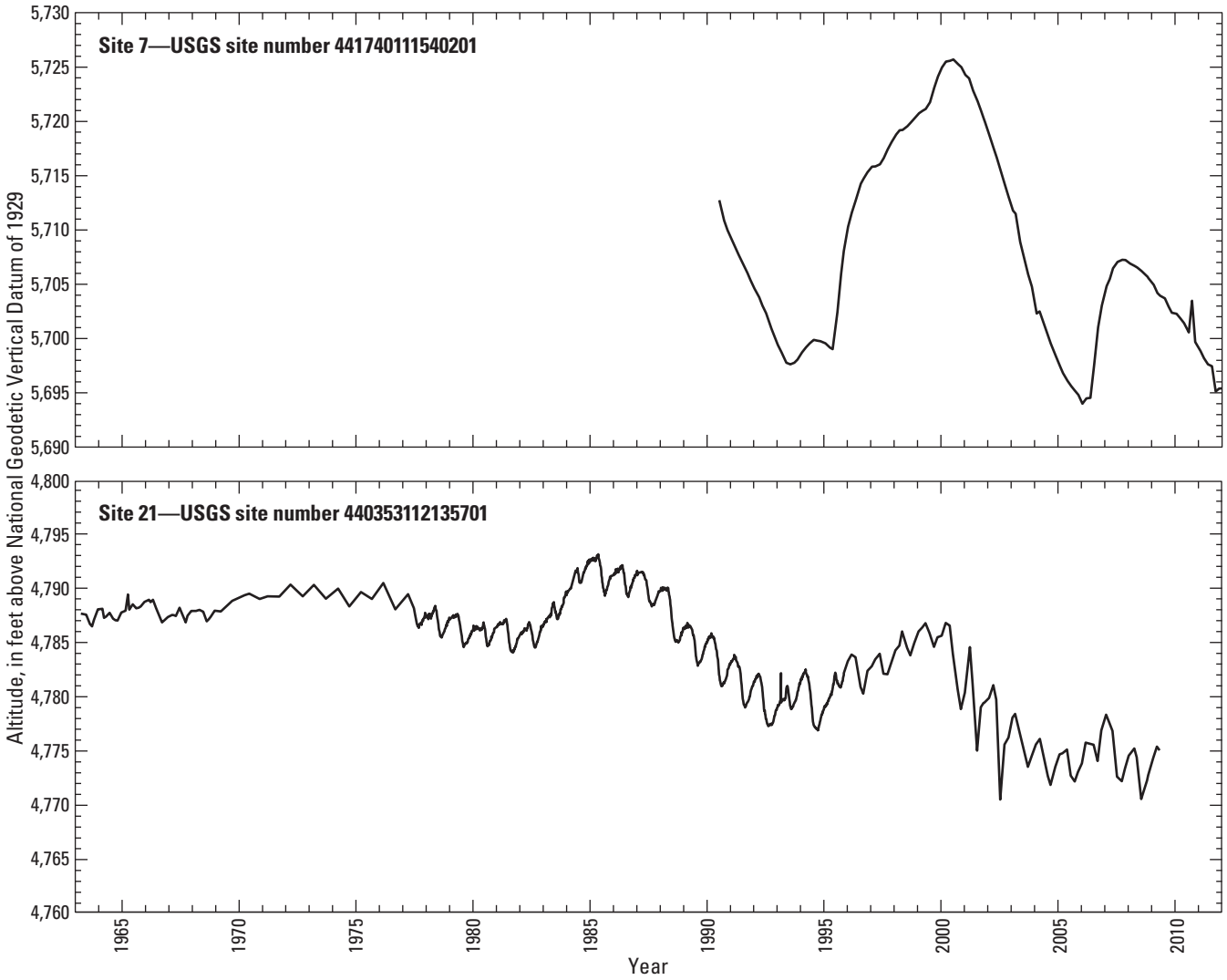

Figure 10. Water levels measured from a well south of Kilgore and a well north of Camas, Beaver and Camas Creek drainage basins, eastern Idaho. Site (well) locations shown in figure 3. Well at site 21 is an irrigation well. USGS, U.S. Geological Survey.

Sample Collection, Analytical Methods, and Quality Assurance

Sediment, rock, and water-quality samples were collected and analyzed for their geochemistry in order to understand the geochemical evolution of groundwater in the study area. Sediment and rock samples were analyzed for their mineralogy to identify possible phases to include in geochemical modeling. Water-quality samples were collected from surface-water and groundwater sites in order to characterize the water chemistry of the study area and to use as initial and final solutions in geochemical models. Quality assurance (QA) of water-quality samples was evaluated with four quality-control (QC) samples and calculation of the charge balance of the samples.

Sample Collection

Sediment and Rock Samples

Two sediment and three rock samples were collected (fig. 5) and analyzed for mineralogy and petrology to supplement information about the mineralogy and petrology of the study area acquired from literature review. Sediment samples were collected in Camas Meadows by digging holes about 1-ft-deep in creek channel deposits and removing approximately 1.5 kg of sediment from the bottom of the holes. Rock samples were collected from road outcrops to identify the primary minerals, as well as any alteration and secondary minerals, in the rhyolite and basalt in the study area.

Water-Quality Samples

Water-quality samples used in this study include 4 surface-water samples and 18 groundwater samples. Two surface-water samples (table 3 and fig. 2, sites 96 and 99) and 11 groundwater samples (sites 1, 3, 5, 6, 7, 8, 11, 12, 15, 18, and 20) were collected during August 2011 specifically for this study, and 2 surface-water samples (sites 97 and 98, collected in 1981 and 1995, respectively) and 9 groundwater samples (sites 2, 4, 9, 10, 13, 14, 16, 17, and 19; collected in 1979, 2007, 2008, 2009 and 2011) were collected for other USGS studies but were used to aid with the geochemical interpretation of the drainage basins. However, two groundwater samples (table 2 and fig. 2, sites 6 and 7) collected during August 2011 were not used in this study because their analytical results appear to be contaminated from exposure to the atmosphere. Four QC samples were collected; two field replicates and one field blank in August, 2011 and one field blank in June 2012.

One surface-water sample was from Beaver Creek and three were from Camas Creek. One groundwater sample was from sedimentary rocks in the Beaverhead Mountains, 2 from sedimentary rocks in the Centennial Mountains, 1 from rhyolite comprising Sheridan Ridge at the eastern extent of the study area, 1 from alluvium in Camas Meadows (fig. 5), and 13 from basalt in the ESRP.

Table 3. Results of measurements of field parameters (temperature, pH, specific conductance, alkalinity, and dissolved oxygen) and calculated partial pressure of carbon dioxide (log PCO_2) in water from selected sites, Beaver and Camas Creek drainage basins, eastern Idaho.

[Location of sites are shown in figure 2. Surface-water sites are shown in shaded gray. **pH**: negative base-10 logarithm of hydrogen activity in moles per liter. **Carbon dioxide:** log PCO_2, base-10 logarithm of carbon dioxide partial pressure. **Abbreviations:** °C, degrees Celsius; µS/cm, microsiemens per centimeter at 25°C; mg/L, milligrams per liter, $CaCO_3$, calcium carbonate]

Site No.	Date sampled	Temperature (°C)	pH	Specific conductance (µS/cm)	Alkalinity (mg/L as $CaCO_3$)	Carbon dioxide (log PCO_2)	Dissolved oxygen	
							(mg/L)	(percent saturation)
1	08-16-2011	8.8	7.2	147	53	-2.47	2.2	24
2	09-24-2008	9.8	7.9	146	74	-3.03	7.5	84
3	08-10-2011	7.1	7.0	99	49	-2.31	12.9	137
4	07-27-2009	6.9	7.8	205	86	-2.88	5.4	56
5	08-15-2011	7.1	8.1	223	110	-3.08	0.2	2
8	08-10-2011	9.7	6.9	70	92	-1.93	5.7	64
9	06-08-2011	11.2	7.7	240	117	-2.63	9.6	110
10	08-22-2011	9.9	7.7	180	84	-2.77	[1]10.9	[1]118
11	08-09-2011	15.6	8.0	241	114	-2.92	8.7	107
12	08-08-2011	7.9	7.8	325	162	-2.61	0.1	1
13	06-22-2007	8.3	7.2	336	161	-2.01	4.5	47
14	08-30-1979	12	7.7	341	160	-2.50	8.3	95
15	08-09-2011	14.4	7.9	292	110	-2.84	8.3	99
16	08-01-2011	11.2	7.7	270	99	-2.70	[1]10.8	[1]116
17	07-12-2011	15.5	8.0	278	118	-2.91	[1]8.5	[1]101
18	08-08-2011	12.1	8.3	249	112	-3.25	8.1	90
19	07-20-2011	10.6	7.0	431	210	-1.68	2.3	25
20	08-09-2011	12.8	7.8	301	136	-2.66	4.8	54
96	08-10-2011	15.5	7.1	242	130	-1.96	7.2	93
97	06-07-1981	13.5	7.7	157	70	-2.83	8	97
98	09-18-1995	11.0	8.6	437	223	-3.29	8.7	98
99	08-08-2011	19.3	7.8	147	76	-2.86	5.8	76

[1]Dissolved oxygen data for sites 10, 16, and 17 are from water samples collected in 2005, 2006, and 2004, respectively.

The maximum depths of open intervals of wells, in feet below the water table, were less than or equal to 130 ft for 13 wells, 183–239 ft for 3 wells, 500 ft for 1 well, and unknown for 1 well (table 2 and fig. 8). As a result, this study primarily investigates groundwater from aquifer (ESRP or local) depths of about 240 ft or less below the water table.

Samples used in the study were collected in accordance with established sample collection procedures and guidelines documented by the U.S. Geological Survey (variously dated), the USGS INL Project Office QA plan (Knobel and others, 2008), and USGS Techniques and Methods (Revesz and Coplen, 2008a, 2008b; Singleton and others, 2012) except for groundwater samples from sites 6 and 7. These two groundwater samples were collected with bailers without purging the wells. All other groundwater samples were collected with dedicated submersible pumps, and the wells were purged for as long as it took for measurements of field parameters to stabilize. Surface water (sites 96, 97, 98, and 99) was collected as grab samples. After sample collection, preservatives were added to sample bottles (if required), and the bottles were capped, labeled, and chilled (if required). Sample bottles, along with chain-of-custody forms, were mailed to the appropriate laboratory in sealed coolers either twice a week or at the end of a short sampling event.

All water-quality samples collected for this study were analyzed for major ions, silica, nutrients, selected trace elements, DOC, tritium, and the stable isotopes of hydrogen, oxygen, and carbon. Water samples collected for other studies were all analyzed for major ions and silica; most were analyzed for selected nutrients and trace elements; and a few were analyzed for the stable isotope ratios of hydrogen, oxygen, and carbon. In addition, the stable isotope ratio of sulfur was analyzed from water samples collected in 1981 from two sites (4 and 97) and the stable isotope ratio of nitrogen was analyzed from water samples collected in 2000 from four sites (9, 11, 17, and 18). The sulfur and nitrogen stable isotope ratios were used to aid with geochemical interpretation of the drainage basins. All water-quality data are available from the USGS National Water Quality Information System (NWIS) database (U.S. Geological Survey, 2013a).

The field replicates were collected at two groundwater sites. Each replicate consists of a replicate water sample and its companion environmental water sample, with the replicate water sample collected immediately after collection of the environmental water sample. The replicate water samples were collected by using the same collection methods as the environmental water samples. One replicate was collected specifically for this study and was analyzed for major ions, silica, nutrients, DOC, trace elements, tritium, and the stable isotope ratios of hydrogen, oxygen, and carbon. The other replicate was collected for another study and was analyzed for major ions, silica, nutrients, and selected trace elements (aluminum, iron, and manganese). No replicate samples were analyzed for the stable isotope ratios of sulfur and nitrogen.

Field blanks were collected and analyzed for DOC. One field blank was collected on August 10, 2011, for this study, and a second DOC field blank was collected on June 4, 2012, for a study of the Medicine Lodge Creek drainage basin (Ginsbach, 2013). Because both blanks were collected using the same sample collection methods by the same sample collectors, the results from both blanks were suitable for evaluating bias in the DOC results from samples collected in August 2011. The field blanks were prepared at a field site by filtering blank water through a Whatman 0.1 µm polytetrafluoroethylene membrane filter into the blank sample bottle. The blank water was nitrogen-purged volatile-grade organic blank water purchased from the NWQL and certified free of organic constituents.

Analytical Methods and Data Reporting Conventions

The mineralogy of two fluvial sediment samples was determined from X-ray diffraction and the mineralogy, chemical weathering, and alteration products of one basalt and two rhyolite rock samples were determined from X-ray diffraction and thin section analyses. Analysis of the sediment and rock samples was performed at the Laboratory for Environmental Geochemistry in the Geosciences Department at Idaho State University.

Water samples were measured in the field for temperature, pH, specific conductivity, dissolved oxygen (DO), and alkalinity. Major ions, silica, nutrients, trace metals, and DOC were analyzed at the USGS National Water Quality Laboratory (NWQL) in Denver, Colo. Tritium was analyzed at the USGS Stable Isotope and Tritium Labs (SITL) in Menlo Park, Calif., and the stable isotope ratios of hydrogen, oxygen, carbon, sulfur, and nitrogen were analyzed at the USGS Stable Isotope Laboratory (RSIL) in Reston, Va.

Sediment and Rock Samples

Mineralogy was determined with X-ray diffraction for the bulk sediment samples (2 samples), for each 1 phi (φ) size interval of the sediment samples [8 φ intervals for each sediment sample, with sediment size ranging from -2 φ to >4 φ, where φ = -log (base 2) of particle diameter in mm], and for the rock samples (3 samples). Approximately 5 g of material was removed from each of the samples and ground in a tungsten-carbide ring grinder to homogenize the samples. Other sample preparation procedures and sample analysis were described by Bartholomay (1990a, p. 12–16) and Ginsbach (2013, p. 41–47).

Petrographic analysis was performed on thin sections of the rock samples to look for mineralogical composition, textures, and alteration products. Thin sections were prepared by cutting billets, approximately 27 by 46 mm in size, from the rock samples. After the billets were cut they were commercially made into thin sections. Each thin section was analyzed through plane- and cross-polarized light with a petrographic microscope. Interference colors, extinction angles, interference figures, and visual characteristics (cleavage, twinning, zoning, exsolution, inclusions, and relief) were used to identify primary minerals and alteration products.

Water-Quality Samples

Field measurement methods are described in the USGS National Field Manual for the Collection of Water-Quality Data (U.S. Geological Survey, variously dated). Analytical methods used by the NWQL for measurement of major ions, silica, nutrients, and trace elements are described by Fishman and Friedman (1989), Brenton and Arnett (1993), Fishman (1993), Struzeski and others (1996), the American Public Health Association and others (1998), Garbarino (1999), Garbarino and others (2006), and Patton and Kryskalla (2011).

Reporting levels used by the NWQL were minimum reporting levels (MRLs), long-term method detection levels (LT-MDLs), and laboratory reporting levels (LRLs) and were used to determine when a constituent was detected with sufficient confidence to be reported uncensored or without remarks (Childress and others, 1999). The MRL was the smallest measured constituent concentration that could be reliably reported using a specific analytical method (Timme, 1995). The LT-MDL was determined by calculating the standard deviation of a sample with at least 24 spike sample measurements over an extended period of time (Childress and others, 1999, p. 19). The LRL generally was equal to twice the yearly determined LT-MDL (Childress and others, 1999, p. 19). Results that were between the LT-MDL and the LRL, or between the LRL and the lowest calibration standard, were reported with the "E" remark code (Childress and others, p. 9), which means the result was estimated and had a greater uncertainty than data without the "E" remark. Non-detections were reported by the NWQL as censored values (reported with the "<" symbol) that were less than the MRL or LRL.

Changes to data reporting conventions and qualifier codes used by the NWQL were implemented in October 2010 (U.S. Geological Survey, 2010). For inorganic analytes using the LRL convention, the reporting level was set at the LT-MDL concentration and concentrations less than the LT-MDL are reported as less than the LT-MDL. The LRL convention as described above is still used for organic constituents.

Tritium samples were prepared and analyzed at the SITL with electrolytic enrichment and liquid scintillation counting (Thatcher and others, 1977). Combined standard uncertainties (CSUs) for tritium were reported at a confidence level of one standard deviation (*s*). These propagated random uncertainties were calculated by using variables such as yields, appropriate half-lives, counting efficiencies, and count times. A lower CSU relative to the result indicates a lower measurement uncertainty, and a higher CSU relative to the result indicates a higher measurement uncertainty. Guidelines for interpreting radiological data used by the USGS were provided by McCurdy and others (2008). In this report, radionuclide concentrations less than 3*s* were considered to be less than a "reporting level." The reporting level should not be confused with the analytical method detection limit, which is based on laboratory procedures.

Stable isotopes were analyzed at the RSIL by using an automated carbon dioxide (CO_2) equilibration technique for the stable isotopes of oxygen and carbon (Revesz and Coplen, 2008b; Singleton and others, 2012) and a hydrogen equilibration technique for the stable isotopes of hydrogen (Revesz and Coplen, 2008a). Sulfur and nitrogen stable isotopes were analyzed by following procedures in Revesz and others (2012) and Coplen and others (2012).

The stable isotope ratios of hydrogen ($^2H/^1H$), oxygen ($^{18}O/^{16}O$), carbon ($^{13}C/^{12}C$), sulfur ($^{34}S/^{32}S$), and nitrogen ($^{15}N/^{14}N$) were reported as permil, by using delta notation (δ), the ratio of the abundance of the minor isotope to the predominant isotope for an element in a sample relative to the same isotopes in a reference material. For example, for the oxygen stable isotope ratio the delta notation is:

$$\delta^{18}O_{sample} = \frac{\left(^{18}O / {}^{16}O\right)_{sample} - \left(^{18}O / {}^{16}O\right)_{reference}}{\left(^{18}O / {}^{16}O\right)_{reference}} \quad (1)$$

where

$\left(^{18}O / {}^{16}O\right)_{sample}$ is the isotope ratio of oxygen-18 and oxygen-16 of the sample, and

$\left(^{18}O / {}^{16}O\right)_{reference}$ is the isotope ratio of oxygen-18 and oxygen-16 of the reference material.

The δ-values are multiplied by a factor of 1,000 and then expressed as parts per thousand or permil. Delta notations for the other stable isotope ratios are δ^2H for hydrogen, and $\delta^{13}C$ for carbon, $\delta^{34}S$ for sulfur, and $\delta^{15}N$ for nitrogen.

Quality Assurance

QA of water-quality measurements included laboratory practices and procedures; the collection and analysis of field quality control samples (Knobel and others, 2008); and determination of the charge balance, or electroneutrality, of water samples.

Laboratory Practices and Procedures

Laboratory QA/QC practices and procedures for the National Water Quality Laboratory (NWQL) are described in analytical method documents as well as by Friedman and Erdmann (1982) and Pritt and Raese (1995). Summaries of NWQL QA/QC data are available online (U.S. Geological Survey, 2012a, 2012b). QA for the SITL includes analysis of standards and blanks with environmental samples, periodic analysis of blanks to evaluate instrument bias, and maintenance of a long-term record of instrument performance metrics to ensure that instrument performance remains stable (Megan Young, U.S. Geological Survey, written commun., June 28, 2013). The standard operating procedures used by the RSIL are presented in Revesz and Coplen (2008a, 2008b), Coplen and others (2012), Revesz and others (2012), and Singleton and others (2012).

Quality-Control Samples

QC samples collected in the field included two replicates and two field blanks. The variability associated with measured constituent concentrations, whether from sample collection, processing, or analysis, was evaluated with statistical analysis of concentrations from replicates and their associated environmental samples (hereafter called a replicate pair). Routine collection and analysis of field blanks has shown that bias is uncommon in major ion, nutrient, trace metal, and tritium water-quality samples collected by the USGS INL Project Office (Rattray, 2012). However, DOC samples are not routinely collected by the INL Project Office and are easily contaminated. Consequently, blank samples were collected to estimate the potential bias of DOC in environmental samples. Bias was estimated from DOC concentrations using order statistics and binomial probability.

Analysis of Quality-Control Samples

Statistical analysis of replicate pair concentrations was performed using relative standard deviation (RSD) and normalized absolute difference (NAD). Replicate pair concentrations had acceptable reproducibility if the (1) RSD was less than14 percent (or both measurements were censored and/or estimated because they were below the reporting level for that analysis, or one measurement was censored or estimated and the other measurement was within one detection limit of the larger of the estimated value or the reporting level) or (2) NAD was less than or equal to 1.96 at the 95-percent confidence level. Further discussion of these statistical methods and their use for evaluating quality-control samples was provided by Rattray (2012).

The distribution of constituent concentrations from field blank samples is typically highly skewed (Rattray, 2012), so a non-parametric statistical method was used to estimate the potential bias of DOC from blank sample measurements. The statistical method used here, using order statistics (with the ranking from low to high concentration) and binomial probability (Mueller, 1998, p. 5–6), determined a one-sided confidence interval, or a confidence level (cl), that represented "the probability that m observed values from a total of n observations are less than or equal to the 100pth percentile of the sampled population" (Mueller, 1998, p. 5). The confidence level was calculated as:

$$cl = \mathrm{Prob}(n, m, p). \quad (2)$$

At the 100cl, the concentration of the $m+1$ ranked observation represented the concentration that exceeded 100p percent of the values in the population.

Quality-Control Sample Results

Relative standard deviations were calculated from replicate concentrations of major ions, silica, nutrients, trace elements, and DOC (tables 4–6). Relative standard deviations for the major ions, which were calculated for both replicate pairs, ranged from 0.1 to 3.6 percent. These values were much less than the criterion for acceptable reproducibility of less than 14 percent. Censored concentrations for ammonia and nitrite in both replicate pairs precluded calculating RSDs for these constituents, but their analytical results were acceptable following the criteria described above. Relative standard deviations for nitrate and orthophosphate, also calculated from both replicate pairs, ranged from 0.1 to 1.3 percent. The RSD calculated for DOC, from just one replicate pair, was 12 percent. Relative standard deviations for trace elements were calculated from one replicate pair except for aluminum, iron, and manganese, which were calculated from two replicate pairs, and chromium, which had a censored concentration. The trace elements all had acceptable reproducibility, except for the results from one replicate pair for aluminum, iron, and lead (RSDs of 46, 21, and 34 percent, respectively). The results for aluminum and lead that did not have acceptable reproducibility were calculated from concentrations that were within three times their reporting levels, while the result for aluminum with acceptable reproducibility was calculated from concentrations that were more than 10 times the reporting level. For iron, the result with acceptable reproducibility was calculated from low concentrations, whereas the result with unacceptable reproducibility was calculated from high concentrations.

Table 4. Concentrations of dissolved major ions and silica in water from selected sites, and the charge balance for each analysis, Beaver and Camas Creek drainage basins, eastern Idaho.

[Location of sites are shown in figure 2. Surface-water sites are shown in shaded gray. Concentrations of dissolved major ions and silica (as SiO_2) are in milligrams per liter. **Site No. or quality control (QC) sample:** RSD, relative standard deviation, in percent; R3 and R8 are replicate samples from sites 3 and 8. **Charge balance:** Calculated from major ion concentrations and nitrate in milliequivalents per liter. **Abbreviations**: na, not applicable; nd, not determined; –, not calculated]

Site No. or QC sample	Date sampled	Calcium	Magnesium	Potassium	Sodium	Bicarbonate	Chloride	Fluoride	Sulfate	Silica	Charge balance (percent)
1	08-16-2011	18	3.1	1.7	7.5	65	2.1	2.1	1.5	33	8.3
2	09-24-2008	18	5.1	2.0	5.5	90	1.4	0.4	2.5	41	-0.3
3	08-10-2011	11	2.4	0.9	3.5	60	1.2	0.04	2.2	27	-10.7
R3	08-10-2011	10	2.4	0.9	3.6	nd	1.2	0.04	2.2	28	–
RSD	na	3.0	1.5	2.0	1.0	–	0.7	1.7	0.7	3.6	–
4	07-27-2009	30	5.1	2.2	4.0	104	1.5	0.1	2.4	38	7.9
5	08-15-2011	30	6.6	3.1	5.8	134	2.3	0.27	1.7	39	1.3
8	08-10-2011	24	3.4	4.4	8.9	112	2.8	0.43	11	59	-4.2
R8	08-10-2011	24	3.4	4.4	8.9	nd	2.8	0.42	11	59	–
RSD	na	0.4	0.1	0.2	0.1	–	0.2	1.7	0.5	0.2	–
9	06-08-2011	29	11	2.1	7.2	141	4.6	0.25	2.7	36	3.1
10	08-22-2011	21	6.2	2.0	6.4	102	3.5	0.20	5.4	37	-1.1
11	08-09-2011	23	10	2.1	9.4	139	5.6	0.30	3.2	39	-2.4
12	08-08-2011	28	19	1.1	16	198	4.0	0.08	16	13	-0.9
13	06-22-2007	50	11	1.0	7.4	198	3.6	0.2	7.0	29	2.7
14	08-30-1979	46	12	1.9	8.9	200	6.3	0.2	10	26	0.1
15	08-09-2011	30	10	2.7	11	134	15	0.25	13	34	-1.3
16	08-01-2011	25	8.6	2.4	12	120	7.3	0.29	15	30	-2.6
17	07-12-2011	30	9.5	2.2	12	142	9.6	0.41	6.0	35	0.6
18	08-08-2011	30	8.3	2.4	9.0	137	5.6	0.49	9.3	34	-2.1
19	07-20-2011	62	14	2.9	11	256	6.0	0.32	10	30	0.9
20	08-09-2011	32	9.6	2.9	13	166	9.5	0.41	9.1	34	-3.9
96	08-10-2011	33	7.9	2.1	5.3	158	1.5	0.14	1.7	36	-2.0
97	06-07-1981	20	4.7	1.7	4.1	85	2.0	0.10	1.6	26	3.9
98	09-18-1995	62	15	1.4	8.9	264	5.1	0.17	5.2	17	1.7
99	08-08-2011	19	4.7	2.0	3.6	93	1.0	0.11	1.4	18	-1.4

Table 5. Concentrations of dissolved nutrients and organic carbon in water from selected sites, Beaver and Camas Creek drainage basins, eastern Idaho.

[Location of sites are shown in figure 2. Surface-water sites are shown in shaded gray. **Site No. or quality control (QC) sample:** RSD, relative standard deviation, in percent; R3 and R8 are replicate samples from sites 3 and 8; B1 and B2 are field blanks. **Abbreviations**: A, acceptable result; nd, not determined; na, not analyzed; mg/L, milligrams per liter; <, less than]

Site No. or QC sample	Date sampled	Ammonia (mg/L as nitrogen)	Nitrite (mg/L as nitrogen)	Nitrite plus nitrate (mg/L as nitrogen)	Orthophosphate (mg/L as phosphorus)	Dissolved organic carbon (mg/L)
1	08-16-2011	< 0.01	< 0.001	0.10	0.01	0.31
2	09-24-2008	< 0.02	< 0.002	0.40	0.05	na
3	08-10-2011	< 0.01	< 0.001	0.74	0.08	0.73
R3	08-10-2011	< 0.01	< 0.001	0.74	0.08	na
RSD	na	A	A	0.1	0.6	nd
4	07-27-2009	< 0.02	< 0.002	0.43	0.04	na
5	08-15-2011	0.06	< 0.001	< 0.02	0.07	1.13
8	08-10-2011	< 0.01	< 0.001	0.16	0.07	0.48
R8	08-10-2011	< 0.01	< 0.001	0.15	0.07	0.41
RSD	na	A	A	1.3	0.7	12
9	06-08-2011	< 0.01	< 0.001	0.66	0.03	na
10	08-22-2011	< 0.01	< 0.001	0.50	0.03	na
11	08-09-2011	< 0.01	< 0.001	0.72	0.02	0.38
12	08-08-2011	0.03	< 0.001	< 0.02	0.01	0.40
13	06-22-2007	<0.02	<0.002	0.72	na	na
14	08-30-1979	na	na	0.59	na	na
15	08-09-2011	< 0.01	< 0.001	0.74	0.02	1.07
16	08-01-2011	< 0.01	< 0.001	2.46	0.05	na
17	07-12-2011	0.01	< 0.001	1.09	0.03	na
18	08-08-2011	< 0.01	< 0.001	1.73	0.04	0.82
19	07-20-2011	< 0.01	< 0.001	1.74	0.05	na
20	08-09-2011	< 0.01	< 0.001	0.95	0.03	0.40
96	08-10-2011	< 0.01	< 0.001	0.04	0.05	3.80
97	06-07-1981	na	na	0.05	na	na
98	09-18-1995	0.02	<0.01	0.07	0.02	na
99	08-08-2011	0.02	< 0.001	< 0.02	0.01	3.80
B1	08-10-2011	na	na	na	na	0.25
B2	06-04-2012	na	na	na	na	0.77

Table 6. Concentrations of selected trace elements in water from selected sites, Beaver and Camas Creek drainage basins, eastern Idaho.

[Location of sites are shown in figure 2. Surface-water sites are shown in shaded gray. Concentrations of trace elements are in micrograms per liter. **Site No. or quality control (QC) sample:** RSD, relative standard deviation, in percent; R3 and R8 are replicate samples from sites 3 and 8. **Aluminum:** Concentrations shown in **bold** were estimated with PHREEQC from saturation indices for gibbsite. See section "Solutions" in text for further discussion of this method. **Abbreviations**: A, acceptable reproducibility; E, estimated; na, not analyzed; nd, not determined; <, less than]

Site No. or QC sample	Date sampled	Aluminum	Barium	Boron	Chromium	Iron	Lead	Lithium	Manganese	Strontium	Zinc
1	08-16-2011	82	13	31	0.16	31	0.18	79	3.8	46	436
2	09-24-2008	**34**	na	na	na	<8	na	na	<0.4	na	na
3	08-10-2011	18	10	6.3	1.4	12	0.23	1.3	0.48	46	141
R3	08-10-2011	20	na	na	na	14	na	na	0.56	na	na
RSD	na	7	nd	nd	nd	11	nd	nd	11	nd	nd
4	07-27-2009	**15**	na	na	na	E 3	na	na	0.3	na	na
5	08-15-2011	<1.7, **1.6**	37	9.4	<0.06	90	<.015	24	209	72	2.2
8	08-10-2011	2.2	35	9.9	0.07	71	0.04	12	12	108	83
R8	08-10-2011	4.3	35	10	<0.06	53	0.03	12	12	109	84
RSD	na	46	0.0	0.7	A	21	34	0.0	0.0	1	1
9	06-08-2011	**8**	na	na	na	35	na	na	2.1	na	na
10	08-22-2011	**0.9**	na	na	na	48	na	na	11.1	na	na
11	08-09-2011	3.6	6.5	20	2.4	<3.2	0.22	14	<0.13	75	81
12	08-08-2011	1.8	85	14	0.06	635	0.06	17	27	1,701	5.2
13	06-22-2007	**0.3**	26	na	na	E3.1	na	na	E0.16	na	na
14	08-30-1979	**1.2**	na	na	na	<10	na	na	na	na	na
15	08-09-2011	2.7	26	25	2.5	<3.2	1.2	7	1.6	131	49
16	08-01-2011	**1.1**	na	na	na	<3	na	na	<0.2	na	na
17	07-12-2011	**3.7**	na	na	na	<3	na	na	<0.2	na	na
18	08-08-2011	10	21	19	1.2	5.0	<.015	12	<0.13	100	<1.4
19	07-20-2011	**0.3**	na	na	na	<3	na	na	<0.2	na	na
20	08-09-2011	<1.7, **1.7**	30	21	1.5	3.6	0.03	13	<0.13	127	18
96	08-10-2011	13	72	9.5	0.17	61	0.02	3.7	18	156	<1.4
97	06-07-1981	2	40	na	0	46	na	<4	29	78	na
98	09-18-1995	**9**	200	na	na	10	na	na	10	na	na
99	08-08-2011	14	33	7.6	0.17	31	0.03	2.6	2.3	77	2.3

These results indicate that analytical uncertainties may be nearly 50 and 35 percent for low concentrations of aluminum and lead, respectively, and as much as 20 percent for any concentration of iron.

Normalized absolute differences were calculated from concentrations from one replicate pair for tritium and the stable isotopes of hydrogen, oxygen, and carbon. The NADs ranged from 0.1 for tritium to 1.3 for the stable isotopes of carbon (table 7). These results were less than 1.96 so, at the 95-percent confidence level, the concentrations between the replicate and environmental water samples did not differ significantly.

Two field blank measurements of DOC, 0.25 and 0.77 mg/L (table 5), were available to evaluate the bias in DOC analyses from contamination during sampling, processing, and analysis of environmental water samples. Because only two measurements were available, a *p*-value of 0.60 was used in the binomial probability calculation instead of the more inclusive value of 0.95. Also, the $m+1$ ranked observation equaled the *n*th-ranked observation, or the highest-ranked observation. For these two field blanks ($n=2$), the contamination bias for at least 60 percent of the environmental samples ($p=0.60$) was below the 2nd-ranked ($m+1$ ranked) field blank concentration of 0.77 mg/L with a confidence level (*cl*) of 64 percent.

Table 7. Measurements of the stable isotope ratios of hydrogen, oxygen, carbon, sulfur, and nitrogen and the radiogenic isotope tritium in water from selected sites, Beaver and Camas Creek drainage basins, eastern Idaho.

[Location of sites are shown in figure 2. Surface-water sites are shown in shaded gray. Stable isotope uncertainties are 2σ and tritium uncertainties are 1σ. Sulfur and nitrogen isotopes from 1981 and 2000, respectfully. **Site No. or quality control (QC) sample:** R8 is a replicate sample from site 8; NAD, normalized absolute difference. **Abbreviations**: E, estimated; na, not analyzed; pCi/L, picocuries per liter]

Site No. or QC sample	Date sampled	Stable isotopes, permil					Tritium (pCi/L)
		Hydrogen (δ^2H±2)	Oxygen (δ^{18}O±0.2)	Carbon (δ^{13}C±0.2)	Sulfur (δ^{34}S±0.4)	Nitrogen (δ^{15}N±0.1)	
1	08-16-2011	-138.8	-18.36	-14.71	na	na	4.7±1.9
3	08-10-2011	-131.4	-17.43	-19.10	na	na	42.4±2.4
4	07-27-2009	-135	-18	-12.9	-3.2	na	na
5	08-15-2011	-135.0	-17.66	-15.23	na	na	5.1±1.9
8	08-10-2011	-133.7	-17.75	-14.07	na	na	11.2±2
R8	08-10-2011	-134.5	-17.73	-14.44	na	na	11.4±1.9
NAD	na	0.3	0.07	1.3	na	na	0.1
9	08-30-2000	na	na	na	na	E37.1	na
11	08-09-2011	-133.1	-17.48	-13.02	na	E-1.4	6.5±2
12	08-08-2011	-131.8	-17.48	-10.35	na	na	-0.5±1.9
15	08-09-2011	-131.5	-17.33	-11.21	na	na	-4±2.3
17	07-26-2000	na	na	na	na	E1.59	na
18	08-08-2011	-132.9	-17.62	-13.41	na	E10	13.3±2.1
20	08-09-2011	-134.4	-17.62	-13.21	na	na	8.6±1.9
96	08-10-2011	-130.0	-17.30	-10.33	na	na	25.9±2.2
97	06-07-1981	-127.0	-16.80	-11.2	6.9	na	na
99	08-08-2011	-125.0	-16.24	-7.98	na	na	26.6±2.1

Charge Balance

The charge balance of water samples was determined from concentrations, in milliequivalents per liter (meq/L), of the major ions plus nitrate. The charge balance was calculated as:

$$CB = \frac{\sum_1^i C_i - \sum_1^j C_j}{\sum_1^i C_i + \sum_1^j C_j} \times 100 \quad (3)$$

where

CB is the charge balance for a water sample,
C_i is the concentration of a cation in the water sample,
C_j is the concentration of an anion in the water sample, and
i and j is the number of measured cation and anion species, respectively, in the water sample.

Charge balance errors of 5 percent or less generally are considered acceptable for analyses of water samples (Freeze and Cherry, 1979, p. 97), although larger errors may be acceptable if the sum of ions is less than 5 meq/L (Hem, 1992, p. 164). Of the 22 water samples used in this report, 19 had absolute value charge balance errors ranging from 0.3 to 4.2 percent (table 4). Three water samples had absolute value charge balance errors ranging from 7.9 to 10.7 percent, but the sum of ions for each of these three samples was less than or equal to 4.0 meq/L.

Analytical Results

Mineralogy and Petrology

X-ray diffraction was performed on two bulk sediment samples (S1 and S2), sixteen sediment size fraction samples (subsets of samples S1 and S2), and three rock samples (two rhyolite samples, R1 and R2, and one basalt sample, B1). Thin section analysis was performed on the basalt and rhyolite rock samples.

X-ray diffraction of the bulk sediment and sediment size fractions indicated mineralogical compositions that consisted of silica minerals (quartz, tridymite), plagioclase (albite, anorthite, labradorite), potassium feldspars (orthoclase, sanidine, microcline, anorthoclase), and clays (kaolinite, illite) (table 8). X-ray diffraction of the basalt rock sample indicated a mineralogical composition of plagioclase (albite, anorthite, labradorite), olivine, clinopyroxene, iron oxides (magnetite, hematite), apatite, and glass. X-ray diffraction of the rhyolite rock samples indicated mineralogical compositions that consisted predominantly of a potassium feldspar groundmass, plagioclase (albite, anorthite, labradorite), tridymite, iron oxides (magnetite, ilmenite, hematite), clinopyroxene, smectite, apatite, and trace amounts of goethite, zircon, and biotite.

Basalt rock sample B1 was a porous, relatively unweathered porphyritic basalt with some caliche coating the surface of the sample. Thin section analysis indicated that the basalt contained plagioclase, olivine, clinopyroxene, magnetite, ilmenite, apatite, and volcanic glass. The basalt had a diktytaxitic texture with vesicles found tangential to crystals. Microphenocrysts of plagioclase showed oscillatory zoning and clinopyroxene crystals were found forming around the plagioclase crystals. Some reddish color, from oxidation of iron, was observed on several olivine crystals but no other evidence of alteration was found in the sample.

Rhyolite rock sample R1 was a weathered porphyritic rhyolite with a felty texture that contained phenocrysts of potassium feldspar, plagioclase, tridymite, magnetite, hematite, clinopyroxene, apatite, and zircon. The aphanitic groundmass comprised about 60 percent of the thin section and was predominantly potassium feldspar. Glomerocrysts of plagioclase were found, with complex and oscillatory zoning and alteration to smectite and a smectitic texture in the interior of numerous grains. Pyroxene pseudomorphs were observed, with clinopyroxenes mostly removed and heavily altered to goethite and smectite. Magnetite grains showed reddish staining along the outside of the grains. Tridymite was found in vesicles and showed characteristics of deposition from the vapor phase.

Rhyolite rock sample R2 was a slightly weathered porphyritic rhyolite with a low porosity, felty texture, and evidence for flow-banding. The rhyolite contained phenocrysts of potassium feldspar, plagioclase, tridymite, magnetite, ilmenite, hematite, clinopyroxene, apatite, and biotite. The aphanitic groundmass comprised about 50 percent of the thin section and was predominantly potassium feldspar. Glomerocrysts of plagioclase were found with corroded cores consisting of smectite. Clinopyroxene grains were found stuck on magnetite grains and as individual anhedral grains and glomerocrysts of differing sizes. Biotite grains were not found in the matrix, showed no evidence of alteration, and were found near magnetite grains. Magnetite and ilmenite grains were slightly ragged, and the matrix contained a brownish discoloration around these minerals. Apatite was found as long blades. Tridymite was found in vesicles and showed characteristics of deposition from the vapor phase.

Table 8. Site number, location, rock type, mineralogy, and percent abundance of minerals in rock samples, Beaver and Camas Creek drainage basins, eastern Idaho.

[Samples were collected on October 17, 2010. Location of sites are shown in figure 5. Latitude and longitude are shown in degrees (dd), minutes (mm), and seconds (ss). **Mineralogy:** Sediment mineralogy in table combines minreralogy of bulk sediment and sediment size fractions. **Abbreviations**: nd, not determined; tr, trace]

Site No.	Latitude (ddmmss)	Longitude (ddmmss)	Rock type	Mineralogy	Percent abundance
S1	441720	1115338	Sediment	Quartz, albite, anorthite, labradorite, orthoclase, sanidine, microcline, anorthoclase, kaolinite, illite	nd
S2	442407	1115513	Sediment	Quartz, tridymite, albite, anorthite, labradorite, orthoclase, sanidine, microcline, kaolinite	nd
B1	441721	1115340	Basalt	Plagioclase (albite, anorthite, labradorite)	38
				Olivine	35
				Clinopyroxene	15
				Iron oxides (magnetite, ilmenite)	10
				Apatite	2
				Glass	tr
R1	442516	1115658	Rhyolite	Groundmass (predominantly potassium feldspar)	60
				Plagioclase (albite, anorthite)	14
				Tridymite	9
				Iron oxides (magnetite, hematite)	9
				Clinopyroxene	5
				Smectite	3
				Goethite	tr
				Apatite	tr
				Zircon	tr
R2	442840	1120240	Rhyolite	Groundmass (predominantly potassium feldspar)	50
				Plagioclase (albite, anorthite, labradorite)	25
				Tridymite	12
				Iron oxides (magnetite, ilmenite, hematite)	5
				Clinopyroxene	4
				Smectite	2
				Apatite	2
				Biotite	tr

Water Chemistry

Water chemistry analyses are presented in tables 3–7. Table 3 shows measurements of field parameters; calculations for the partial pressure of carbon dioxide (as log PCO_2); and the percent saturation of oxygen with respect to the atmospheric concentration of oxygen at the sample temperature of the water-quality samples. Concentrations of major ions, silica, and the calculated charge balance for each water-quality sample are shown in table 4. Concentrations of nutrients, DOC, and selected trace elements are shown in tables 5 and 6. Measurements of tritium and the stable isotope ratios of δ^2H, $\delta^{18}O$, $\delta^{13}C$, $\delta^{34}S$, and $\delta^{15}N$ are shown in table 7. The measurements of the stable isotope ratios of nitrogen all have an "E" remark, which means these results were estimated and have a greater uncertainty than data without the "E" remark.

Analytical results from sites 6 and 7 were not used in interpretations of the geochemistry of groundwater in the study area or in geochemical modeling. These results were excluded from tables 3–7, but are shown in tables B1–B5 (in appendix B). Dissolved gases were collected and analyzed from several pumped groundwater samples, but were not used in interpretations of the geochemistry of groundwater in the study area. Analytical results for dissolved gases are presented in table C1 (in appendix C).

Geochemistry of Groundwater

The geochemistry of groundwater in the Beaver and Camas Creek drainage basins is characterized by the distribution of dissolved gases, solutes, and isotopes in the aquifer. The distribution of dissolved gases and solutes is controlled by sources and sinks of these constituents that are a function of the geology, mineralogy, land cover and use, and hydrology in the basins. The distribution of isotopes in the aquifer reflects the source of the isotopes and any isotope fractionation processes that may have occurred in the unsaturated zone and aquifer. Sources of dissolved gases, solutes, and isotopes are unsaturated zone gases, source waters, anthropogenic inputs, and chemical reactions between gaseous, aqueous, and solid phases in the aquifer. These sources are the physical (mixing, evaporation) and chemical (carbonate reactions, silicate weathering, etc.) processes that control the geochemistry of the groundwater. After evaluating the distribution of chemical species in the aquifer, and their potential sources, geochemical inverse (mass balance) modeling was performed to identify which physical and chemical processes were most important in controlling the geochemistry of the groundwater.

Distribution of Chemical Species

Field Parameters

The pH ranged from 7.1 to 8.6 pH units in surface water, and 6.9 to 8.3 pH units in groundwater (table 3); specific conductance ranged from 147 to 437 µS/cm at 25 °C in surface water, and 70 to 431 µS/cm at 25 °C in groundwater (table 3). Larger pH and specific conductance values were measured in groundwater from the Beaverhead Mountains and the ESRP, and smaller values were measured in groundwater from the Centennial Mountains. Values for pH and specific conductance in groundwater were relatively uniform between the Beaverhead Mountains and Dubois and generally increased between the Centennial Mountains and Mud Lake, although a small pH (7.0) and the largest specific conductance in groundwater was measured at site 19 in the southern end of wetlands in the CNWR. Alkalinity ranged from 70 to 223 mg/L as $CaCO_3$ in surface water and from 49 to 210 mg/L as $CaCO_3$ in groundwater. The smallest alkalinity measurements in groundwater (49–92 mg/L as $CaCO_3$) were from water in or near the Centennial Mountains, and alkalinity generally increased with distance downgradient from the Centennial Mountains. Relatively large alkalinity (160–162 mg/L as $CaCO_3$) was measured in groundwater from, or immediately downgradient of, the Beaverhead Mountains (sites 12, 13, 14), and the largest alkalinity was measured at site 19 in the CNWR . Water temperatures ranged from 11.0 to 19.3 °C in surface water and 6.9 to 15.6 °C in groundwater. Groundwater temperatures generally increased in a downgradient direction except where potentially influenced by streamflow infiltration (sites 4, 16, 18, and 19).

Dissolved Gases

Oxygen

The percent saturation of DO (table 3) in water was calculated with DOTABLES (U.S. Geological Survey, 2013b) by using measured DO concentrations, water temperatures, and specific conductivities and an estimate of barometric pressure (estimated from land-surface altitude for each site). DO in surface water ranged from 76 to 98 percent saturation (table 3). DO in groundwater ranged from anoxic (1–2 percent saturation) in the Beaverhead Mountains (site 12) and Camas Meadows (site 5) to supersaturated (137 percent saturation) in the Centennial Mountains (site 3). Other groundwater from the mountains (sites 1 and 8) was significantly undersaturated (24–64 percent saturation). Most groundwater in the ESRP ranged from slightly undersaturated to slightly supersaturated (84–118 percent saturation), although undersaturated (25–54 percent saturation) groundwater was present at Spencer (site 13) and south of the CNWR (sites 19 and 20).

Carbon Dioxide

The partial pressure of CO_2 was calculated for surface-water and groundwater samples using the concentrations of dissolved CO_2 calculated by PHREEQC, temperature-dependent equilibrium constants for CO_2 tabulated by Plummer and Busenberg (1982, p. 1,014), and the equation for calculating the equilibrium constant for CO_2:

$$K_{CO_2} = \frac{[H_2CO_3]}{P_{CO_2}[H_2O]} \quad (4)$$

where

K_{CO_2} is the equilibrium constant for CO_2,
$[H_2CO_3]$ is the activity of dissolved CO_2 in the water,
P_{CO_2} is the partial pressure of CO_2 in the water, and
$[H_2O]$ is the activity of water, assumed to be one for the dilute water from the study area.

The partial pressure of CO_2 was converted into base-10 logarithmic form (table 3), where log PCO_2 values larger than -3.5 indicate supersaturation with the atmosphere and values smaller than -3.5 indicate undersaturation with respect to the atmosphere. The partial pressure of CO_2 ranged from -3.29 to -1.96 in surface water and -3.25 to -1.68 in groundwater (table 3). The partial pressure of CO_2 in groundwater generally was large (-2.61 to -1.93) in or near the mountains (sites 1, 3, 8, 12, 13), was smaller (-3.08 to -2.88) in Camas Meadows (sites 4 and 5), and generally decreased in the ESRP with distance downgradient from the mountains (except at sites 2, 16 and 19).

Major Elements

Cations and Silica

Concentrations of calcium ranged from 19 to 62 mg/L in surface water, and from 11 to 62 mg/L in groundwater [table 4 and fig. 11, cation and silica concentrations in the figure are in millimoles per liter (mmol/L)]. The smallest calcium concentration in groundwater was from the Centennial Mountains (site 3), and concentrations generally increased in a downgradient direction from the Centennial Mountains until reaching a concentration of about 30 mg/L (site 9). At about this concentration of calcium, calcite was frequently at or near equilibrium with groundwater from the ESRP. The largest calcium concentrations in groundwater were from groundwater south of the Beaverhead Mountains (sites 13 and 14) and the CNWR (site 19). Magnesium concentrations ranged from 4.7 to 15 mg/L in surface water, and from 2.4 to 19 mg/L in groundwater; sodium concentrations ranged from 3.6 to 8.9 mg/L in surface water, and from 3.5 to 16 mg/L in groundwater. Concentrations of magnesium and sodium in groundwater generally increased in a downgradient direction from the Centennial Mountains, with the smallest concentrations from the Centennial Mountains (site 3). The largest magnesium and sodium concentrations in groundwater were from the Beaverhead Mountains (site 12). Concentrations of potassium ranged from 1.4 to 2.1 mg/L in surface water and from 0.9 to 4.4 mg/L in groundwater. The smallest and largest potassium concentrations in groundwater were from the Centennial Mountains (sites 3 and 8). Silica concentrations ranged from 17 to 36 mg/L in surface water and from 13 to 59 mg/L in groundwater. The smallest silica concentration in groundwater was from the Beaverhead Mountains (site 12) and largest concentration was from the Centennial Mountains (site 8, downgradient of rhyolite bedrock).

Anions

Bicarbonate concentrations ranged from 85 to 264 mg/L as $CaCO_3$ in surface water and from 65 to 256 mg/L as $CaCO_3$ in groundwater (table 4). Bicarbonate concentrations in groundwater were smallest in the Centennial Mountains (sites 1 and 3) and largest in the Beaverhead Mountains (sites 12 and 13) and the CNWR (site 19). Concentrations of chloride ranged from 1.0 to 5.1 mg/L in surface water and from 1.2 to 15 mg/L in groundwater; sulfate concentrations ranged from 1.5 to 5.2 mg/L in surface water and 1.5 to 16 mg/L in groundwater. Chloride and sulfate concentrations in groundwater generally increased in the downgradient direction with noticeably larger concentrations near and south of Dubois than elsewhere in the study area (fig. 12, anion concentrations in mmol/L). Exceptions to the increasing concentration trend in the downgradient direction were the large chloride concentration in groundwater north of Dubois (site 15), the large sulfate concentration in groundwater in the Beaverhead Mountains (site 12), and a decrease in sulfate concentration between sites 4 and 5 in Camas Meadows. Fluoride concentrations ranged from 0.10 to 0.17 mg/L in surface water and from 0.04 to 2.1 mg/L in groundwater. The smallest fluoride concentration in groundwater was from the Centennial Mountains (site 3), and the largest concentration in groundwater was from the rhyolite outcrop comprising Sheridan Ridge (site 1).

Hydrochemical Facies

Groundwater in the study area was classified into hydrochemical facies based on the relative concentrations (in milliequivalents per liter) of specific cations (calcium, magnesium, sodium, potassium) and anions (bicarbonate, carbonate, chloride, sulfate). For example, the calcium bicarbonate hydrochemical facies is defined by water in which calcium makes up greater than 50 percent of the total cations and bicarbonate makes up greater than 50 percent of the total anions (Knobel and others, 1998, p. 10). When a single cation or anion does not make up greater than 50 percent of the total cations or anions, the cations or anions are listed in order of decreasing concentration. For example, water would be designated a magnesium-calcium bicarbonate type water if magnesium made up 45 percent of the cations, calcium made up 40 percent of the cations, and bicarbonate made up more than 50 percent of the anions.

Hydrochemical facies of surface waters and groundwaters in the study area were interpreted from trilinear diagrams (fig. 13) (Drever, 1997, p. 409–411). All surface water in the study area and groundwater from the Centennial Mountains and Camas Meadows were calcium bicarbonate type water. All groundwater from the ESRP was calcium bicarbonate type water except for groundwater from two sites (sites 11 and 16) that were a calcium-magnesium bicarbonate type water. The groundwater sample (site 12) from the Beaverhead Mountains was a magnesium-calcium bicarbonate type water.

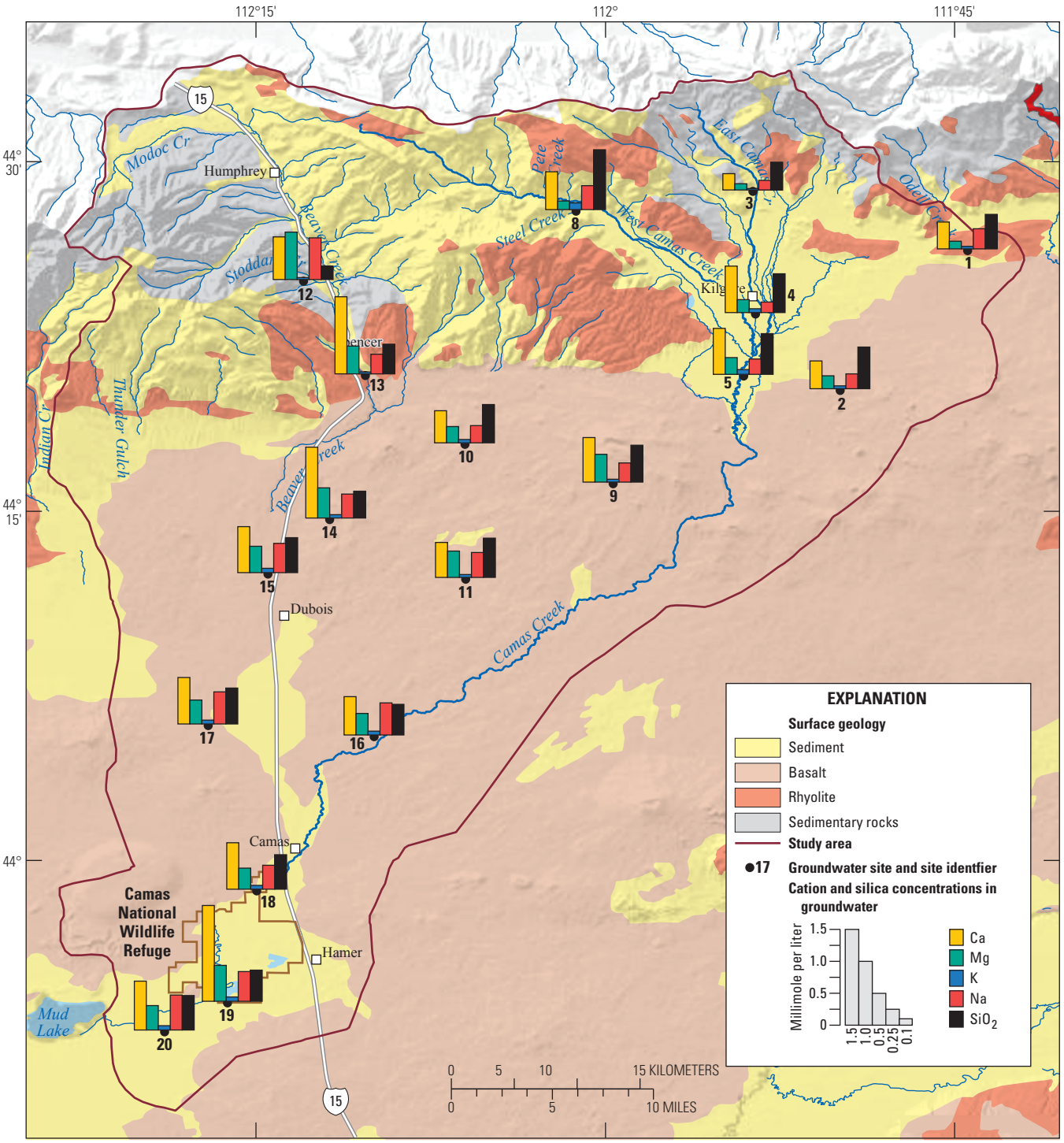

Base from U.S. Geological Survey digital data, 1:24,000 and 1:100,000. Coordinate system and datum: NAD 1927 (definition 1976).

Figure 11. Concentrations of cations and silica in groundwater and surface geology of the study area, Beaver and Camas Creek drainage basins, eastern Idaho.

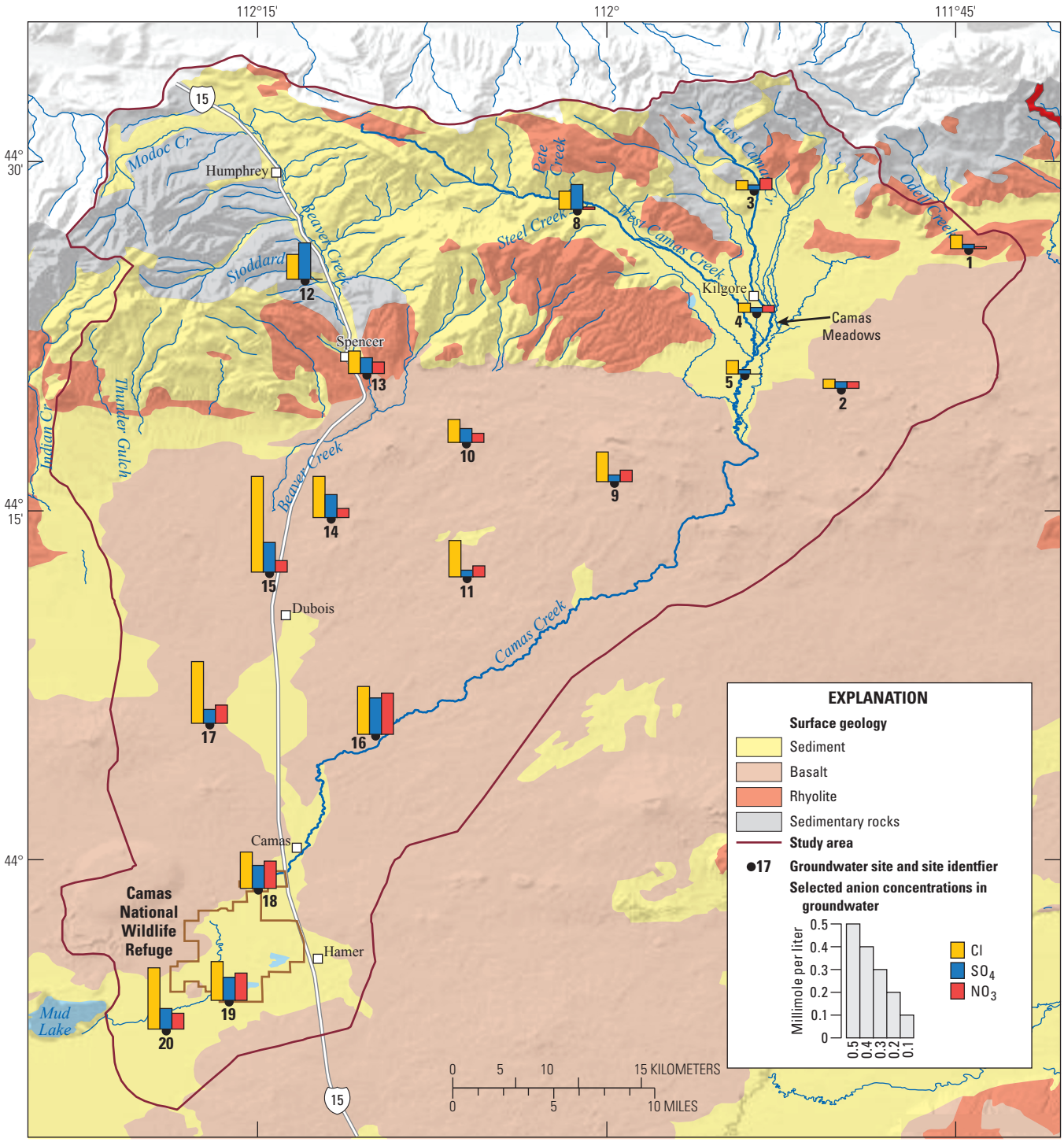

Base from U.S. Geological Survey digital data, 1:24,000 and 1:100,000. Coordinate system and datum: NAD 1927 (definition 1976).

Figure 12. Concentrations of selected anions in groundwater and surface geology of the study area, Beaver and Camas Creek drainage basins, eastern Idaho.

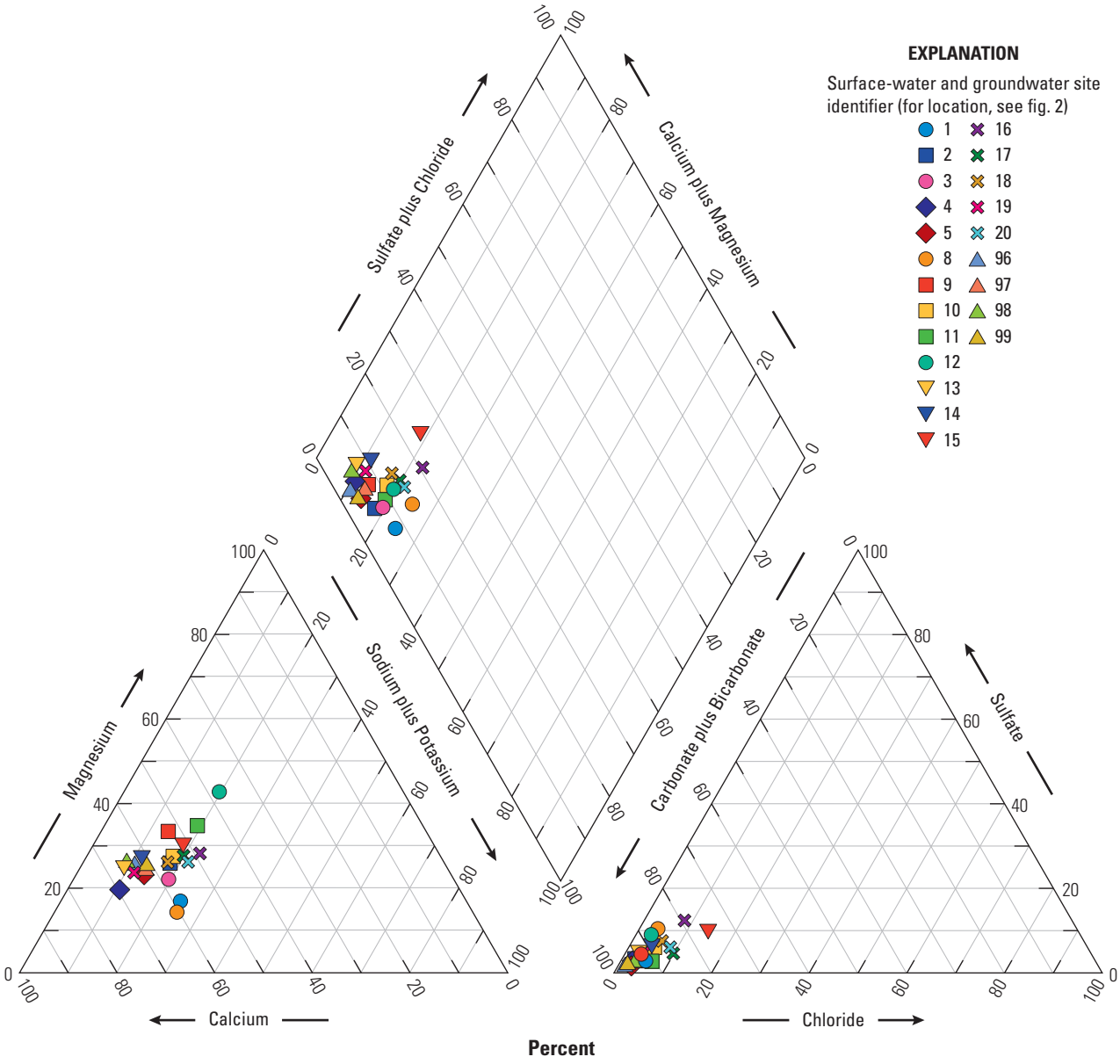

Figure 13. Major-ion composition of water from surface-water and groundwater sites, Beaver and Camas Creek drainage basins, eastern Idaho.

Nutrients

Concentrations of nitrate + nitrite (hereafter referred to as nitrate), nitrite, ammonia, and orthophosphate in surface water were all less than or equal to 0.07 mg/L (as N for nitrogen species and as P for orthophosphate). Nitrite and orthophosphate concentrations in groundwater were all less than 0.002 mg/L as N for nitrite and less than or equal to 0.08 mg/L as P for orthophosphate. Ammonia concentrations in groundwater were all less than 0.02 mg/L as N except for detectable concentrations that ranged from 0.01 to 0.06 mg/L as N at sites 5, 12, and 17. Concentrations of nitrate in groundwater ranged from less than 0.02 to 2.46 mg/L as N (table 5), with the largest nitrate concentrations in groundwater in irrigated areas south of Dubois (fig. 12). Nitrate concentrations generally increased in a downgradient direction, although decreasing concentrations in the downgradient direction were observed in Camas Meadows (where nitrate concentrations decreased to undetectable levels between sites 4 and 5) and south of Dubois (nitrate concentrations decreased between sites 16 and 18 and sites 19 and 20).

Dissolved Organic Carbon

Concentrations of DOC were potentially affected by sample contamination, as shown by the evaluation of blank samples. Two surface-water samples, collected from West Camas Creek (northwest of Kilgore, fig. 2) in the headwaters of the study area, and from Camas Creek at the CNWR, had DOC concentrations of 3.80 mg/L. Nine groundwater samples had concentrations that ranged from 0.31 to 1.13 mg/L. All of these DOC concentrations fall within typical ranges for streams and groundwater (Drever, 1997, p. 118).

Trace Elements

Concentrations of dissolved trace elements (table 6) in surface water were all less than or equal to 14 µg/L except for barium (33–200 µg/L), iron (10–61 µg/L), manganese (2.3–29 µg/L), and strontium (77–156 µg/L). Concentrations in groundwater ranged from less than 1.7 to 82 µg/L for aluminum, 6.5 to 85 µg/L for barium, 6.3 to 21 µg/L for boron, less than 0.06 to 2.5 µg/L for chromium, less than 3 to 635 µg/L for iron, less than 0.015 to 1.2 µg/L for lead, 1.3 to 79 µg/L for lithium, less than 0.13 to 209 µg/L for manganese, 46 to 1,701 µg/L for strontium, and less than 1.4 to 436 µg/L for zinc. The largest aluminum, boron, lithium, and zinc concentrations were all from groundwater from site 1, located in rhyolite comprising Sheridan Ridge, and the largest barium, iron, and strontium concentrations were all from site 12, located in carbonate rocks in the Beaverhead Mountains. Boron concentrations were 2 to 4 times larger in groundwater from the ESRP than from the Centennial Mountains or Camas Meadows. Lithium concentrations on the ESRP were relatively uniform, with concentrations ranging from 7 to 14 µg/L. Iron and manganese concentrations increased between sites 4 and 5 in Camas Meadows, with iron increasing from an estimated value of 3 to 90 µg/L and manganese increasing from 0.3 to 209 µg/L.

Tritium

Tritium was measured from two surface-water and nine groundwater samples. Tritium concentrations in surface water were 25.9±2.2 and 26.6±2.1 (table 7). These surface-water samples were collected in August 2011, a time of year when the stream is typically at baseflow (fig. 7). Consequently, the tritium concentrations in surface water were probably representative of recent (within the past few years) precipitation and groundwater recharge. Tritium concentrations in groundwater ranged from -4±2.3 to 42.4±2.4 pCi/L (table 7). The smallest tritium concentrations in groundwater were from or immediately downgradient of the Beaverhead Mountains (sites 12 and 15), and the largest concentration was from the Centennial Mountains (site 3) (table 7). No clear pattern of increasing or decreasing tritium concentrations with distance downgradient from the mountains was apparent for groundwater samples from the ESRP.

Stable Isotopes

Hydrogen and Oxygen

The stable isotope ratios of hydrogen (δ^2H) and oxygen ($\delta^{18}O$) were measured from 3 surface-water and 10 groundwater sites (table 7). The stable isotope ratios of hydrogen had δ^2H values that ranged from -130.0 to -125.0 permil for surface water and -138.8 to -131.4 permil for groundwater, and the stable isotope ratios of oxygen had $\delta^{18}O$ values that ranged from -17.30 to -16.24 permil for surface water and -18.36 to -17.33 permil for groundwater. All isotopic ratios from surface-water samples were heavier (less negative) than the isotopic ratios of the groundwater samples. The lightest (most negative) isotopic ratios were measured from groundwater samples from Sheridan Ridge (site 1) and Kilgore (site 4). All other isotopic ratios from groundwater samples are intermediate between the heavy isotopic ratios from surface water and the light isotopic ratios for groundwater from Sheridan Ridge and Kilgore. No clear pattern of increasing or decreasing isotopic ratios was apparent between upland mountain sites and downgradient sites on the ESRP.

Carbon

The stable isotope ratio of carbon ($\delta^{13}C$) was measured from 3 surface-water and 10 groundwater sites (table 7). The stable isotope ratios of carbon in the study area had $\delta^{13}C$ values that ranged from -11.2 to -7.98 permil in surface water and -19.10 to -10.35 permil in groundwater. Two of the isotopic ratios from surface water (sites 96 and 99) had heavier isotopic ratios (-10.33 and -7.98) than any of the isotopic ratios from groundwater. The lightest isotopic ratio in groundwater was from the Beaverhead Mountains (site 12) and the heaviest was from the Centennial Mountains (site 3). The isotopic ratio in groundwater downgradient of the Centennial Mountains generally decreased with distance from the mountains except for site 4 in Camas Meadows and site 18 in the CNWR.

Sulfur

The stable isotope ratio of sulfur ($\delta^{34}S$) was measured from one surface-water (site 97) and one groundwater (site 4) site (table 7). At site 4, at Kilgore in Camas Meadows, a $\delta^{34}S$ value of -3.2 permil was measured from groundwater. At site 97, just south of Camas Meadows, a $\delta^{34}S$ value of 6.9 permil was measured from Camas Creek.

Nitrogen

The stable isotope ratio of nitrogen ($\delta^{15}N$) was measured from four groundwater sites (sites 9, 11, 17, and 18) (table 7). At site 9, southwest of Camas Meadows, the $\delta^{15}N$ value was estimated to be 37.1 permil (table 7). Sites 11 and 17, both on the ESRP, had estimated $\delta^{15}N$ values of -1.4 and 1.59 permil, respectively. Site 18, at the CNWR, had an estimated $\delta^{15}N$ value of 10 permil.

Interpretation of Isotopic Data

Tritium

Large quantities of tritium, the radioactive isotope of hydrogen, were introduced into the atmosphere by thermonuclear bomb testing in the 1950s and 1960s (Solomon and Cook, 2000, p. 397). Because tritium is readily incorporated into water molecules in the atmosphere and is rapidly removed from the atmosphere in meteoric precipitation, the large peak and subsequent radioactive decay of tritium concentrations in the atmosphere make tritium a useful tracer for determining the age of water. Because the half-life of tritium is just 12.34 years, tritium is at present most useful for qualitatively estimating the residence time of water as older or younger than the year (1952) when thermonuclear bomb testing in the atmosphere began.

The qualitative residence times of groundwater samples were estimated from guidelines for interpreting tritium values presented by Mazor (1991). The guidelines were adjusted for radioactive decay of tritium in groundwater during the period when the guidelines were published (1991) and the time when the water samples were collected (2011). The adjusted guidelines suggest that water with tritium concentrations less than 0.5 pCi/L represents pre-1952 (pre-thermonuclear bomb testing in the atmosphere) water, greater than 11 pCi/L represents mostly post-1952 (post-thermonuclear bomb testing) water, and from 0.5 to 11 pCi/L probably represents a mixture of pre- and post-1952 water.

Based on the adjusted guidelines for interpreting tritium results, groundwater from sites 12 and 15, both with measured tritium concentrations less than 0 pCi/L and consisting of water that originated in the Beaverhead Mountains, are pre-1952 water. One groundwater sample from the Centennial Mountains, site 3, has a large tritium concentration of 42.2 ± 2.4 pCi/L and is post-1952 water that includes some water recharged during the 1960s, the period when tritium from thermonuclear testing in the atmosphere reached peak concentrations. Another groundwater sample from the Centennial Mountains, site 8, has a tritium concentration of 11.2 ± 2 pCi/L and may be mostly post-1952 water. The other five groundwater samples with tritium measurements are from Sheridan Ridge or the ESRP. Four of these samples (sites 1, 5, 11, and 20) have tritium concentrations that indicate the water is a mixture of pre- and post-1952 water. The other sample, site 18, has a tritium concentration of 13.3 ± 2.1 pCi/L, and is probably a mixture of pre-1952 water and recent recharge from streamflow infiltration.

Stable Isotopes

Hydrogen and Oxygen

The stable isotopes of hydrogen and oxygen in precipitation reflect the origin of the airmass and the conditions under which precipitation occurs (Benjamin and others, 2004, p. 1). For example, the $\delta^{2}H$ and $\delta^{18}O$ values in precipitation become progressively lighter as temperature decreases, and the temperature of precipitation is affected by changes in altitude, latitude, or seasons. In the Beaver and Camas Creek drainage basin, the change in latitude across the study area is not large enough to effect a change in temperature. However, colder temperatures and relatively lighter $\delta^{2}H$ and $\delta^{18}O$ values are expected at higher altitudes and during winter, as opposed to summer, precipitation.

Local, seasonal meteoric water lines were developed for the region encompassing the Beaver and Camas Creek drainage basins by Benjamin and others (2004). The winter and summer local meteoric water lines, along with selected

data points used to generate these lines, and the δ^2H and $\delta^{18}O$ values from surface-water and groundwater samples in the study area are shown in figure 14. Within analytical uncertainty limits, all δ^2H and $\delta^{18}O$ values from surface-water and groundwater samples plot on or near local winter or summer meteoric water lines. The surface-water and groundwater data plot parallel to the meteoric water lines, which indicates that the water in the study area is of meteoric origin. The δ^2H and $\delta^{18}O$ values of groundwater are all isotopically lighter than summer precipitation data and plot on or near the winter precipitation trend line, which indicates that most recharge in the study area is from winter precipitation. Recharge from summer precipitation is probably small due to low rainfall amounts along with high air temperatures (table 1) that produce high rates of evapotranspiration (Stearns and others, 1939, p. 68–69). Consequently, most groundwater recharge probably occurs in the spring when snow melts and streams are at their highest flows (fig. 7).

The δ^2H and $\delta^{18}O$ values from Camas Creek were heavier than any of the δ^2H and $\delta^{18}O$ values from groundwater samples. These heavy values plot near the summer precipitation trend line and, because these samples were collected in June and August, the heavy values may represent groundwater with a component of summer precipitation or evaporated stream water. For example, the heaviest δ^2H (-125 permil) and $\delta^{18}O$ (-16.24 permil) values were from site 99, Camas Creek at the CNWR. This data point plots to the right of the summer precipitation trend line in figure 14, which indicates that this water may have undergone evaporation. This water was collected in August 2011, after it had flowed approximately 40 mi across the ESRP during the hottest part of summer, so the water would be expected to have undergone some evaporation.

The δ^2H (-138.8 permil) and $\delta^{18}O$ (-18.36 permil) values for water from Sheridan Ridge (site 1) are lighter than the δ^2H and $\delta^{18}O$ values of all the other water samples. It is not apparent from the altitude of site 1 that recharge to this site would be from a higher altitude than recharge to other mountain sites in the study area. However, the thick unsaturated zone and confined aquifer at site 1 (table 2 and fig. 8) may inhibit infiltration of summer precipitation at site 1 and may cause the source of recharge at site 1 to be from an altitude that is much higher than site 1.

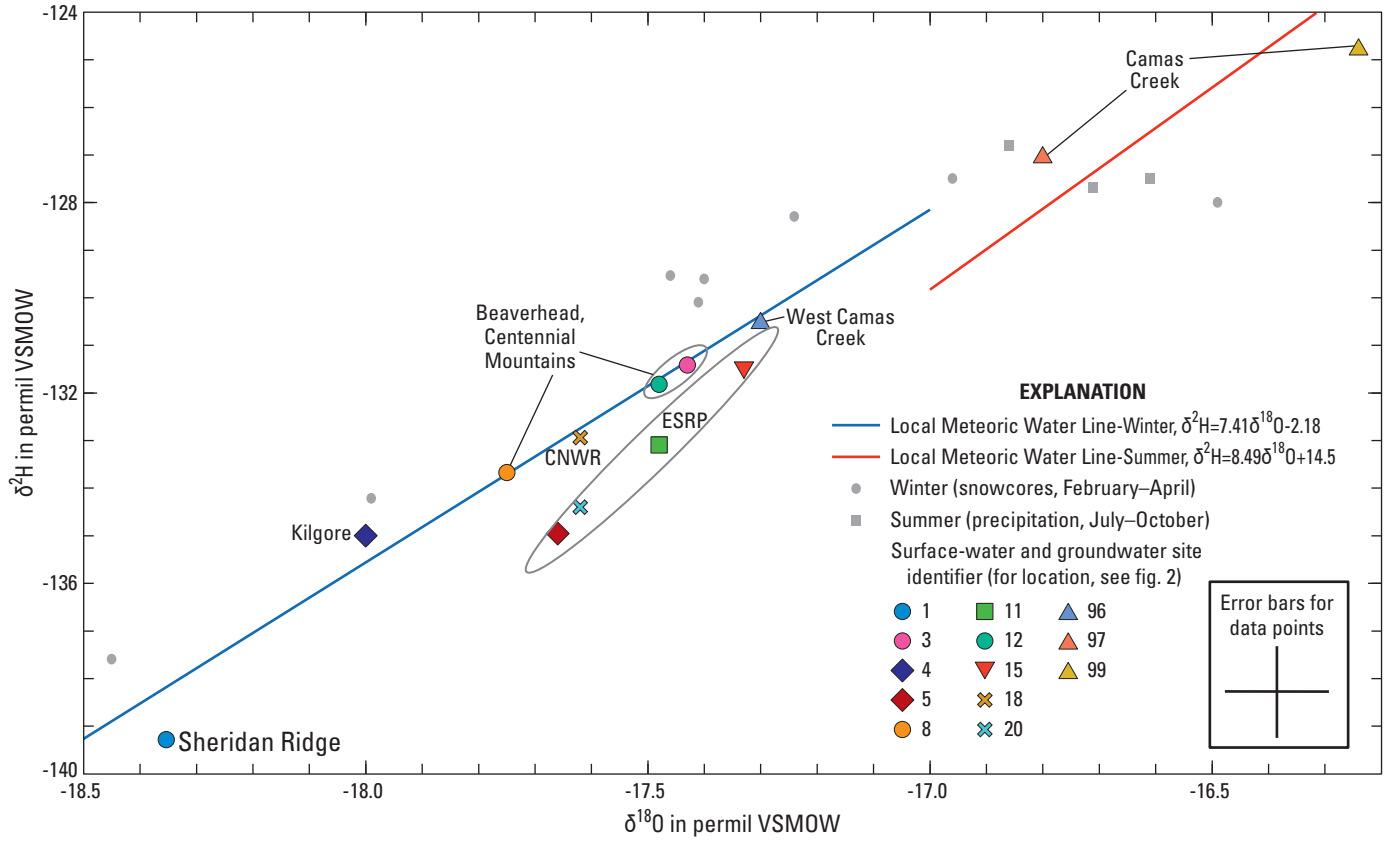

Figure 14. Stable isotope ratios of hydrogen and oxygen and local seasonal meteoric water lines, Beaver and Camas Creek drainage basins, eastern Idaho. δ^2H, delta notation for stable hydrogen isotopes; $\delta^{18}O$, delta notation for stable oxygen isotopes; VSMOW, Vienna Standard Mean Ocean Water. The summer and winter stable isotope data are from Benjamin and others (2004). CNWR, Camas National Wildlife Refuge; ESRP, eastern Snake River Plain.

The δ^2H (-135 permil) and $\delta^{18}O$ (-18 permil) values from water at Kilgore (site 4) are lighter than all other water samples except for water from site 1 (fig. 14) (note that the oxygen isotope ratio from site 4 was only reported to the nearest integer, so the uncertainty for the $\delta^{18}O$ measurement is ±0.5 permil instead of ±0.2 permil for the other $\delta^{18}O$ measurements). These light values may indicate that the source(s) of recharge to site 1 also may provide recharge to site 4.

The δ^2H and $\delta^{18}O$ values from groundwater collected from the ESRP (except for site 18) plot slightly to the right of the winter precipitation trend line. These slightly heavier δ^2H and $\delta^{18}O$ values may result from greater amounts of infiltration recharge from summer precipitation or, at sites 5 and 20, from infiltration of evaporated surface water from Camas Creek or from nearby wetlands. Site 18, at the CNWR, has a shallow depth to water (about 16 ft) and is located near Camas Creek; consequently, the δ^2H and $\delta^{18}O$ values from this site, relative to the δ^2H and $\delta^{18}O$ values from other ESRP groundwater, may result from infiltration of cold spring runoff from Camas Creek. An unusually cold, wet spring extended into June in 2011, and this cold, wet spring may have allowed a large amount of cold surface water to recharge at site 18 during the spring of 2011.

Carbon

The stable isotopes of carbon in groundwater are initially influenced by recharge moving through the soil and unsaturated zones in the mountains. This recharge is influenced by the decay of organic matter, which has typical $\delta^{13}C$ values of soil CO_2 (of C3-type plants typical in temperate, high-latitude regions) estimated to range from about -24 to -30 permil (Clark and Fritz, 1997, p. 119), although Wood and Low (1988, p. 22) estimated that $\delta^{13}C$ values of soil CO_2 in upland tributary basins to the INL were about -22 permil. On the ESRP at the INL, Wood and Low (1988, p. 21) noted that the $\delta^{13}C$ values of CO_2 in soil gas averaged -14 permil and Conrad and DePaolo (2004, p. 145) measured background (uncontaminated) $\delta^{13}C$ values from the shallow (30 to 230 ft depth) unsaturated zone and determined an average $\delta^{13}C$ value for soil CO_2 of -18.2 permil. As CO_2 dissolves in groundwater, fractionation of the carbon isotopes produces a $\delta^{13}C$ value for bicarbonate that is enriched (heavier or less negative) by about 9 permil relative to the soil CO_2 (Clark and Fritz, 1997, p. 120). Marine carbonate rocks typically have $\delta^{13}C$ values near zero, so as water enters and moves through the unsaturated and saturated zones, carbonate rocks may dissolve, and $\delta^{13}C$ values in groundwater may become heavier. Organic matter in the study area was assumed to have $\delta^{13}C$ values ranging from -24 to -30 permil (Clark and Fritz, 1997, p. 119), so decay of organic matter in the saturated zone generally will result in lighter $\delta^{13}C$ values in groundwater.

The lightest $\delta^{13}C$ value in groundwater (-19.10 permil) was from site 3 in the Centennial Mountains and may indicate that groundwater recharging site 3 exchanged CO_2 with the soil zone, and the low alkalinity, 49 mg/L as $CaCO_3$, indicates little dissolution of carbonate minerals has taken place. The heaviest $\delta^{13}C$ value (-10.35 permil) was from site 12 in the Beaverhead Mountains, and indicates reaction of water with carbonate minerals. Other $\delta^{13}C$ values from the Centennial Mountains and Sheridan Ridge were -14.07 permil (site 8) and -14.71 permil (site 1), respectively. These $\delta^{13}C$ values probably indicate groundwater that has had a small amount of reaction with carbonate minerals, which is supported by their low alkalinity concentrations. In Camas Meadows, $\delta^{13}C$ values became heavier between sites 3 and 4, due to dissolution of carbonate minerals, and became lighter between sites 4 and 5 due to decay of organic matter. On the ESRP, $\delta^{13}C$ values in groundwater became heavier with distance downgradient from Camas Meadows and Sheridan Ridge until reaching the CNWR, indicating that carbonate minerals dissolved in groundwater throughout most of the ESRP. At sites 18 and 20, in the vicinity of the CNWR, lighter $\delta^{13}C$ values were observed in groundwater. These lighter $\delta^{13}C$ values may be from (1) exchange of CO_2 gas with the soil or unsaturated zone as surface-water recharge percolates downward and (2) CO_2 from aerobic decay of organic matter associated with wetlands at the CNWR.

Sulfur

The stable isotopes of sulfur can be used to determine whether sulfate in water was derived from dissolution of calcium sulfate (anhydrite, gypsum) or iron sulfide (pyrite) minerals. Typical ranges of $\delta^{34}S$ values for these minerals are 10 to 20 permil for anhydrite or gypsum and -20 to 0 permil for pyrite (Clark and Fritz, 1997, p. 139). The stable isotopes of sulfur from the Snake and Boise Rivers, at locations where they drain Permian sulfate deposits and pyritized granite, respectively, had $\delta^{34}S$ values of 14.9 and -6.6 permil (Wood and Low, 1988, p. 22). Based on the typical ranges of $\delta^{34}S$ values for anhydrite, gypsum, and pyrite, sulfate in groundwater at Kilgore (site 4, $\delta^{34}S$ value of -3.2 permil) was primarily from dissolution of pyrite and sulfate in surface water downstream of Kilgore (site 97, $\delta^{34}S$ value of 6.9 permil) was primarily from dissolution of anhydrite or gypsum.

Nitrogen

The stable isotopes of nitrogen were used to determine whether nitrogen (as nitrate) in groundwater was derived from inorganic fertilizer, manure, septic systems, or had undergone denitrification. Ranges typical of $\delta^{15}N$ values for these inputs are -5 to 5 permil for inorganic fertilizer and 10 to 20 permil for manure or septic systems (Clark and Fritz,

1997, p. 148–154). The $\delta^{15}N$ value for the residual fraction of nitrate that has undergone denitrification (the nitrate remaining after N_2 gas produced from denitrification leaves the system) increases as the residual fraction of nitrate decreases; $\delta^{15}N$ values for the residual fraction have been reported to be as large as 80 permil (Clark and Fritz, 1997, p. 152–153).

Groundwater from sites 11 and 17 had estimated $\delta^{15}N$ values (-1.4 and 1.59 permil, respectively) consistent with a source of nitrogen from inorganic fertilizer. Groundwater from site 18 had an estimated $\delta^{15}N$ value (10 permil) consistent with a source of nitrogen from manure or septic system waste. The large estimated $\delta^{15}N$ value (37.1 permil) in groundwater from site 9 indicates that the nitrate is a residual fraction from a source that has undergone significant denitrification.

Sources of Chemical Species

Dissolved Gases

Concentrations of dissolved gases in groundwater are a function of (1) recharge water that equilibrates with soil gases in the unsaturated zone and (2) chemical reactions in the unsaturated and saturated zones that include dissolved gases as a reactant or product of the reaction. Consequently, groundwater below the water table tends to preserve its dissolved-gas composition unless modified by biological and or chemical reactions (Busenberg and others, 1993, p. 8–10).

In the Beaver and Camas Creek drainage basins, groundwater hydrographs indicate that most recharge occurs in the mountains, not on the ESRP. This interpretation of recharge is consistent with geohydrologic and chemistry data from the ESRP at the INL. For example, in a study of sources of recharge to the ESRP aquifer at the INL, Schramke and others (1996) assumed that groundwater at the INL recharged in the mountains and did not equilibrate with gases in the soil zone of the ESRP. Their conclusion was based on the thick unsaturated zone (260–460 ft) in their study area at the INL and the relatively low carbon-14 concentrations (as low as 20 percent modern carbon) observed in some wells (Schramke and others, 1996, p. 527–528). Although most recharge in the Beaver and Camas Creek drainage basins occurs in the mountains, some recharge does occur on the ESRP from vertical infiltration of surface water from streams percolating through the unsaturated zone of the ESRP. Some vertical recharge also may occur in areas where the aquifer is relatively shallow, such as at Camas Meadows and the CNWR. Infiltration recharge may be a source of dissolved gases to the aquifer. However, a study of recharge to the ESRP aquifer at the INL indicated that most, but not all, recharge from infiltrating water at the INL is rapid and focused and has little contact with the unsaturated zone (Busenberg and others, 2001, p. 17). In areas of the ESRP in the Beaver and Camas Creek drainage basins where sediment is not very thick (everywhere but Camas Meadows and the CNWR), streamflow infiltration also is probably rapid and focused, has little contact with the unsaturated zone, and may not equilibrate with gases in the unsaturated zone. Consequently, most dissolved gas concentrations in the study area probably are influenced by gas concentrations in the soil zones in the mountains and chemical reactions in the ESRP aquifer.

Oxygen

DO is transported to the unsaturated zone from the atmosphere and dissolves in the unsaturated zone water. Where DO in the unsaturated zone is in contact with atmospheric oxygen, the DO would have 100 percent saturation at the ambient temperature. Once recharge is no longer in contact with the atmosphere, groundwater may remain saturated with DO for long distances or periods of time if there are no chemical reactions in the aquifer that consume oxygen (Appelo and Postma, 2005, p. 447). DO could become supersaturated (greater than 100 percent saturation) if groundwater recharges at a cold temperature and then warms. DO will be consumed if organic carbon or reduced minerals (sulfide or ferrous minerals, for example) react as groundwater moves downgradient.

It is not clear why there is anoxic water in the Beaverhead Mountains (site 12, table 3). However, anoxic or undersaturated water in Camas Meadows (sites 4 and 5) and the CNWR (site 19) probably result from aerobic and anaerobic decay (oxidation) of organic matter. Supersaturated water at site 3, in the Centennial Mountains, probably resulted from warming of cold recharge. Excepting the sites where decay of organic matter modified the oxygen content of water, DO in groundwater from the ESRP was near saturation with the atmosphere, indicating that reactions that consume oxygen are only locally important in the ESRP aquifer.

Carbon Dioxide

The partial pressure of CO_2 in the atmosphere is about -3.5 (as log PCO_2) (Clark and Fritz, 1997, p. 115). The partial pressure of CO_2 in recharge that has percolated through the soil zone generally is much larger than in the atmosphere due to (1) biochemical reactions in the soil zone that release CO_2 and (2) equilibration of CO_2 between infiltrating water and the soil zone. The partial pressure of CO_2 in the soil zone generally ranges from about -3 to -1 (Clark and Fritz, 1997, p. 115). In the shallow unsaturated zone (30 to 230-ft depth) of the ESRP at the INL, the background (uncontaminated) partial pressure of CO_2 ranged from -3.0 to -2.4 (Conrad and DePaolo, 2004, p. 145). In the saturated zone, little exchange of CO_2 gas with the groundwater can occur, and any dissolution of carbonate and silicate minerals consumes CO_2, thereby reducing the partial pressure of CO_2 and increasing the alkalinity of the water. Where aerobic decay of organic matter occurs CO_2 will be released to the saturated or unsaturated zone and the partial pressure of CO_2 will increase slightly; a maximum of about 0.25 mmol of dissolved CO_2 can be produced by consuming all DO in groundwater (in a closed system).

Large partial pressures of CO_2, ranging from -2.47 to -1.93, were calculated for samples collected from sites located on Sheridan Ridge or in the Centennial Mountains (sites 1, 3, and 8; table 3). These groundwaters were close to recharge areas and had low alkalinities (ranging from 49 to 92 mg/L as $CaCO_3$), which indicates that reactions of carbonate and/or silicate minerals has been minimal. Consequently, these large partial pressures probably represent a lower bound for the partial pressure of CO_2 in soil zones in the Centennial Mountains and Sheridan Ridge. Smaller CO_2 partial pressures of -2.88 and -3.08 were calculated for sites 4 and 5, respectively, in Camas Meadows. Because alkalinity in groundwater from these sites were greater relative to groundwater from the upgradient site (site 3), the smaller partial pressures probably were the result of carbonate and silicate minerals reacting with groundwater. A partial pressure of CO_2 of -2.61 was calculated for groundwater from site 12 in the Beaverhead Mountains, which is less than the partial pressures calculated for the groundwater samples from Sheridan Ridge and the Centennial Mountains. Groundwater from site 12 had a relatively large alkalinity (162 mg/L as $CaCO_3$), so the smaller partial pressure probably was caused by reaction of carbonate minerals with groundwater. A large partial pressure of CO_2 (-2.01) was calculated from site 13. Groundwater at this site probably is a mixture of surface water from Beaver Creek and groundwater from the Beaverhead and Centennial Mountains, and the large partial pressure of CO_2 may represent a mixture of infiltrating surface water equilibrating with CO_2 in the unsaturated zone and groundwater from the Beaverhead and Centennial Mountains.

The partial pressure of CO_2 in groundwater from the ESRP, excluding sites 18 and 19 in the CNWR, ranged from -2.50 to -3.03. These values were smaller than the values in groundwater entering the ESRP aquifer from the mountains, and probably indicate that CO_2 was consumed in groundwater by reactions with carbonate and/or silicate minerals.

At the CNWR, a small partial pressure of CO_2 (-3.25) was calculated for groundwater from site 18. This smaller partial pressure probably resulted from surface-water recharge that was in approximate equilibrium with a CO_2-poor soil or unsaturated zone. A large partial pressure of CO_2 (-1.68) was calculated for groundwater from site 19. This large value reflects a source of CO_2 to the system, most likely from streamflow-infiltration recharge with a partial pressure of dissolved CO_2 that was in approximate equilibrium with a CO_2-rich soil or unsaturated zone (potentially from oxidation of organic matter).

Sources of Groundwater

Potential sources of groundwater include infiltration of meteoric water, groundwater inflow from adjacent drainage basins, and upwelling of geothermal water. The δ^2H and $\delta^{18}O$ values of groundwater indicate that meteoric water, or precipitation, is a source of water to the study area (hydrogen and oxygen stable isotopes were discussed in section, "Interpretation of Isotopic Data"). Groundwater inflow from adjacent drainage basins, either the Henry's Fork basin to the east or the Medicine Lodge Creek basin to the west (fig. 1), probably is small because a topographic divide between the Henry's Fork and Camas Creek drainage basins acts as a groundwater divide and the northeast-to-southwest regional hydraulic gradient (Spinazola, 1994, p. 28) likely impedes eastward groundwater movement from the Medicine Lodge Creek drainage basin (fig. 9). Upwelling of a significant amount of geothermal water is unlikely because relatively cool water temperatures of less than or equal to 12.8 °C were measured for 15 of the 18 groundwater samples, and the three groundwater samples with higher water temperatures (site 11, 15.6 °C; site 15, 14.4 °C; site 17, 15.5 °C), all from the ESRP, do not have elevated concentrations of major ions (Na, HCO_3; table 4) or trace elements (B, Li; table 6) that might indicate significant upwelling of geothermal water from below the ESRP (Mann, 1986, p. 17).

Anthropogenic Inputs

Potential anthropogenic sources of solutes in the study area include leachate of manure from grazing cattle and sheep, inorganic fertilizer used as crop amendments, waste from septic systems, and road salt or anti-icing liquids. Leachate of manure from stock may occur on rangeland on the ESRP north and east of Dubois (including U.S. Sheep Experimental Station lands north of Dubois). Inorganic fertilizer (and minor amounts of manure) (U.S. Department of Agriculture, 2009, p. 428) is applied to agricultural lands in Camas Meadows and south of Dubois (fig. 6). Waste from septic systems is a minor source of anthropogenic solutes in the study area (Rupert, 1996, p. 5), due to the very low population density, but may be present locally in groundwater near Dubois, Spencer, and Kilgore. Leachate from road salt or anti-icing liquid (Idaho Transportation Department, 2013) may be applied to U.S. Interstate Highway15 and show up in groundwater near the U.S. Interstate Highway15 corridor (figs. 11–12).

The most abundant elements leached from cattle manure are nitrogen, potassium, and chloride (Appelo and Postma, 2005, p. 46). Inorganic fertilizer primarily is comprised of nitrogen, potassium, and phosphorus. Nitrogen in fertilizer may be present as nitrate or ammonium, but nitrogen leached from fertilizer (or manure) that infiltrates through the unsaturated zone to the aquifer will be in an oxidized form as nitrate. Potassium in commercial fertilizer is often present as potassium chloride. Leachate from road salt (NaCl) or anti-icing liquid (MgCl, CaCl) may include sodium, magnesium, calcium, or chloride.

Phosphorus, potassium, and chloride in water from irrigation wells are potentially from fertilizer or manure. However, orthophosphate concentrations are smaller in water from irrigation wells than in water from upland wells (tables 2 and 5), indicating that fertilizer is not a significant source of

phosphorus to groundwater in the study area. Concentrations of potassium and chloride in water from irrigation wells do not show an increasing pattern as nitrate concentrations increase (fig. 15). Consequently, nitrate appears to be the only solute from fertilizer or manure that is reaching the aquifer in significant concentrations.

Concentrations of nitrate in groundwater in three of the upland sites (sites 1, 8, and 12) were less than or equal to 0.16 mg/L as N (table 5; fig. 12). The other upland site (site 3) was a domestic well that had a NO_3 concentration of 0.74 mg/L as N. This larger NO_3 concentration may be from septic waste, cattle manure, or fertilizer. Nitrate concentrations in Camas Meadows include the concentration at site 3 at the upgradient end of Camas Meadows, a concentration of 0.43 mg/L as N from an irrigation well (site 4) at Kilgore, and a concentration of less than 0.02 mg/L as N from a domestic well (site 5) downgradient of Kilgore. The undetectable nitrate concentration and anoxic water at site 5 indicates that groundwater from this area underwent denitrification. Nitrate concentrations in water from stock wells on the ESRP (north and east of Dubois) ranged from 0.40 to 0.74 mg/L as N. The $\delta^{15}N$ value (37.1 permil) for site 9, one of the stock wells and directly downgradient of Camas Meadows, indicates that nitrate at this site represents a residual fraction of a nitrate reservoir that has undergone denitrification (Clark and Fritz, 1997, p. 148–154). The likely source of groundwater to site 9 is either groundwater from site 5 or other groundwater from Camas Meadows that has undergone denitrification. The $\delta^{15}N$ value (-1.4 permil) for site 11, another stock well, was too small to be from manure or septic waste, and probably indicates that the nitrate source was inorganic fertilizer (Clark and Fritz, 1997, p. 151). The only upgradient source of inorganic fertilizer is irrigated land in Camas Meadows. The nitrate concentration in water from a domestic well near Spencer (site 13) was 0.72 mg/L as N and may be from septic waste, manure, or fertilizer. Nitrate concentrations in water from irrigation wells on the ESRP south of Dubois (tables 2 and 5, fig. 12) ranged from 1.09 to 2.46 mg/L as N. These concentrations are larger than those in the upgradient stock or domestic (site 13) wells and show that the aquifer in this area has an anthropogenic source of nitrogen. The $\delta^{15}N$ values measured in water from two of the irrigation wells (1.6 permil, site 17; 10 permil, site 18) indicate that the source of nitrate probably was inorganic fertilizer at site 17 and leachate from manure or septic system waste at site 18. Because septic systems are sparse in this area, nitrate in water from site 18 probably is derived from manure.

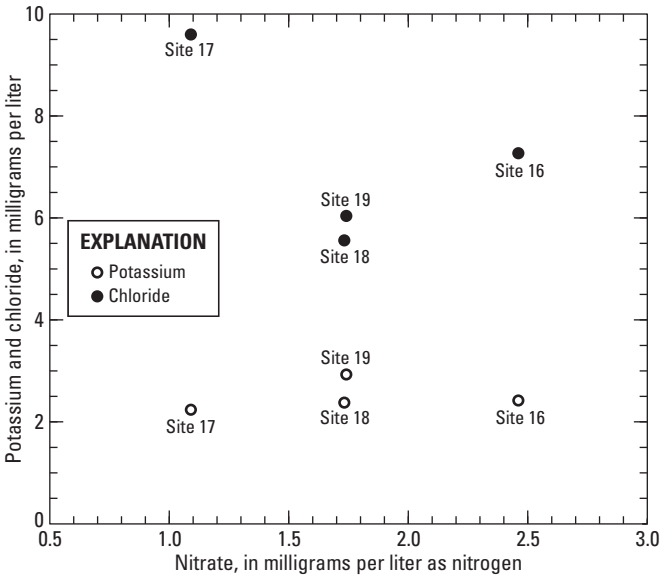

Figure 15. Potassium and chloride concentrations versus nitrate concentrations in water from irrigation wells in the Beaver and Camas Creek drainage basins, Idaho.

Chemical Reactions

Important chemical reactions that may affect the chemistry of groundwater in the study area were identified from groundwater chemistry and the minerals and gases available to react with groundwater. Potentially important reactions included carbonate reactions, silicate weathering, dissolution of evaporite minerals, oxidation-reduction reactions, and cation exchange. Carbonate reactions and dissolution of evaporite minerals involve minerals that dissolve rapidly in groundwater, so these reactions probably have a significant influence on groundwater chemistry. Silicate weathering and oxidation-reduction reactions may be rate-limited. Dissolution rates of silicate minerals are discussed in section, "Silicate Weathering." Oxidation-reduction reactions often proceed at significant rates only when mediated by bacterial catalysis (Appelo and Postma, 2005, p. 415). Biochemistry investigations were beyond the scope of this report, so if the groundwater chemistry indicated that oxidation-reduction reactions took place the appropriate bacteria were assumed to be present.

Carbonate Reactions

Carbonate rocks are present in both the Beaverhead and Centennial Mountains, and physical weathering of these rocks and fluvial, landslide, or eolian transport onto the ESRP means that carbonate minerals were present in surficial and interbed sediments on the ESRP. Consequently, carbonate minerals were available to react with groundwater throughout the study area. Groundwater from the Beaverhead Mountains (site 12) had about equal molar concentrations of calcium and magnesium (fig. 11), indicating that dissolution of dolomite influenced the chemistry of this water. Elsewhere in the study area, molar concentrations of calcium were larger than concentrations of magnesium, as would be expected from dissolution of a magnesium-poor limestone or calcite.

Groundwater in the study area ranged from being undersaturated, at equilibrium, or saturated with respect to calcite, so calcite may dissolve into or precipitate from solution. Dolomite was undersaturated in all groundwater except for one site (site 18). Precipitation of dolomite is kinetically unfavorable at low temperatures, and is rare unless the ratio of the molar activities of magnesium and calcium are considerably larger than one (Drever, 1997, p. 59), so dolomite in the study area may dissolve but is unlikely to precipitate. Dissolution of calcite or dolomite will consume CO_2 while releasing calcium, magnesium (from dolomite), and bicarbonate ions to solution (table 9). Precipitation of calcite is the reverse reaction.

Silicate Weathering

Silicate minerals are present in the study area in rhyolite along the margins of the ESRP, in basalt that comprises the ESRP, and in surficial and interbed sediment in the ESRP. Weathering of silicate minerals in the ESRP aquifer is indicated from the oxidation of iron in olivine crystals in basalt collected for this and other studies (Nace and others, 1956, p. 97–98; Rightmire, 1984; Rightmire and Lewis, 1987, p. 36). Clinopyroxene in one rhyolite sample (R1) collected for this study shows alteration to smectite and goethite, and titanaugite in basalt from the ESRP was observed by Nace and others (1956, p. 99–101) to alter to clinopyroxene and ilmenite. Plagioclase in both rhyolite samples collected for this study shows alteration to smectite, similar to observations from other studies of basalt from the ESRP (Knobel and others, 1997, p. 35). Based on such evidence of weathering of silicate minerals in the ESRP, geochemical mass-balance models of the ESRP aquifer (Wood and Low, 1988) and the ESRP aquifer at and near the INL (McLing, 1994; Schramke and others, 1996; Busenberg and others, 2001; Swanson and others, 2003) included dissolution of silicate minerals such as amorphous silica, plagioclase, pyroxene, olivine, and potassium feldspar. However, the extent of silicate weathering in the ESRP aquifer may be quite limited because most of the mineral grains in ESRP basalt appear fresh and unaltered (Nace and others, 1956, p. 97). At INEL-1, a 10,365 ft geothermal test well, basalt was observed to be mostly fresh to 1,600 ft below land surface (BLS), at which point basalts began to show alteration (Doherty and others, 1979, p. 3). Consequently, the shallower, active part of the ESRP aquifer (approximately less than 900 ft) appears to be mostly unaltered relative to the deeper aquifer (Mazurek, 2004, p. 3).

Based on evidence that silicate minerals dissolve slowly, Knobel and others (1997, p. 13) assumed that slow-reacting silicate minerals had a negligible effect on the chemistry of ESRP groundwater unless, like plagioclase, they were relatively abundant in the aquifer. Most silicate minerals dissolve in groundwater slowly due to the kinetics of a rate-limiting reaction step or steps. The relative rates of dissolution of some silicate minerals were inferred from calculations of the mean lifetime of 1 mm crystals (Lasaga and others, 1994, p. 2,362). These calculations, performed with data for a dilute solution at 25 °C and a pH of 5, showed mean lifetimes of 34×10^6 years for quartz, 9.2×10^5 years for microcline, 5.8×10^5 years for albite, 6.8×10^3 to 10×10^3 years for diopside and enstatite, 2.9×10^3 years for sanidine, 2.3×10^3 years for forsterite, and 1.1×10^2 years for anorthite. In the near-neutral pH region (pH 4–8), which includes water from the Beaver and Camas Creek drainage basins, the pH dependence of dissolution rates is slight (Lasaga and others, 1994, p. 2,374).

The discussion of tritium in section, "Interpretation of Isotopic Data," indicates that all groundwater samples in the ESRP appear to contain some pre-1952 water. However, it is not clear from the tritium concentrations if the pre-1952 groundwater in the ESRP is old water that has had a long enough residence time to be significantly influenced chemically by weathering of silicate minerals.

The residence time of groundwater in the ESRP was evaluated from the average linear flow velocities estimated for groundwater in the ESRP. The distance between site 1, at the extreme eastern edge of the ESRP, and sites 2 and 20, the next site downgradient from site 1 and the farthest downgradient site in the study area, respectively, are about 8.25 and 48 mi. Given the rapid groundwater flow rates (a conservative estimate of 2–20 ft/d) expected in the ESRP in the study area, the range of estimated groundwater residence times in the ESRP is about 6 to 60 years at site 2 and 35 to 350 years at site 20. Considering the distance from sources of recharge in the mountains and hydraulic gradients (about 100 ft/mi north and east of Dubois and 7 ft/mi south of Dubois), the residence time of groundwater in the ESRP that was recharged in the mountains is probably less than 50 years in the high hydraulic gradient region north and east of Dubois and 100 to 350 years in the low hydraulic gradient region south of Dubois. These short residence times indicate that weathering of silicate minerals with slow dissolution rates, such as olivine, pyroxene, and potassium feldspar, probably contribute only minor amounts of solutes to the ESRP aquifer in the study area.

Volcanic glass is metastable at environmental conditions due to its lack of crystallinty and large surface area (Deutsch and others, 1982), is abundantly present in the ESRP, and may be an important source of solutes to groundwater in the ESRP. Volcanic glass is present in rhyolite of the ESRP as vitrophere zones (Morgan and others, 1984; Morgan, 1992; Morgan and McIntosh, 2005). The large potassium and silica concentrations in groundwater from site 8 (table 4, fig. 11) in the Centennial Mountains, located downgradient of rhyolite bedrock, may be evidence of weathering of volcanic glass from rhyolite. Volcanic glass also is present in basalt of the ESRP, where volcanic glass was estimated to comprise as much as 10 percent of the basalt (McLing, 1994, p. 16), and was observed at the base of many flows (Nace and

Table 9. Chemical reactions that may act as sources or sinks of gases and solutes to or from groundwater, Beaver and Camas Creek drainage basins, eastern Idaho.

[Ex, exchanging substrate; X, a stoichiometric variable that ranges from 0 to 1]

Carbonate reactions
Calcite
$CaCO_3 + CO_2 + H_2O \leftrightarrow Ca^{2+} + 2HCO_3^-$
Dolomite
$CaMg(CO_3)_2 + 2CO_2 + 2H_2O \rightarrow Ca^{2+} + Mg^{2+} + 4HCO_3^-$
Dissolution of evaporite minerals
Gypsum
$CaSO_4 \cdot H_2O \rightarrow Ca^{2+} + SO_4^{2-} + 2H_2O$
Halite
$NaCl \rightarrow Na^+ + Cl^-$
Fluorite
$CaF_2 \rightarrow Ca^{2+} + 2F$
Silicate weathering
Plagioclase (An_{60}) to Ca-montmorillonite
$Ca_{0.6}Na_{0.4}Al_{1.6}Si_{2.4}O_8 + 0.13H_4SiO_4 + 1.36CO_2 + 1.12H_2O \rightarrow 0.69Ca_{0.17}Al_{2.33}Si_{3.67}O_{10}(OH)_2 + 0.48Ca^{2+} + 0.4Na^+ + 1.36HCO_3^-$
Plagioclase (An_{25}) to Na-montmorillonite
$Ca_{0.25}Na_{0.75}Al_{1.25}Si_{2.75}O_8 + 1.07CO_2 + 2.64H_2O \rightarrow 0.54Na_{0.33}Al_{2.33}Si_{3.67}O_{10}(OH)_2 + 0.78H_4SiO_4 + 0.25Ca^{2+} + 0.57Na^+ + 1.07HCO_3^-$
Volcanic glass (basalt) to Ca-montmorillonite
$SiAl_{0.3}Fe_{0.19}Fe_{0.2}Mg_{0.1}Ca_{0.26}Na_{0.1}K_{0.02}O_{3.36} + 1.18CO_2 + 1.88H_2O \rightarrow$ $0.13Ca_{0.17}Al_{2.33}Si_{3.67}O_{10}(OH)_2 + 0.53H_4SiO_4 + 0.19Fe^{2+} + 0.2FeOOH + 0.1Mg^{2+} + 0.24Ca^{2+} + 0.1Na^+ + 0.02K^+ + 1.18HCO_3^-$
Volcanic glass (rhyolite) to Na-montmorillonite
$SiAl_{0.22}K_{0.12}Na_{0.08}O_{2.43} + 0.17CO_2 + 1.48H_2O \rightarrow 0.54Na_{0.33}Al_{2.33}Si_{3.67}O_{10}(OH)_2 + 0.65H_4SiO_4 + 0.12K^+ + 0.05Na^+ + 0.17HCO_3^-$
Agricultural and anthropogenic inputs
Inorganic fertilizer (ammonium nitrate)
$NH_4NO_3 + 2O_2 \rightarrow 2NO_3^- + 2H^+ + H_2O$
Road anti-icing liquids
$MgCl_2 \rightarrow Mg^{2+} + 2Cl^-$
$CaCl_2 \rightarrow Ca^{2+} + 2Cl^-$
Oxidation-reduction reactions
Oxidation of organic matter
$CH_2O + O_2 \rightarrow CO_2 + H_2O$
Oxidation of pyrite
$FeS_2 + 3.5O_2 + H_2O \rightarrow Fe^{2+} + 2SO_4^{2-} + 2H^+$
Denitrification (reduction of nitrate)
$5CH_2O + 4NO_3^- \rightarrow 2N_2 + 5HCO_3^- + 2H_2O + H^+$
Reduction of manganese oxide
$CH_2O + 2MnO_2 + 3H^+ \rightarrow 2Mn^{2+} + HCO_3^- + 2H_2O$
Reduction of ferric iron
$CH_2O + 4FeOOH + 7H^+ \rightarrow 4Fe^{2+} + HCO_3^- + 6H_2O$
Sulfate reduction
$CH_2O + SO_4^{2-} \rightarrow HCO_3^- + HS^- + O_2$
Precipitation of pyrite
$Fe^{2+} + 2HS^- + 0.5O_2 \rightarrow FeS_2 + H_2O$
Cation Exchange
$(1\text{-}X)Ca^{2+} + XMg^{2+} + Na_2 \cdot Ex \leftrightarrow 2Na^+ + (Ca_{1-x}Mg_x) \cdot Ex$

others, 1956, p. 96) where, below the water table, it would be in constant contact with groundwater. Volcanic glass has previously been interpreted as dissolving and contributing solutes to groundwater from rhyolite at Frenchman Flat and Oasis Valley in Nevada (Thomas and others, 2002; Hershey and others, 2005) and from basalt of the ESRP at the INL (Busenberg and others, 2001, p. 48).

Based on estimated groundwater residence times in the ESRP, mineral kinetics and stability, the abundance of glass and plagioclase in rhyolite (very and moderately abundant, respectively) and basalt (moderately and very abundant, respectively) (table 8), and the location of volcanic glass at the base of basalt flows (and therefore in contact with groundwater moving rapidly through interflow zones), volcanic glass and plagioclase probably are more important contributors of solutes to groundwater in the ESRP than olivine, pyroxene, or potassium feldspar. Both volcanic glass and plagioclase dissolve incongruently, forming aluminosilicate clay minerals and releasing silica, calcium, sodium, iron, magnesium, potassium, and bicarbonate to solution (table 9). Based on the alteration of plagioclase to smectite in the rhyolite samples, and the ubiquitous presence of smectite in sediments in the study area, incongruent dissolution of volcanic glass and plagioclase probably forms a smectite clay mineral.

Thermodynamic data for aluminosilicate minerals are not well known, so calculated saturation indices for these minerals are not reliable predictors of mineral stability (Knobel and others, 1997, p. 24). To evaluate whether it was reasonable that incongruent dissolution of volcanic glass and plagioclase would form smectite (montmorillonite) minerals, the groundwater solutions were plotted on aluminosilicate stability diagrams that plot the $\log_{10}$ activity of Na^+/H^+ or $Ca^{2+}/(H^+)^2$ versus the $\log_{10}$ activity of H_4SiO_4 (figs. 16–17).

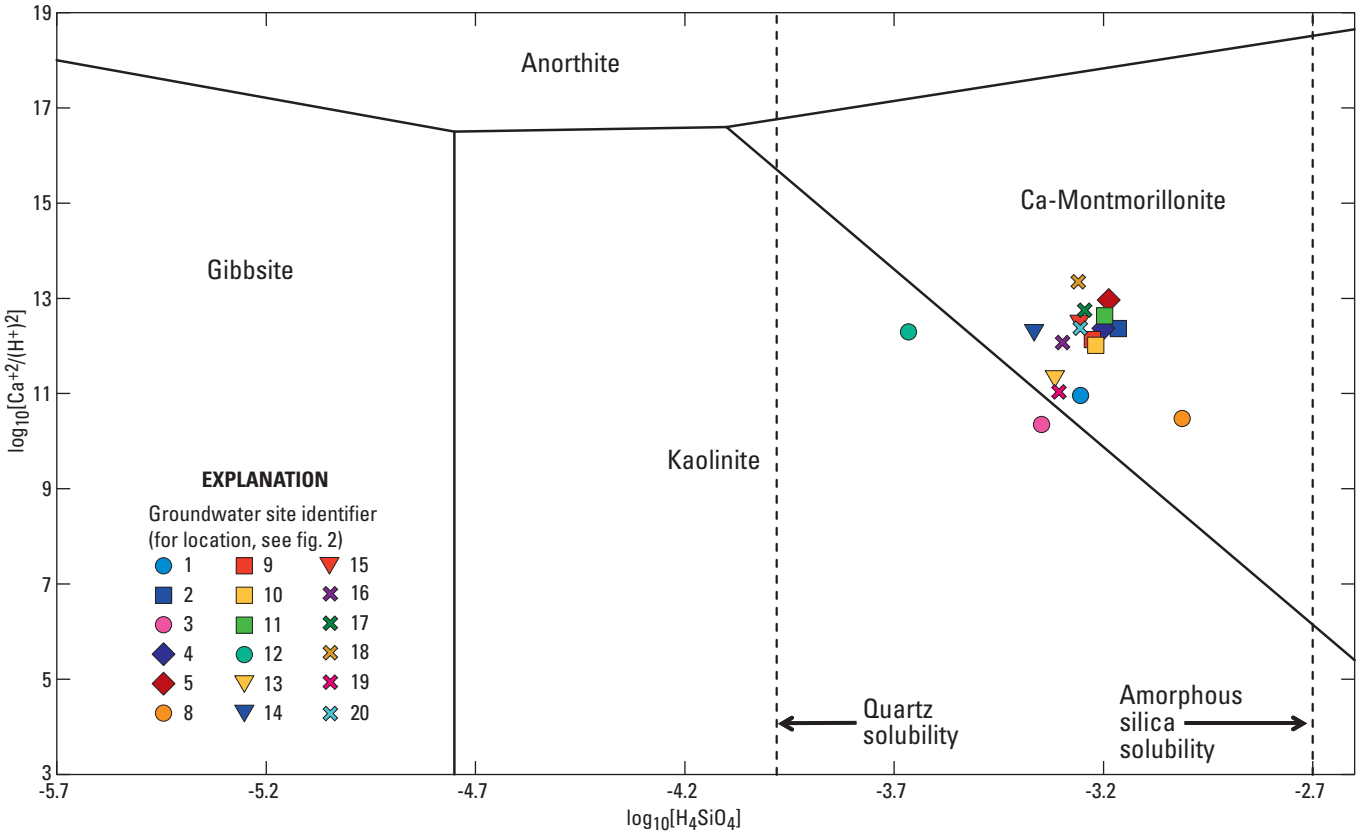

Figure 16. Stability relations among anorthite, gibbsite, kaolinite, and calcium montmorillonite (Ca-Montmorillonite) with superposed compositions of water samples, Beaver and Camas Creek drainage basins, eastern Idaho. Modified from Knobel and others (1997, p. 28–30). Brackets indicate thermodynamic activity of indicated species.

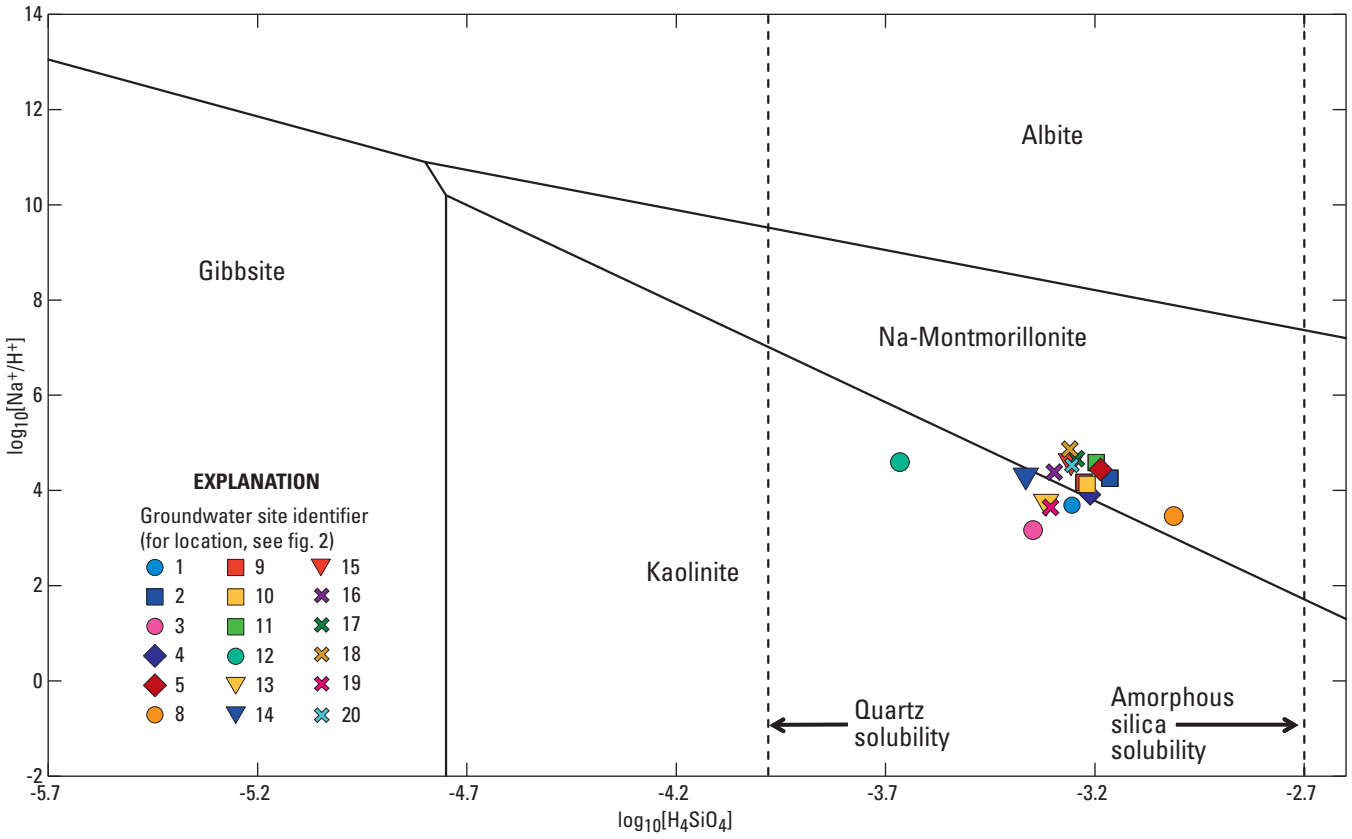

Figure 17. Stability relations among albite, gibbsite, kaolinite, and sodium montmorillonite (Na-Montmorillonite) with superposed compositions of water samples, Beaver and Camas Creek drainage basins, eastern Idaho. Modified from Knobel and others (1997, p. 31–33). Brackets indicate thermodynamic activity of indicated species.

These mineral stability diagrams contain uncertainties in the thermodynamic data used to generate the diagrams (Drever, 1997, p. 210–213), and conclusions about water equilibrium and aluminosilicate mineral stability based solely on these diagrams should be considered tentative (Knobel and others, 1997, p. 24). All groundwater samples, except for sites 3 and 12, plotted within the calcium-montmorillonite field for the system anorthite-gibbsite-kaolinite-calcium montmorillonite, and 12 of the 18 groundwater samples plotted in the sodium montmorillonite field for the system albite-gibbsite-kaolinite-sodium montmorillonite. Of the six groundwater samples that plotted in the kaolinite field on the plot of the system albite-gibbsite-kaolinite-sodium montmorillonite, three of the samples (sites 1, 3, and 12) were located in the mountains, two of the samples (sites 13 and 14) were located on the ESRP downgradient of the Beaverhead Mountains, and one sample (site 19) was located at the southern end the CNWR. These results indicate that incongruent dissolution of volcanic glass and plagioclase would form (1) smectites at most of the groundwater sites and (2) that kaolinite may form at groundwater sites in the mountains, downgradient of the Beaverhead Mountains, and at the southern end of the CNWR.

Dissolution of Evaporite Minerals

Concentrations of sodium, chloride, and fluoride in groundwater from the southeastern part of the INL, where the groundwater source area is from northeast of the INL, are higher than expected in the dilute groundwater from the ESRP aquifer at the INL (Olmstead, 1962; Busenberg and others, 2001, p. 8, 41). Sources for high sodium and chloride concentrations have been suggested in several previous studies. Robertson and others (1974, p. 52) attributed high sodium and chloride concentrations in water from Mud Lake to evaporation of irrigated water, atmospheric fallout, and rapid solution from irrigated soils. Wood and Low (1988, p. 18) in modeling the solute geochemistry of the ESRP, noted that sodium and chloride concentrations were anomalously high and attributed the high concentrations to flushing of grain boundaries and pores of detrital marine sediments in the interbeds. Schramke and others (1996, p. 528) developed a geochemical model of the northern part of the INL and indicated that dissolution of fluid-inclusion NaCl or grain boundary flushing could contribute sodium and chloride to groundwater.

In this study, the primary sources of sodium, chloride, sulfate, and fluoride were attributed to the minerals halite, gypsum (or anhydrite), and fluorite from carbonate and sedimentary rocks in the Beaverhead and Centennial Mountains, interbed and surficial sediments on the ESRP, and evaporite deposits associated with Pleistocene Lake Terreton in the Dubois-Mud Lake area (Geslin and others, 2002, p. 13). The evaporite deposits associated with Lake Terreton could be an important, unrecognized, source of sodium, chloride, sulfate, and fluoride to the ESRP aquifer northeast of the INL. Gypsum was identified in interbed sediments associated with Lake Terreton (Geslin and others, 2002, p. 13), but neither halite nor fluorite has been identified in the literature as being present in surficial or interbed sediment in this area. It is possible that halite, which is uniformly undersaturated in groundwater in the study area, has dissolved from some surficial and interbed deposits in the study area and thus may not be readily detected in sediment analyses. Fluorite may only be present in the sediments in small quantities. In addition to these major ions, Busenberg and others (2001, p. 9, 41) noted that the trace elements lithium and boron had large concentrations in water recharging the INL from the northeast. Lithium and boron, which were previously suggested as indicator elements for geothermal water, also may be present in evaporite deposits (Hem, 1992, p. 129, 133).

Oxidation-Reduction Reactions

Wetlands, with their abundant organic matter, provide excellent conditions for oxidation-reduction reactions in groundwater. Wetlands in the study area occur in Camas Meadows and the CNWR. DO concentrations decreased in the downgradient direction in Camas Meadows (between sites 3 and 4 and sites 4 and 5) and the CNWR (between sites 18 and 19) (table 3). The decrease in DO was inferred to occur due to reduction of DO and oxidation of organic matter.

Groundwater at site 4 in Camas Meadows and site 19 in the CNWR contained DO, so the only oxidation-reduction reactions occurring between sites 3 and 4 in Camas Meadows and sites 18 and 19 in the CNWR were aerobic oxidation-reduction reactions. Aerobic oxidation of organic matter (CH_2O; table 9) was assumed to take place in both Camas Meadows and the CNWR, and aerobic oxidation of pyrite was considered a likely reaction in groundwater moving between sites 3 and 4 in Camas Meadows. Pyrite was assumed to be present in sediment at Camas Meadows as a detrital mineral associated with seams of coal in the Centennial Mountains; a pyrite source of sulfate is consistent with the sulfur isotope data for groundwater from site 4. Aerobic oxidation of organic matter releases CO_2 to water and, when CO_2 concentrations in groundwater increase, the saturation state of calcite and dolomite in the water is reduced and these minerals may dissolve (Drever, 1997, p. 55). Oxidation of pyrite releases ferrous iron, sulfate, and hydrogen ions to solution.

Groundwater at site 5 in Camas Meadows was anoxic. This indicates that all oxygen in the water was consumed by aerobic oxidation of organic matter and pyrite. Groundwater at site 5 also had undetectable concentrations of nitrate and, relative to site 4, larger concentrations of manganese and iron and a smaller concentration of sulfate. These changes in groundwater chemistry may be due to anaerobic reduction of nitrate (denitrification), manganese oxide, ferric iron (iron oxyhydroxide), and sulfate (table 9). The removal of nitrate from the water, and the large $\delta^{15}N$ (37.1) from groundwater downgradient of Camas Meadows, support the hypothesis that denitrification occurred. Sulfate reduction generally occurs in water with a pe (pe = $-\log_{10}$ of the activity of electrons in solution) of approximately -4 (Drever, 1997, p. 161), and sulfate reduction usually leads to the formation of iron sulfide minerals. All of the anaerobic reduction reactions in table 9 release bicarbonate to solution. When bicarbonate concentrations in groundwater increase, calcite (but probably not dolomite) may precipitate.

Cation Exchange

Cation exchange may occur with clay minerals, zeolites, colloidal oxyhydroxides, and natural organic compounds (Drever, 1997, p. 82). All these materials except for zeolites are present in sediments in the study area and provide capacity for exchange processes. Of these materials, clays probably are most abundant. Clays are present in surface and interbed sedimentary deposits, which are most abundant in the mountains, Camas Meadows, and south of Dubois. Exchange between sodium and calcium or magnesium are plausible exchange reactions, based on the concentrations of cations in groundwater in the study area (table 4). These exchange reactions were previously modeled in ESRP groundwater by McLing (1994, p. 44) and Busenberg and others (2001, p. 133–136). Exchange of calcium or magnesium for sodium will remove calcium and magnesium from solution and add sodium to solution (table 9).

Geochemical Modeling

Geochemical modeling was performed by using the inverse (mass balance) modeling capability of PHREEQC (Parkhurst and Appelo, 2013) to test interpretations about the distribution of chemical species in the drainage basins and the sources of solutes to groundwater. Inverse modeling attempts to identify the net chemical reactions that account for observed changes in chemistry between initial (one or more) and final (one) water compositions along a single flowline or joined (mixture) flowlines (Parkhurst and Appelo, 2013, p. 7). The thermodynamic conditions of water compositions place constraints on plausible and actual chemical reactions. Model inputs included aqueous solutions, gas and solid phases, and chemical elements and constraints (isotopic compositions). The nonunique model results are set(s) of gas and solid phase mass transfers into and out of the system that account for the change in chemistry from the initial to the final solutions.

Saturation Indices

The thermodynamic conditions of surface water and groundwater were evaluated to determine whether specific minerals may precipitate from, dissolve into, or were in equilibrium with surface-water and groundwater compositions. The thermodynamic state of each water composition was calculated, with respect to selected minerals that are present in the aquifers, with PHREEQC (Parkhurst and Appelo, 2013) by using the WATEQ4F thermodynamic database. The results are shown as saturation indices (SIs) in table 10, where SIs are the $\log_{10}$ of the ratio of an ion activity product of a solution for a specific mineral and the equilibrium constant for the mineral. Positive and negative SIs indicate supersaturation (mineral may precipitate) and undersaturation (mineral may dissolve), respectively. Saturation indices of 0 ± 0.1 were interpreted as indicating that the mineral was in equilibrium with a water composition and that the mineral may precipitate or dissolve.

The minerals shown in table 10 include minerals that are present, or represent minerals that are present, in the study area that have thermodynamic data available. Saturation indices for two end members of plagioclase, albite and anorthite, were included in table 10. Plagioclase in the study area is intermediate in composition between these end members, but if both end members were undersaturated in, or in equilibrium with, a groundwater then dissolution of the intermediate plagioclase composition is a reasonable possibility. Saturation indices for amorphous silica were used to represent the saturation state of volcanic glass in groundwater.

The calculated SIs for calcium montmorillonite and goethite were all positive, indicating that these minerals will only precipitate. The calculated SIs were all negative for dolomite (except for sites 18 and 98), gypsum, halite, fluorite, amorphous silica, and plagioclase (albite and anorthite) indicating that these minerals, or the minerals that they represent, will only dissolve (except for plagioclase at site 2; albite has an SI of -0.05, is in approximate equilibrium with the solution, so plagioclase may dissolve or precipitate). Calculated SIs for calcite were positive and negative, indicating that calcite may precipitate or dissolve.

Table 10. Mineral/water thermodynamic saturation indices for selected minerals for selected surface water and groundwater samples, Beaver and Camas Creek drainage basins, eastern Idaho.

[Location of sites are shown in figure 2. Saturation indices are log IAP/K (ion activity product/equilibrium constant); positive values indicate saturation, negative values indicate undersaturation, and zero plus or minus 0.1 indicates equilibrium]

Site No.	Calcite	Dolomite	Gypsum	Halite	Fluorite	Silica (amorphous)	Albite	Anorthite	Calcium Montmorillonite	Goethite
1	-1.34	-3.34	-3.76	-9.31	-0.62	-0.40	-0.45	-2.29	5.96	6.16
2	-0.48	-1.39	-3.55	-9.61	-2.09	-0.32	-0.05	-1.45	5.54	6.65
3	-1.81	-4.19	-3.78	-9.84	-4.21	-0.48	-0.96	-2.68	6.20	5.07
4	-0.36	-1.42	-3.38	-9.71	-2.71	-0.33	-0.44	-1.94	5.27	6.42
5	0.04	-0.51	-3.54	-9.38	-2.16	-0.32	-1.23	-3.87	2.42	1.13
8	-1.27	-3.28	-2.81	-9.11	-1.88	-0.17	-1.00	-4.29	4.34	5.66
9	-0.29	-0.86	-3.39	-9.00	-2.32	-0.40	-1.71	-4.44	2.02	7.39
10	-0.58	-1.55	-3.18	-9.16	-2.61	-0.38	-1.72	-4.68	2.05	7.53
11	-0.04	-0.20	-3.41	-8.80	-2.33	-0.40	-1.29	-3.58	2.05	6.17
12	-0.15	-0.39	-2.67	-8.72	-3.44	-0.81	-2.26	-4.84	1.22	8.72
13	-0.48	-1.53	-2.78	-9.09	-2.26	-0.46	-2.39	-5.54	1.76	5.02
14	0.03	-0.36	-2.67	-8.78	-2.36	-0.54	-2.07	-4.50	1.50	6.53
15	-0.06	-0.39	-2.71	-8.32	-2.36	-0.45	-1.46	-3.81	1.93	6.17
16	-0.43	-1.17	-2.70	-8.58	-2.26	-0.47	-1.71	-4.65	1.75	6.03
17	0.08	-0.11	-3.04	-8.49	-1.95	-0.45	-1.33	-3.54	1.93	6.15
18	0.30	0.21	-2.84	-8.82	-1.74	-0.44	-0.81	-2.58	2.83	6.78
19	-0.46	-1.44	-2.58	-8.71	-1.83	-0.47	-2.45	-5.73	1.60	4.23
20	-0.07	-0.49	-2.84	-8.42	-1.89	-0.44	-1.46	-4.14	1.92	6.54
96	-0.72	-1.84	-3.54	-9.63	-2.83	-0.43	-1.10	-2.44	4.99	6.49
97	-0.60	-1.65	-3.71	-9.60	-3.26	-0.56	-2.26	-4.39	1.75	7.54
98	1.13	1.78	-2.88	-8.87	-2.40	-0.73	-1.71	-3.01	1.19	7.09
99	-0.40	-1.13	-3.80	-9.95	-3.28	-0.77	-2.37	-3.24	2.01	7.34

Model Inputs

Input to the geochemical models consisted of the chemical compositions of solutions (tables 3–7), the set of gases and solid phases involved in thermodynamically possible chemical reactions to be modeled (tables 9 and 10), and the set of elements and constraints required or available to chemically describe the solutions and phases.

Solutions

Solutions used in the models were the chemical data from the surface-water and groundwater sites (tables 3–7). Iron concentrations in solutions that were censored were assigned a value in the models of one-half the censored value. Aluminum concentrations in solutions that were either not available or were censored were estimated with PHREEQC (table 6). This was done by calculating (with PHREEQC) the aluminum concentration for a solution that would be in equilibrium with a specific saturation indice for gibbsite. The saturation indice for gibbsite used for a specific solution was approximated from the saturation indices of groundwater with similar sources of water as the specific solution. Groundwater from the Centennial Mountains and Sheridan Ridge had saturation indices for gibbsite ranging from 0.88 to 1.92, and a value of 1.5 was used to calculate the aluminum concentrations in water from sites 2 and 4. This produced an estimated aluminum concentration for site 4 of 15 µg/L, which was close to a measured concentration from this site, from 1981, of 10 µg/L. Saturation indices for groundwater from the ESRP (including site 5) ranged from 0.12 to 0.15 µg/L for four sites and was 0.46 µg/L at site 18. A saturation indice of 0.13 was used to calculate aluminum concentrations for sites 9, 10, 13, 14, 16, 17, 19 as well as for sites 5 and 20 (which had censored concentrations). This produced estimated aluminum concentrations for sites 5 and 20 of 1.6 and 1.7 µg/L, respectively, and these concentrations were near the censored concentrations of aluminum from these sites of less than 1.7 µg/L (table 6). Comparable waters with aluminum concentrations were not available for site 98, Beaver Creek at Spencer. The aluminum concentration for this water was approximated using a saturation indice for gibbsite of 0.13.

The redox state of the solutions, except for solution 5, was calculated by PHREEQC by using the oxygen(-2)/oxygen(0) redox couple. For solution 5, a pe of -4 was specified, which approximates the pe of a solution where sulfate reduction is occurring (Drever, 1997, p. 161). Solution uncertainties assigned in inverse modeling were the larger of the charge balance of a solution (rounded up to the nearest 1 percent) or 5 percent.

The stable isotopes of hydrogen, oxygen, and carbon were only available from specific sites (table 7), and were only used to constrain models between adjacent sites. Consequently, stable isotopes were only used to constrain models of water in Camas Meadows (models that included only sites 3, 4, 5, 8, and 97). Errors assigned to the δ^2H, $\delta^{18}O$, and $\delta^{13}C$ values were ±2 permil, ±0.2 permil, and ±1 permil, respectively. Values and errors assigned to the $\delta^{13}C$ for phases were 0 ± 2 for calcite and dolomite and -23 ± 3 for organic matter.

Phases

Solid phases included in the geochemical models were either present in rocks or sediments in the study area or were inferred to be present based on groundwater chemistry. Gaseous phases included in the models were oxygen (O_2), CO_2, and nitrogen (N_2); O_2 and CO_2 also were assumed to be present in the unsaturated zone.

Phases included in all models were calcite, dolomite, gypsum, halite, fluorite, volcanic glass (rhyolite and basalt), plagioclase (An_{25} and An_{60}), ammonium nitrate, calcium and sodium montmorillonite, and goethite. Montmorillonite and goethite were only allowed to precipitate, calcite was allowed to dissolve or precipitate, and the other phases were only allowed to dissolve. Compositions for rhyolite and basalt volcanic glass used in the models were from McLing (1994, p. 14). The compositions used for plagioclase were within the range of estimated compositions for this mineral in rhyolite and basalt described in section, "Geology." Ammonium nitrate was used as the source of nitrogen from inorganic fertilizer (or from septic system waste or manure).

Phases only included in some models were kaolinite, sodium-calcium cation exchange, calcium chloride, magnesium chloride, potassium feldspar, pyrite, organic carbon (CH_2O), N_2, CO_2, and O_2. Kaolinite was included as a phase when sites 1, 3, 12, 13, 14, and 19 were either initial or final model solutions because kaolinite was shown as a stable phase for these solutions in aluminosilicate stability diagrams (figs. 16–17). Cation exchange was modeled in the CNWR (site 19) where sodium was allowed to be desorbed from exchange sites and calcium was allowed to sorb. Calcium chloride and magnesium chloride was allowed to dissolve for models of water near the U.S. Interstate Highway 15 corridor (sites 14 and 15), and potassium feldspar was allowed to dissolve for one model, site 4 in Camas Meadows, that did not have sufficient sources of potassium from other model phases. The oxidation or precipitation of pyrite was modeled in Camas Meadows (sites 4 and 5) and was dependent on the oxidation state of the groundwater. Organic carbon was allowed to dissolve in groundwater beneath wetlands in Camas Meadows (sites 4 and 5) and the CNWR (site 19), and nitrogen was allowed to precipitate (exsolve; nitrogen also could accumulate in solution as dissolved N_2) during denitrification in Camas Meadows (site 5). Carbon dioxide was included as a phase for models that included site 3 in the Centennial Mountains and sites 18, 19, and 20 in the CNWR. Either the partial pressure of carbon dioxide or the stable isotopes of carbon indicated that these sites may exchange CO_2 with the soil or unsaturated zones.

Oxygen was included as a phase, and allowed to dissolve, when surface water mixed with groundwater. This was necessary because oxygen concentrations in the stream samples, collected during the low flow and hot days of summer (sites 96–99, table 3), were smaller (much smaller for site 99) than would be present in the stream during the high flow and colder temperatures of spring when most streamflow infiltration would occur. Oxygen also was included as a phase, and allowed to exsolve, for a model that used a hypothetical groundwater solution. The hypothetical solution was groundwater from site 3, which was mixed with groundwater from site 1 as initial model solutions in a model where groundwater from site 2 was the final model solution. Exsolution of oxygen allowed for the possibility that the DO concentration of the hypothetical groundwater was too high.

Elements and Constraints

Elements used in the mass-balance models were hydrogen, oxygen, carbon, silica, nitrogen, sulfur, chloride, fluoride, calcium, magnesium, sodium, potassium, aluminum, and iron. δ^2H, $\delta^{18}O$, and $\delta^{13}C$ were included as constraints in some models.

Model Results

The initial and final solutions used for the geochemical models are shown in figure 18 and the solutions, mixing of solutions, evaporation of solutions or solution mixtures, and mass transfer of phases for the models are shown in table 11. The models were run in minimal mode, which means that the models were reduced to the minimum number of phases needed to satisfy the model constraints (Parkhurst and Appelo, 2013, p. 89). Use of the minimal mode means that the simulated model results do not include every possible combination of phases that could result in a successful model. However, the models produced in the minimal mode were suitable for identifying all of the important physical and chemical processes controlling the geochemistry of groundwater in the study area.

Model simulations produced 79 net geochemical mass-balance models that were thermodynamically possible. Twenty-six of the models were considered implausible (the 26 implausible models have a gray background in table 11) after evaluation of stable isotope, tritium, mineral, and hydrologic constraints. In nearly all models, fluorite was a minor dissolving phase, goethite was a minor precipitating phase, and a clay phase, either calcium montmorillonite, sodium montmorillonite, or kaolinite, precipitated. Larger amounts of goethite were modeled to precipitate if iron-bearing volcanic glass from basalt was modeled as dissolving. Other model results, and interpretations made from the model results, are described with respect to the final solution in a northeast-to-southwest (downgradient) direction across the study area.

Site 2.—Site 2 is located in basalt at the northeastern extent of the ESRP aquifer and is downgradient of site 1 on Sheridan Ridge and the eastern part of Camas Meadows (fig. 6). Groundwater flowing to site 2 probably flows through alluvium in Camas Meadows and basalt, rhyolite, and interbedded sediment of the ESRP aquifer. Groundwater chemistry was not available for the eastern part of Camas Meadows, so groundwater at site 2 was initially modeled as entirely from site 1. No successful models were produced when site 1 was the only initial model solution. To evaluate whether groundwater from the eastern part of Camas Meadows may be a source of water to site 2, groundwater from site 1 was modeled as a mixture with groundwater solutions (sites 3 and 4) that may represent the chemistry of groundwater from the eastern part of Camas Meadows (fig. 18). Using these hypothetical solutions, no successful models were produced by mixing water from sites 1 and 4, but three successful models (each model included a different clay phase as a precipitate) were produced by mixing water from sites 1 and 3 (table 11). Groundwater from site 3 had high DO and nitrate concentrations. The high concentrations of dissolved O_2 and nitrate at site 3 seemed unusual and would probably not be present in groundwater from the eastern part of Camas Meadows. Oxygen was included in the models as a precipitating phase and the balance identifier in PHREEQC was used to assign nitrogen an uncertainty of 100 percent to account for the uncertain concentrations of these constituents.

The models were a mixture of 15–16 percent groundwater from site 1 and 84–85 percent groundwater from site 3 (table 11). The large percentage of groundwater from site 3 indicates that most of the groundwater at site 2 originates from or flows through the eastern part of Camas Meadows. The dominant dissolving phase was volcanic glass from rhyolite [189 micromoles per kilogram of water (µmol/kg water)]. Other dissolving phases were dolomite, calcite, plagioclase (An_{25}), gypsum, and halite. Precipitating phases were O_2 (due to the supersaturated O_2 content of groundwater from site 3) and clay minerals.

Site 4.—Site 4 is an artesian well (see table 2) located in alluvium in wetlands near the center of Camas Meadows. Surface-water and groundwater sources to site 4 probably were from the Centennial Mountains and Camas Meadows to the northwest, north, and northeast; all sources of water to site 4 probably moved through alluvium in Camas Meadows. Oxidation-reduction reactions were considered important in this area because of the wetlands in Camas Meadows and the low DO at site 4 (56 percent saturation, table 3).

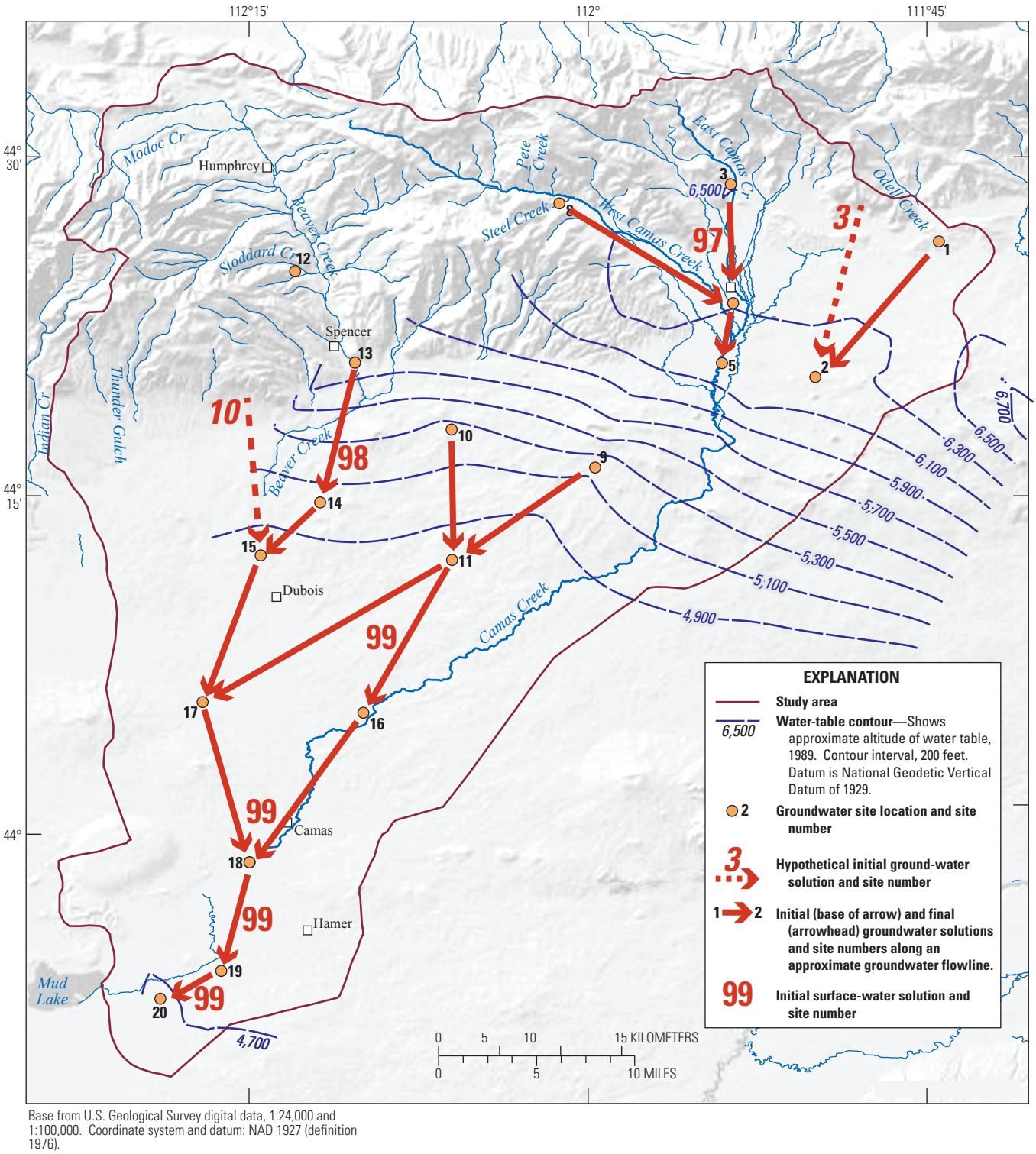

Base from U.S. Geological Survey digital data, 1:24,000 and 1:100,000. Coordinate system and datum: NAD 1927 (definition 1976).

Figure 18. Initial (one or more) and final (one) solutions for geochemical mass-balance models, Beaver and Camas Creek drainage basins, eastern Idaho. Solid red arrows represent flowline(s) between initial groundwater solution(s) and a final groundwater solution. Dashed red arrows represent hypothetical flowlines between a hypothetical initial groundwater solution and a final groundwater solution. Base of arrow represents initial solution and arrowhead represents final solution. Numbers in red indicate that streamflow infiltration was modeled as an initial solution using the composition of the specified site number.

Table 11. Geochemical mass-balance modeling results, Beaver and Camas Creek drainage basins, eastern Idaho.

[Initial and final sites (solutions) are shown in figure 18. Percent solution indicates the amount of initial solution(s) required to produce the final solution. Positive and negative phase mass transfers indicate dissolution and precipitation, respectively. Gray shading indicates an implausible model result. **Abbreviations**: Plag An_{25}, plagioclase with compostion An_{25}; Plag An_{60}, plagioclase with composition An_{60}; –, phase not required by model]

Solution			Phase mass transfer (micromoles per kilogram of water[1])											
Initial sites	Percent	Final site	Calcite	Dolomite	Gypsum	Halite	Fluorite	Rhyolite volcanic glass	Basalt volcanic glass	Plag An_{25}	Plag An_{60}	Potassium feldspar	Ammonium nitrate	Calcium montmorillonite
1, 3	15, 85	2	25	88	6	6	–	199	–	18	–	–	–	–
1, 3	16, 84	2	26	88	7	–	–	189	–	25	–	–	–	-31
1, 3	16, 84	2	19	88	7	6	–	189	–	33	–	–	–	–
3, 8, 97	68, 3, 29	4	264	57	5	–	2	109	–	–	–	7	–	–
3, 8, 97	67, 4, 29	4	269	57	–	–	2	104	–	–	–	8	–	–
97	106	5	–	36	142	–	4	239	184	–	13	–	–	-55
97	106	5	–	41	133	4	4	208	172	30	–	–	–	–
97	106	5	–	44	124	–	4	210	160	39	–	–	–	–
4, 97	65, 35	5	–	63	20	19	4	148	36	66	–	–	–	–
4, 97	68, 32	5	–	63	18	21	4	229	33	–	46	–	–	-57
4, 97	78, 24	5	–	57	–	20	4	209	13	–	70	–	–	-70
4	100	5	–	65	–	24	3	103	16	42	21	–	–	-49
9	100	11	-198	–	5	29	1	–	119	–	135	–	–	-108
9	100	11	-192	–	5	29	1	–	–	80	137	–	–	–
9	100	11	-131	19	5	28	1	–	–	139	–	–	–	-74
9	100	11	-159	–	5	29	1	–	–	74	118	–	–	-120
9	100	11	-183	–	5	29	1	12	–	–	191	–	–	-132
9, 10	79, 21	11	-94	–	–	46	2	–	201	–	–	–	3	-26
9, 10	81, 19	11	-85	–	–	35	2	–	–	136	–	–	3	–
9, 10	83, 17	11	-127	–	–	35	2	–	–	–	147	–	3	-101
9, 10	83, 17	11	-74	–	–	35	2	–	–	134	–	–	3	-72
9, 10	95, 5	11	-141	25	4	31	1	–	34	115	–	–	–	–
13, 98	73, 27	14	-488	–	37	–	–	140	–	–	472	–	–	–
13, 98	73, 27	14	-489	–	37	–	–	140	–	–	472	–	–	–
10, 98	43, 57	15	-994	–	82	–	1	235	–	–	647	–	18	–
10, 98	56, 44	15	-641	–	81	–	1	217	–	–	411	–	16	-302
10, 98	66, 34	15	-365	–	81	140	1	190	–	–	231	–	15	–
10, 98	68, 32	15	-261	–	80	131	1	171	–	–	160	–	15	-126
10, 14	23, 77	15	-723	–	42	–	1	164	–	–	575	–	6	–
10, 14	40, 60	15	-449	–	50	–	1	162	–	–	369	–	6	-269
10, 14	52, 48	15	-271	–	56	113	1	161	–	–	235	–	7	–
10, 14	54, 46	15	-204	–	57	86	1	161	–	–	185	–	8	-142
10, 14	58, 42	15	-67	48	50	167	1	119	–	–	–	–	10	-11
10, 14	58, 42	15	-171	100	50	171	1	119	–	–	–	–	10	–
10, 14	58, 42	15	-171	100	50	167	1	119	–	–	–	–	10	-11
10, 14	58, 42	15	-71	50	50	171	1	119	–	–	–	–	10	–
11, 99	50, 50	16	-90	51	125	125	2	33	–	82	–	–	75	-47
11, 99	70, 30	16	-112	–	129	85	1	49	–	–	137	–	70	-99
11, 15	72, 28	17	56	–	6	44	3	–	–	–	–	–	16	–
11, 15	69, 31	17	51	–	–	36	3	1	–	–	–	–	13	–
16, 17, 99	13, 49, 38	18	4	–	–	–	97	–	–	108	–	–	27	–
16, 17, 99	14, 49, 37	18	–	–	40	–	5	82	–	–	74	–	27	–
16, 17, 99	17, 47, 36	18	–	–	36	–	5	–	152	–	–	–	25	–
16, 17, 99	17, 47, 36	18	–	26	37	–	5	–	–	61	–	–	28	–
16, 17, 99	17, 47, 36	18	–	29	37	–	5	–	–	58	–	–	28	-31
16, 17, 99	17, 47, 36	18	–	–	36	–	6	–	152	–	–	–	25	-20
16, 17, 99	20, 45, 35	18	–	22	35	–	6	–	94	–	–	–	27	–

Table 11. Geochemical mass-balance modeling results, Beaver and Camas Creek drainage basins, eastern Idaho.—Continued

[Initial and final sites (solutions) are shown in figure 18. Percent solution indicates the amount of initial solution(s) required to produce the final solution. Positive and negative phase mass transfers indicate dissolution and precipitation, respectively. Gray shading indicates an implausible model result. **Abbreviations**: Plag An_{25}, plagioclase with compostion An_{25}; Plag An_{60}, plagioclase with composition An_{60}; –, phase not required by model]

Solution			Phase mass transfer (micromoles per kilogram of water[1])											
Initial sites	Percent	Final site	Sodium montmorillonite	Kaolinite	Goethite	Calcium chloride	Magnesium chloride	Calcium exchange	Sodium exchange	Pyrite	Organic matter	Nitrogen	Carbon dioxide	Oxygen
1, 3	15, 85	2	–	-33	-1	–	–	–	–	–	–	–	–	-119
1, 3	16, 84	2	–	–	-1	–	–	–	–	–	–	–	–	-115
1, 3	16, 84	2	-35	–	-1	–	–	–	–	–	–	–	–	-116
3, 8, 97	68, 3, 29	4	-13	–	-1	–	–	–	–	–	230	–	–	–
3, 8, 97	67, 4, 29	4	-13	–	-3	–	–	–	–	2	221	–	–	–
97	106	5	–	–	–	–	–	–	–	-71	522	-2	–	–
97	106	5	-58	–	–	–	–	–	–	-66	512	-2	–	–
97	106	5	-61	–	–	–	–	–	–	-62	501	-2	–	–
4, 97	65, 35	5	-54	–	–	–	–	–	–	-13	278	-11	–	–
4, 97	68, 32	5	–	–	–	–	–	–	–	-12	273	-11	–	–
4, 97	78, 24	5	–	–	–	–	–	–	–	-4	245	-13	–	–
4	100	5	–	–	–	–	–	–	–	-5	234	-16	–	–
9	100	11	–	–	-47	–	–	–	–	–	–	–	–	–
9	100	11	-137	–	-1	–	–	–	–	–	–	–	–	–
9	100	11	–	–	-1	–	–	–	–	–	–	–	–	–
9	100	11	–	–	-1	–	–	–	–	–	–	–	–	–
9	100	11	–	–	-1	–	–	–	–	–	–	–	–	–
9, 10	79, 21	11	–	–	-79	–	–	–	–	–	–	–	–	–
9, 10	81, 19	11	-73	–	-1	–	–	–	–	–	–	–	–	–
9, 10	83, 17	11	–	–	-1	–	–	–	–	–	–	–	–	–
9, 10	83, 17	11	–	–	-1	–	–	–	–	–	–	–	–	–
9, 10	95, 5	11	-66	–	-14	–	–	–	–	–	–	–	–	–
13, 98	73, 27	14	-337	–	–	35	–	–	–	–	–	–	–	84
13, 98	73, 27	14	-337	–	–	–	35	–	–	–	–	–	–	84
10, 98	43, 57	15	-466	–	-1	154	–	–	–	–	–	–	–	–
10, 98	56, 44	15	–	–	-1	156	–	–	–	–	–	–	–	–
10, 98	66, 34	15	-176	–	-1	–	77	–	–	–	–	–	–	–
10, 98	68, 32	15	–	–	-1	–	90	–	–	–	–	–	–	–
10, 14	23, 77	15	-410	–	-1	132	–	–	–	–	–	–	–	–
10, 14	40, 60	15	–	–	-1	139	–	–	–	–	–	–	–	–
10, 14	52, 48	15	-177	–	-1	–	86	–	–	–	–	–	–	–
10, 14	54, 46	15	–	–	-1	–	91	–	–	–	–	–	–	–
10, 14	58, 42	15	–	–	-1	–	52	–	–	–	–	–	–	–
10, 14	58, 42	15	-11	–	-1	50	–	–	–	–	–	–	–	–
10, 14	58, 42	15	–	–	-1	52	–	–	–	–	–	–	–	–
10, 14	58, 42	15	-11	–	-1	–	50	–	–	–	–	–	–	–
11, 99	50, 50	16	–	–	-1	–	–	–	–	–	–	–	–	257
11, 99	70, 30	16	–	–	-1	–	–	–	–	–	–	–	–	229
11, 15	72, 28	17	–	–	–	–	–	–	–	–	–	–	–	–
11, 15	69, 31	17	–	–	–	–	–	–	–	–	–	–	–	–
16, 17, 99	13, 49, 38	18	-56	–	-1	–	–	–	–	–	–	–	–	–
16, 17, 99	14, 49, 37	18	-59	–	-1	–	–	–	–	–	–	–	–	–
16, 17, 99	17, 47, 36	18	-20	–	-60	–	–	–	–	–	–	–	–	–
16, 17, 99	17, 47, 36	18	-32	–	-1	–	–	–	–	–	–	–	–	–
16, 17, 99	17, 47, 36	18	–	–	-1	–	–	–	–	–	–	–	–	–
16, 17, 99	17, 47, 36	18	–	–	-60	–	–	–	–	–	–	–	–	–
16, 17, 99	20, 45, 35	18	-12	–	-37	–	–	–	–	–	–	–	–	–

Table 11. Geochemical mass-balance modeling results, Beaver and Camas Creek drainage basins, eastern Idaho.—Continued

[Initial and final sites (solutions) are shown in figure 18. Percent solution indicates the amount of initial solution(s) required to produce the final solution. Positive and negative phase mass transfers indicate dissolution and precipitation, respectively. Gray shading indicates an implausible model result. **Abbreviations**: Plag An_{25}, plagioclase with compostion An_{25}; Plag An_{60}, plagioclase with composition An_{60}; –, phase not required by model]

Solution			Phase mass transfer (micromoles per kilogram of water[1])											
Initial sites	Percent	Final site	Calcite	Dolomite	Gypsum	Halite	Fluorite	Rhyolite volcanic glass	Basalt volcanic glass	Plag An_{25}	Plag An_{60}	Potassium feldspar	Ammonium nitrate	Calcium montmorillonite
16, 17, 99	26, 40, 34	18	–	50	26	–	6	73	–	–	–	–	23	-7
16, 17, 99	27, 40, 33	18	–	49	26	–	6	73	–	–	–	–	23	–
16, 17, 99	27, 40, 33	18	–	40	26	–	6	93	–	–	–	–	22	–
16, 17, 99	43, 28, 29	18	100	–	–	–	6	66	–	–	–	–	15	–
16, 17, 99	43, 28, 29	18	100	–	–	–	6	66	–	–	–	–	15	-6
99	100	19	355	342	90	141	6	159	265	–	354	–	62	-293
99	100	19	350	369	90	141	6	203	–	–	412	–	62	-214
99	100	19	555	369	90	142	6	150	–	182	–	–	62	-112
99	100	19	642	369	90	141	6	225	–	–	–	–	62	–
99	100	19	644	369	90	141	6	247	–	–	–	–	62	-24
99	148	19	419	275	83	127	4	–	–	128	–	–	62	-69
99	155	19	461	261	81	125	4	–	–	–	–	–	62	–
99	155	19	461	261	81	125	4	–	–	–	–	–	62	
99	164	19	259	245	80	122	4	–	–	–	250	–	62	-172
18, 99	44, 95	19	329	228	48	74	–	–	–	–	208	–	35	-143
18, 99	44, 95	19	472	228	48	74	–	–	–	–	–	–	35	–
18, 99	44, 95	19	472	228	48	74	–	–	–	–	–	–	35	-1
18, 99	47, 80	19	473	245	47	85	–	–	–	57	–	–	33	-31
18, 99	55, 45	19	405	287	44	71	–	156	–	–	270	–	28	-201
18, 99	55, 45	19	591	287	44	71	–	121	–	–	–	–	28	–
18, 99	55, 45	19	591	287	44	71	–	144	–	–	–	–	28	-14
19, 99	36, 64	20	-191	61	43	193	6	2	368	56	–	–	14	-78
19, 99	39, 61	20	-307	–	45	185	6	–	459	–	225	–	9	-213
19, 99	52, 48	20	-701	–	34	165	5	–	440	–	586	–	–	–
19, 99	55, 45	20	-336	–	26	167	5	–	327	–	–	–	–	–
19, 99	57, 43	20	-336	–	29	159	5	–	111	118	–	–	–	–
19, 99	57, 43	20	-354	–	24	164	5	–	284	–	–	–	–	–
19, 99	59, 41	20	-312	–	28	157	5	73	–	128	–	–	–	-76
19, 99	59, 41	20	-354	–	27	157	5	73	–	–	113	–	–	–
19, 99	59, 41	20	-301	–	27	157	5	73	–	60	–	–	–	–
19, 99	59, 41	20	-323	–	28	157	5	73	–	128	–	–	–	–
19, 99	56, 47	20	-359	–	25	167	4	72	275	128	–	–	–	–

Table 11. Geochemical mass-balance modeling results, Beaver and Camas Creek drainage basins, eastern Idaho.—Continued

[Initial and final sites (solutions) are shown in figure 18. Percent solution indicates the amount of initial solution(s) required to produce the final solution. Positive and negative phase mass transfers indicate dissolution and precipitation, respectively. Gray shading indicates an implausible model result. **Abbreviations**: Plag An_{25}, plagioclase with compostion An_{25}; Plag An_{60}, plagioclase with composition An_{60}; –, phase not required by model]

Solution			Phase mass transfer (micromoles per kilogram of water[1])											
Initial sites	Percent	Final site	Sodium montmorillonite	Kaolinite	Goethite	Calcium chloride	Magnesium chloride	Calcium exchange	Sodium exchange	Pyrite	Organic matter	Nitrogen	Carbon dioxide	Oxygen
16, 17, 99	26, 40, 34	18	–	–	-1	–	–	–	–	–	–	–	–	–
16, 17, 99	27, 40, 33	18	-7	–	-1	–	–	–	–	–	–	–	–	–
16, 17, 99	27, 40, 33	18	-12	–	-36	–	–	–	–	–	–	–	–	–
16, 17, 99	43, 28, 29	18	-6	–	-1	–	–	–	–	–	–	–	–	–
16, 17, 99	43, 28, 29	18	–	–	-1	–	–	–	–	–	–	–	–	–
99	100	19	–	–	-104	–	–	–	–	–	86	–	2,595	–
99	100	19	–	-102	-1	–	–	–	–	–	98	–	2,535	–
99	100	19	–	–	-1	–	–	–	–	–	98	–	2,331	–
99	100	19	–	-25	-1	–	–	-81	163	–	98	–	2,243	–
99	100	19	–	–	-1	–	–	-81	161	–	98	–	2,241	–
99	148	19	–	–	-1	–	–	–	–	–	240	–	1,762	–
99	155	19	–	-1	-1	–	–	-55	110	–	262	–	1,613	–
99	155	19	–	–	-1	–	–	-55	110	–	262	–	1,613	–
99	164	19	–	–	-1	–	–	–	–	–	286	–	1,695	–
18, 99	44, 95	19	–	–	-1	–	–	–	–	–	250	–	1,799	–
18, 99	44, 95	19	–	-1	-1	–	–	-42	83	–	250	–	1,657	–
18, 99	44, 95	19	–	–	-1	–	–	-42	83	–	250	–	1,657	–
18, 99	47, 80	19	–	–	-1	–	–	–	–	–	218	–	1,797	–
18, 99	55, 45	19	–	–	-1	–	–	–	–	–	144	–	2,250	–
18, 99	55, 45	19	–	-13	-1	–	–	-55	111	–	144	–	2,063	–
18, 99	55, 45	19	–	–	-1	–	–	-55	109	–	144	–	2,063	–
19, 99	36, 64	20	–	–	-144	–	–	–	–	–	–	–	–	–
19, 99	39, 61	20	–	–	-179	–	–	–	–	–	–	–	–	–
19, 99	52, 48	20	-459	–	-172	–	–	–	–	–	–	–	–	–
19, 99	55, 45	20	-42	–	-128	–	–	–	–	–	–	–	-606	–
19, 99	57, 43	20	-78	–	-43	–	–	–	–	–	–	–	-674	–
19, 99	57, 43	20	–	-43	-111	–	–	–	–	–	–	–	-668	–
19, 99	59, 41	20	–	–	-1	–	–	–	–	–	–	–	-729	–
19, 99	59, 41	20	–	-99	-1	–	–	–	–	–	–	–	-728	–
19, 99	59, 41	20	–	-46	-1	–	–	–	–	–	–	–	-781	–
19, 99	59, 41	20	-76	–	-1	–	–	–	–	–	–	–	-742	–
19, 99	56, 47	20	-42	–	-108	–	–	–	–	–	–	–	-669	–

[1]For solutions or mixtures of solutions that were evaporated: micromoles/kilograms of water where kilograms of water = sum of percent of initial solution(s)/100.

Measurements of δ^2H, $\delta^{18}O$, and $\delta^{13}C$ were available for all sources of water to site 4, except from the eastern part of Camas Meadows (table 7), and stable isotopes were initially included as constraints in the geochemical models. The lighter δ^2H and $\delta^{18}O$ values at both sites 1 and 4, relative to the δ^2H and $\delta^{18}O$ values of the other groundwater samples, may indicate that these sites share a common source of recharge, with the most likely shared source coming from the Centennial Mountains northeast of site 4. Groundwater chemistry was not available for the eastern part of Camas Meadows, so groundwater at site 4 was initially modeled as a mixture of groundwater from site 3 and surface water from Camas Creek (site 97). Using just these two initial waters did not produce any successful models.

A model mixing groundwater from sites 3 and 8 and surface water from Camas Creek (site 97) was tested and resulted in two successful models (fig. 18, table 11). These models were only successful after removing the stable isotopes of hydrogen and oxygen as constraints (stable isotopes of carbon were included in the models), which provided additional support for a source of water to site 4 from the eastern part of Camas Meadows. The percentage of solutions in the models was 67–68 percent groundwater from site 3, 3–4 percent groundwater from site 8, and 29 percent from Camas Creek (table 11). The models required carbonate reactions (dissolution of calcite and dolomite), oxidation-reduction reactions (oxidation of organic matter), silicate weathering (dissolution of rhyolitic volcanic glass and potassium feldspar), dissolution of a sulfur mineral (gypsum or pyrite), and precipitation of clays. The dominant dissolving phases were calcite (264–269 µmol/kg water) and organic matter (221–230 µmol/kg water). Groundwater at site 4 had a $\delta^{34}S$ of -3.2, which indicates that dissolution of sulfide minerals was a larger source of sulfate in this groundwater than the dissolution of sulfate minerals. For this reason, the model requiring oxidation of pyrite was preferred over the model requiring dissolution of gypsum.

The small amount of groundwater from site 8 in the models may indicate that the chemical composition of water from this site, which appears to be influenced by dissolution of rhyolite minerals, is not representative of groundwater from the West Camas Creek valley (fig. 2). Groundwater in the West Camas Creek valley may be more influenced by dissolution of carbonate rocks. The model also required dissolution of potassium feldspar. The dissolution of potassium feldspar, plus the mixing of a small fraction of water from site 8, may indicate that the chemistry of groundwater from the eastern part of Camas Meadows is more influenced by dissolution of rhyolite than groundwater from site 3.

Site 5.—Site 5 is located in basalt of the ESRP, underlies wetlands in the southern part of Camas Meadows, and is downgradient of site 4 (fig. 18). Surface water and groundwater potentially flow to site 5 through alluvium in Camas Meadows and basalt and interbedded sediment of the ESRP aquifer. The chemistry of groundwater at site 5 was modeled as evolving from groundwater from site 4 or as a mixture of groundwater from site 4 and surface water from Camas Creek (site 97). Measurements of δ^2H, $\delta^{18}O$, and $\delta^{13}C$ were available for all these waters (table 7) and were included as constraints in the geochemical models.

Groundwater at site 5 was anoxic, had an undetectable concentration of nitrate, and had larger manganese and iron concentrations and smaller sulfate concentrations than groundwater from site 4 (tables 3–6). The change in water chemistry between sites 4 and 5 was consistent with aerobic oxidation of organic matter and pyrite followed by anaerobic reduction of nitrate (denitrification), manganese oxide, iron oxyhydroxide, and sulfate. Pyrite precipitation was modeled to occur along with sulfate reduction. (A pe of -4, a redox value appropriate for water where sulfate reduction is occurring, was assigned to solution 5. This pe was low enough to ensure that dissolved ferrous iron would be stable in the solution.) Evaporation (conceptually of Camas Creek, but the model evaporates the mixture of initial solutions) also was modeled, because the δ^2H and $\delta^{18}O$ values from site 5 plotted to the right of the local winter meteoric water line.

Mixing of groundwater from site 4 with water from Camas Creek (site 97) and evaporation of the mixture produced six successful models; in three of the models, water from Camas Creek was the sole initial water. Modeling of groundwater from site 4 as the only initial solution produced one successful model (table 11). Evaporation was simulated for four of the mixing models and ranged from 2 to 6 percent evaporation. Because groundwater from site 5 was anoxic and groundwater at site 4 was confined, a continual source of water to site 5 with a large concentration of DO, such as Camas Creek (8 mg/L), seemed implausible. Consequently, the models that included Camas Creek as an initial solution were considered implausible. The sole remaining model included only groundwater from site 4 as an initial solution.

In addition to the oxidation-reduction reactions described above, solutes in groundwater from site 5 were derived from carbonate reactions (dissolution of dolomite), dissolution of evaporite minerals (halite, fluorite), and silicate weathering [volcanic glass (from rhyolite and basalt) and plagioclase (An_{25} and An_{60})]. Dissolution of volcanic glass from rhyolite (103 µmol/kg water) and organic matter (234 µmol/kg water) contributed the largest amounts of solutes to solution.

Dolomite, not calcite, was the carbonate mineral that the models show as dissolving. This was because the concentration of calcium between sites 4 and 5 remained the same while the concentration of magnesium, from dissolution of dolomite, increased. Calcite and dolomite were both undersaturated in groundwater from site 4 (negative SIs in table 10), but calcite was at equilibrium with groundwater from site 5 (SI = 0.04) while dolomite

remained undersaturated (SI = -0.51). This could be caused by dissolution of dolomite (reactions with calcite are probable too, even if not required for a successful model). For example, the ion activity product (IAP) of calcite can be expressed as (Drever, 1997, p. 53–54)

$$IAP = \frac{\left[Ca^{2+}\right]\left[HCO_3^-\right]^2}{P_{CO_2}} \quad (5)$$

where

$\left[Ca^{2+}\right]$ is the activity of calcium in solution,

$\left[HCO_3^-\right]$ is the activity of bicarbonate in solution, and

P_{CO_2} is the fugacity (partial pressure at environmental conditions) of carbon dioxide.

The solution becomes more saturated with respect to calcite as IAP increases, which occurs when calcium and/or bicarbonate concentrations increase and/or the partial pressure of CO_2 decreases. All these changes in concentration can occur when dolomite dissolves. For example, between sites 4 and 5, weathering of silicate minerals and dissolution of dolomite added bicarbonate to groundwater and consumed more CO_2 than oxidation of organic matter produced. However, the calcium concentration in groundwater between the two sites did not change, as calcium entering solution from dissolution of dolomite and plagioclase was balanced by precipitation of calcium montmorillonite. The result of the increased bicarbonate and decreased CO_2 in solution was that calcite became saturated in the groundwater (while dolomite remained undersaturated).

Site 9.—Site 9 is located in basalt on the ESRP. This site appears to be downgradient of site 5 in Camas Meadows (fig. 18). Water probably flows to site 9 through basalt and interbedded sediment of the ESRP aquifer. No successful models were produced when modeling groundwater at site 9 with groundwater from site 5 or as a mixture of groundwater from site 5 with surface water from Camas Creek (site 97). Groundwater was then modeled by using all possible combinations of solutions and mixtures of groundwater from sites 2, 3, 4, 5, 8 and 10 and surface water from Camas Creek. None of these combinations were able to produce a successful model. Modeling the transition of groundwater from Camas Meadows to the ESRP at site 9, given the complicated hydrology of this transition zone and the range of groundwater chemistry observed and hypothesized in Camas Meadows, requires additional water chemistry from Camas Meadows and the ESRP.

Site 11.—Site 11 is located in basalt on the ESRP and is downgradient of sites 9 and 10 (fig. 18). Water flows to this site through basalt and interbedded sediment of the ESRP aquifer. Ten successful models were produced by using groundwater from sites 9 and 10 as initial solutions, with five models consisting of an initial solution of groundwater from site 9 and five models consisting of an initial solution that was a mixture of groundwater from sites 9 and 10. These models included carbonate reactions (precipitation of calcite and dissolution of dolomite), silicate weathering [dissolution of volcanic glass (rhyolite and basalt) and plagioclase (An_{60} and An_{25})], and dissolution of evaporite minerals. The dominant dissolving phases were plagioclase (118–191 µmol/kg water for An_{60}, 74–139 µmol/kg water for An_{25}) and the dominant precipitating phases were calcite (74–198 µmol/kg water) and calcium montmorillonite (26–132 µmol/kg water).

Site 13.—Site 13 is located at Spencer, in basalt of the ESRP, at the mouth of the canyon between the Beaverhead and Centennial Mountains formed by Beaver Creek. Sources of water to this site are surface water from Beaver Creek (site 98) and groundwater from the Beaverhead and Centennial Mountains. Chemistry data for groundwater from the Centennial Mountains that flows to site 13 were not available, and groundwater chemistry was only available from one site (site 12) in the Beaverhead Mountains (fig. 18). Groundwater from site 12 appears to be most influenced by dissolution of dolomite, although groundwater from site 13 appears to be influenced by dissolution of limestone and silicate minerals (fig. 11). Modeling groundwater from site 12 to site 13, or as a mixture of groundwater from site 12 and site 8 (groundwater from the Centennial Mountains but in the Camas Creek, not Beaver Creek, drainage basin) with surface water from Beaver Creek, did not produce any successful models. Additional water chemistry data are needed from the Beaver Creek drainage basin to produce a successful model.

Site 14.—Site 14 is located in basalt on the ESRP and is downgradient of site 13 (fig. 18). Sources of water to site 14 are surface water from Beaver Creek (site 98) and groundwater from site 13. Water flows to site 14 through basalt and sediment of the ESRP.

The chemistry of groundwater at site 14 was modeled successfully with two models containing a mixture of groundwater from site 13 (73 percent) and surface water from Beaver Creek (27 percent). Oxygen was included as a phase in the models to account for possible infiltration of water from Beaver Creek during spring runoff, when the creek would be cold and contain more oxygen than the chemistry analysis for Beaver Creek used in the model. The model included carbonate reactions (precipitation of calcite, 488–489 µmol/kg water), silicate weathering [dissolution of rhyolitic volcanic glass (140 µmol/kg water) and plagioclase (An_{60}, 472 µmol/kg water)], and small amounts of dissolution of gypsum and road anti-icing liquid.

Site 15.—Possible sources of water to site 15, which is located in basalt on the ESRP, were groundwater from site 14 and surface water from Beaver Creek (site 98). Water flows to site 15 through basalt and surficial and interbedded sediment of the ESRP.

No successful models were produced by mixing groundwater from site 14 with surface water from Camas Creek. Consequently, it was suspected that water may flow to site 15 from the ESRP aquifer north of site 15. Water chemistry data were not available from the ESRP aquifer north of site 15, so the chemistry of groundwater from site 10 was used to represent a hypothetical composition of groundwater from this area. Twelve successful models were produced when groundwater from site 10 was included in the model simulations. Eight of these models were a mixture of groundwater from the hypothetical solution (site 10) and site 14 and four were a mixture of site 10 and Beaver Creek. The mixtures with Beaver Creek were considered implausible because, based on tritium values, water at site 15 consists of pre-1952 water. Two of the mixtures with groundwater from sites 10 and 14 were considered implausible due to their large mass transfer amounts of calcite (449–723 µmol/kg water), plagioclase (369–575 µmol/kg water), and clay (269–410 µmol/kg water). For the remaining six models, site 10 contributed 52–58 percent of the water to site 15 and site 14 contributed 42–48 percent of the water.

Important dissolving phases in the models were rhyolitic volcanic glass (119–161 µmol/kg water) and evaporite minerals. Other notable dissolving phases were small amounts of ammonium nitrate (7–10 µmol/kg water), indicating leaching of inorganic fertilizer or manure from agricultural practices, and road anti-icing liquids (50–91 µmol/kg water). Calcite (67–271 µmol/kg water) was an important precipitating phase.

Dissolution of evaporite minerals was important in all these models, and a large source for evaporite minerals in this area could be evaporite deposits from Pleistocene Lake Terreton. The depths to water at sites 14 and 15 were about 670 and 450 ft BLS, respectively. Since evaporite deposits from Lake Terreton and eruption of basalt flows in the northeastern part of the ESRP both occurred during the Pleistocene (Kuntz and others, 1992; Geslin and others, 2002), evaporite deposits at 400–700 ft depths is possible. Gypsum inferred to be from evaporite deposits from Lake Terreton was observed as deep as 740 ft BLS in the northern part of the INL (Geslin and others, 2002, p. 25). The chemistry and geochemical modeling of groundwater at site 15 indicates that evaporite deposits at depth extend farther north than surficial sediments in the area (fig. 5). Dissolution of gypsum in the models ranged from 50 to 57 µmol/kg water and dissolution of halite in the models ranged from 86 to 171 µmol/kg water.

Site 16.—Site 16 was located in basalt on the ESRP, was close to Camas Creek, and appeared to be downgradient of site 11 (fig. 18). Sources of water to site 16 are surface water from Camas Creek (site 99) and groundwater from site 11. Water flows to site 16 through basalt and surficial and interbedded sediment of the ESRP.

No successful models were produced when modeling groundwater from site 11 as the sole source of water to site 16, but two successful models were produced when groundwater at site 16 was modeled as a mixture of groundwater from site 11 (50 and 70 percent) and surface water from Camas Creek (50 and 30 percent). The model indicates that gypsum (125 and 129 µmol/kg water) and halite (85 and 125 µmol/kg water) dissolve. The source of these evaporite minerals probably was evaporite deposits from Lake Terreton, which indicates that evaporite deposits at depth may extend several miles farther east than surficial sediment in the area (fig. 5). Other phases that dissolved were plagioclase (An_{60} or An_{25}), rhyolitic volcanic glass (33 and 49 µmol/kg water), and ammonium nitrate (70 and 75 µmol/kg water). Dissolution of ammonium nitrate indicates leaching of nitrate at the land surface due to agricultural practices. Calcite (90 and 112 µmol/kg water) and calcium montmorillonite (47 and 99 µmol/kg water) were modeled as precipitating.

Site 17.—Site 17 was located in basalt of the ESRP. The source of water to this site, based on water-table contours (fig. 18), appears to be groundwater from site 15. Water flows to site 17 through basalt and interbedded sediment of the ESRP aquifer.

No successful models were produced when site 15 was the only initial solution modeled. However, the low hydraulic gradient in the area south of Dubois reflects the relatively flat water table in this area, and the direction of movement of groundwater from site 11 is uncertain. Consequently, groundwater from site 11, which was used to model groundwater at site 16, was also considered a possible source of water to site 17.

Two models reproducing the chemistry of groundwater at site 17 were produced by mixing groundwater from sites 11 (69–72 percent) and 15 (28–31 percent). Reproducing the groundwater chemistry at site 17 required small amounts of dissolution of calcite (51 and 56 µmol/kg water), halite (36–44 µmol/kg water), ammonium nitrate (13–16 µmol/kg water), gypsum, fluorite, and rhyolitic volcanic glass.

Site 18.—Site 18, which has a depth to water of about 16 ft, is located in basalt of the ESRP at the northern extent of the CNWR. Sources of water to this site are surface water from Camas Creek (site 99) and groundwater from sites 16 and 17. Water flows to site 18 through basalt and surficial and interbedded sediment of the ESRP.

Carbon dioxide was included as a phase in the models, but was only allowed to precipitate since the partial pressure of CO_2 in groundwater from site 18 was smaller than the partial pressure of CO_2 in water from sites 16, 17, and 99. To provide a more accurate mass transfer amount of CO_2 in the model, the DO content of Camas Creek was adjusted to 9.4 mg/L. This DO value represents 100 percent saturation of the stream at 10°C, and both values are more representative

of the temperature and DO content in the stream during the spring when most infiltration from the stream would occur.

Twelve models were produced that successfully modeled groundwater at site 18 as a mixture of groundwater from sites 16 (13–43 percent) and 17 (28–49 percent) and surface water from Camas Creek (29–38 percent). Recharge to site 18 from Camas Creek is supported by the tritium value for this site (13.3±2.1 pCi/L), which indicates groundwater from site 18 contains a significant amount of post-1952 water. One of the models was considered implausible due to a large mass transfer of fluorite (97 µmol/kg water).

The models included various combinations of dissolution of carbonates, silicates, and evaporites. Dissolving phases included calcite (100 µmol/kg water) or dolomite (22–50 µmol/kg water), volcanic glass (rhyolite, 66–93 µmol/kg water; basalt, 94–152 µmol/kg water) and/or plagioclase (58–74 µmol/kg water), gypsum (26–40 µmol/kg water) and/or fluorite (5–6 µmol/kg water), and ammonium nitrate (15–28 µmol/kg water). The amount of fluorite dissolved in this model, as well as in the model for site 20, is noticeably larger than elsewhere in the study area and may represent dissolution of fluorite from evaporite deposits associated with Lake Terreton.

Site 19.—Site 19, located in basalt of the ESRP at the southern extent of wetlands in the CNWR, is downgradient of site 18. Potential sources of water to site 19 include groundwater from site 18 and surface water from Camas Creek (site 99) and ponds and lakes on the CNWR (water chemistry data were not available for the ponds and lakes at the CNWR). Water flows to site 19 through basalt and surficial and interbedded sediment of the ESRP. Evaporation of water was modeled, even though no δ^2H and $\delta^{18}O$ values were available for site 19, because the (1) δ^2H and the $\delta^{18}O$ values from Camas Creek and site 20, downgradient of site 19, plot to the right of the local winter meteoric water line (fig. 14) and (2) ponds and lakes on the CNWR provide opportunity for evaporation of surface water at the CNWR.

Carbon dioxide was included as a phase in the models, but was only allowed to dissolve because the partial pressure of CO_2 in groundwater from site 19 was much larger than the partial pressure of CO_2 in groundwater from site 18. This increase in CO_2 content may be a result of oxidation of organic matter and/or exchange of CO_2 with a CO_2-rich soil zone. The DO content of Camas Creek was adjusted to 9.4 mg/L for the same reasons as described for site 18.

Sixteen successful models were produced. Nine of the models only required Camas Creek as an initial solution, and these models were considered implausible because groundwater from site 19 does not appear to be from a perched water zone. The other seven models included mixing and evaporation of groundwater from site 18 (32–55 percent) and surface water from Camas Creek (45–68 percent) (mixing percentages of evaporated mixtures were normalized to 100 percent for the sum of the two initial solutions).

Reactions in all models were oxidation of organic matter (144–250 µmol/kg water), dissolution of calcite (329–591 µmol/kg water), dolomite (228–287 µmol/kg water), gypsum (44–48 µmol/kg water), halite (71–85 µmol/kg water), ammonium nitrate (28–35 µmol/kg water), and CO_2 (1,657–2,250 µmol/kg water). Some models included dissolution of rhyolitic volcanic glass and plagioclase (An_{60} and An_{25}), and sodium-calcium exchange was simulated in four models. The redox state of the water may not have proceeded beyond oxidation of organic matter due to the continual source of oxygen from infiltrating surface water. The large transfer of CO_2 into solution probably indicates that CO_2 in infiltrating surface water was in equilibrium with CO_2 from the soil zone. This infusion of CO_2 into the groundwater facilitated the large amounts of dissolution of calcite and dolomite.

Site 20.—Site 20 is located downgradient of site 19 in basalt of the ESRP. Potential sources of water to site 20 are groundwater from north of site 20, groundwater from site 19, and surface water from Camas Creek (site 99). Water flows to site 20 through basalt and surficial and interbedded sediment of the ESRP.

Water chemistry data were not available for groundwater north of site 20. However, the much smaller partial pressure of CO_2 in groundwater from site 20, relative to site 19, indicates that groundwater north of site 20 (and east of the CO_2-rich soil zone at the CNWR) may be a better source of groundwater to site 20 than groundwater from site 19. Evaporation of water from Camas Creek was modeled because the δ^2H and the $\delta^{18}O$ values from sites 99 and 20 plot to the right of the local winter meteoric water line (fig. 14).

Carbon dioxide was included as a phase in the models, but was only allowed to precipitate since the partial pressure of CO_2 in groundwater from site 20 was much smaller than the partial pressure of CO_2 in groundwater from site 19. The DO content of Camas Creek was adjusted to 9.4 for the same reasons as described for site 18.

Eleven models were produced that simulated groundwater at site 20 as a mixture of groundwater from site 19 and surface water from Camas Creek. Two of the models were considered implausible due to the large amount of surface water included in the models (61–84 percent), which was inconsistent with the tritium value of 8.6±1.9 pCi/L for groundwater from site 20. If greater than 60 percent of the water from site 20 was very recent recharge the tritium concentration in the groundwater probably would be greater than 15 pCi/L. Another model was considered implausible due to large mass transfers of minerals.

The remaining eight models were mixtures of groundwater from site 19 (54–59 percent) and surface water (41–46 percent) from Camas Creek. One model included evaporation (3.4 percent) of the mixture. The important chemical reactions were dissolution of plagioclase (60–128 µmol/kg water), volcanic glass (73 µmol/kg

water for rhyolite and 111–327 µmol/kg water for basalt), halite (157–167 µmol/kg water), gypsum (24–29 µmol/kg water), and fluorite (5 µmol/kg water); precipitation of calcite (301–359 µmol/kg water) and clay minerals (42–99 µmol/kg water); and exsolution of CO_2 (606–781 µmol/kg water). Calcite precipitation probably was a result of reduced partial pressure of CO_2 in the groundwater mixture, as CO_2 from groundwater with a large partial pressure of CO_2 (log PCO_2 of -1.68, site 19) mixed with a CO_2 reservoir with a smaller partial pressure of CO_2 (log PCO_2 of -2.86, site 99). It also is possible that calcite precipitation resulted from dissolved CO_2 in groundwater exchanging with a CO_2-poor unsaturated zone (log PCO_2 of -2.4 – -3.0 for the unsaturated zone of ESRP).

Summary of Geochemical Modeling Results.—Geochemical modeling results indicate that groundwater geochemistry was influenced by reactions with rocks of the geologic terranes—carbonate rocks, rhyolite, basalt, evaporite deposits (associated with Lake Terreton), and sediment comprised of all of these rocks. Agricultural practices near and south of Dubois and application of road anti-icing liquids to U.S. Interstate Highway 15 were likely sources of nitrate, chloride, calcium, and magnesium to groundwater.

Calcite was modeled as dissolving in groundwater at and near Camas Meadows (sites 2, 4, and 5), mostly precipitating from groundwater of the ESRP (sites 11, 14, 15, and 16), and dissolving in groundwater at the CNWR (sites 18 and 19); dolomite was modeled as dissolving in most of the groundwater. Silicate minerals believed to be important contributors of solutes to groundwater are volcanic glass and plagioclase. Volcanic glass with a rhyolitic composition is a more important contributor of solutes than volcanic glass with a basalt composition, particularly in areas immediately downgradient of rhyolite outcrops (fig. 5) in the Beaverhead (sites 14 and 15) and Centennial Mountains (sites 4 and 5) and Sheridan Ridge (site 2). Dissolution of the evaporite minerals gypsum and halite are important contributors of solutes in the Mud Lake-Dubois area (sites 15, 16, 19, and 20). Oxidation-reduction reactions are important influences on the chemistry of groundwater at Camas Meadows (sites 4 and 5) and the CNWR (site 19). Of these reactions, the primary geochemical processes controlling groundwater in the study area appear to be precipitation or dissolution of calcite and dissolution of silicate minerals. In addition, mixing of different groundwaters or surface water with groundwater appears to be an important physical process influencing the geochemical evolution of groundwater in much of the study area, and evaporation may be an important physical process influencing the geochemistry of groundwater at the CNWR (site 19).

Summary and Conclusions

The U.S. Geological Survey, in cooperation with the U.S. Department of Energy, is studying the fate and transport of waste solutes in the eastern Snake River Plain (ESRP) aquifer at the Idaho National Laboratory (INL) in eastern Idaho. This effort requires an understanding of the natural and anthropogenic geochemistry of groundwater at the INL and of the important physical and chemical processes controlling the geochemistry. In this study, the USGS applied geochemical modeling to investigate the geochemistry of groundwater in the Beaver and Camas Creek drainage basins, which provide groundwater recharge to the ESRP aquifer underlying the northeastern part of the INL.

Data used in this study include petrology and mineralogy from 2 sediment and 3 rock samples, and water-quality analyses from 4 surface-water and 18 groundwater samples. The mineralogy of the sediment and rock samples was analyzed with X-ray diffraction, and the mineralogy and petrology of the rock samples were examined in thin sections. The water samples were analyzed for field parameters, major ions, silica, nutrients, dissolved organic carbon, trace elements, tritium, and the stable isotope ratios of hydrogen, oxygen, carbon, sulfur, and nitrogen.

Physical and chemical processes that control the geochemistry of groundwater in the Beaver and Camas Creek drainage basins were investigated through analysis of the climate, geology, mineralogy, land cover and use, hydrology, and surface-water and groundwater chemistry in the study area. Groundwater geochemistry was influenced by reactions with rocks of the geologic terranes—carbonate rocks, rhyolite, basalt, evaporite deposits, and sediment comprised of all of these rocks. Agricultural practices near and south of Dubois, and application of road anti-icing liquids to U.S. Interstate Highway 15, were sources of nitrate, chloride, calcium, and magnesium to groundwater. Local recharge on the ESRP from streams was an important control on the saturation state of calcite in groundwater.

Groundwater in the Beaverhead Mountains was a magnesium-calcium bicarbonate type water and was older than groundwater from the Centennial Mountains or Camas Meadows. Groundwater from the Centennial Mountains and Camas Meadows was a calcium bicarbonate type water, and all groundwater from the ESRP was either a calcium bicarbonate or a calcium-magnesium bicarbonate type water. Groundwater in the Beaverhead Mountains had larger calcium, magnesium, sodium, bicarbonate, chloride, and sulfate concentrations than groundwater from the Centennial Mountains and Camas Meadows; groundwater from the Centennial Mountains and Camas Meadows had larger

silica and potassium concentrations than groundwater in the Beaverhead Mountains. Nitrate, sodium, chloride, and sulfate concentrations in groundwater of the ESRP increased as groundwater approached and moved south of Dubois. Nitrate increased due to leaching of inorganic fertilizer or manure, and sodium, chloride, and sulfate probably increased due to dissolution of evaporite deposits associated with Pleistocene Lake Terreton.

Groundwater geochemistry was successfully modeled in the alluvial aquifer in Camas Meadows and the ESRP fractured basalt aquifer using the geochemical modeling code PHREEQC. However, there were not enough groundwater sites with chemistry data to develop mass-balance models for groundwater in the Beaverhead and Centennial Mountains. The transition of groundwater from the mountains to the ESRP also was modeled at three areas, but the transition was only successfully modeled for a mixture of groundwater from Camas Meadows and Sheridan Ridge to the northeastern extent of the ESRP.

Geochemical modeling results indicate that the physical and chemical processes controlling the geochemistry of groundwater in the Beaver and Camas Creek drainage basins are carbonate reactions, silicate weathering, dissolution of evaporite minerals, oxidation-reduction reactions, surface-water recharge, mixing, and evaporation. The primary geochemical processes appear to be precipitation or dissolution of calcite and dissolution of primary silicate minerals. Calcite was modeled as dissolving in groundwater at and near Camas Meadows, mostly precipitating from groundwater of the ESRP, and dissolving in groundwater at the CNWR; dolomite was modeled as dissolving in most of the groundwater. Silicate minerals believed to be important contributors of solutes to groundwater are volcanic glass and plagioclase of intermediate compositions. Volcanic glass with a rhyolitic composition is a more important contributor of solutes than volcanic glass with a basalt composition, particularly in areas immediately downgradient of rhyolite in the Beaverhead and Centennial Mountains and Sheridan Ridge. Dissolution of the evaporite minerals gypsum and halite are important contributors of solutes in the Mud Lake-Dubois area. Oxidation-reduction reactions are important influences on the chemistry of groundwater at Camas Meadows and the Camas National Wildlife Refuge. In addition, mixing of different groundwaters or surface water with groundwater appears to be an important physical process influencing the geochemical evolution of groundwater in much of the study area, and evaporation may be an important physical process influencing the geochemistry of groundwater at the Camas National Wildlife Refuge. The mass-balance modeling results from this study provide an explanation of the natural geochemistry of groundwater in the ESRP northeast of the INL, and thus provide a starting point for evaluating the natural and anthropogenic geochemistry of groundwater at the INL.

References Cited

Ackerman, D.J., Rattray, G.W., Rousseau, J.P., Davis, L.C., and Orr, B.R., 2006, A conceptual model of ground-water flow in the eastern Snake River Plain aquifer at the Idaho National Laboratory and vicinity with implications for contaminant transport: U.S. Geological Survey Scientific Investigations Report 2006-5122 (DOE/ID-22198), 62 p.

American Public Health Association, American Water Works Association, and Water Environment Federation, 1998, Standard methods for the examination of water and wastewater (20th edition): Washington, D.C., American Public Health Association, American Water Works Association, and Water Environment Federation, variously paged.

Appelo, C.A.J., and Postma, D., 2005, Geochemistry, groundwater, and pollution, 2nd ed.: Leiden, The Netherlands, A.A. Balkema Publishers, 649 p.

Barraclough, J.T., Robertson, J.B., and Janzer, V.J., 1976, Hydrology of the solid waste burial ground, as related to the potential migration of radionuclides, Idaho National Engineering Laboratory: U.S. Geological Survey Open-File Report 76-471 (IDO-22056), 183 p.

Bartholomay, R.C., 1990a, Mineralogy, petrology and grain size of surficial sediment from the Big Lost River, Little Lost River, and Birch Creek drainages, Idaho National Engineering Laboratory, Idaho: Pocatello, Idaho State University, M.S. thesis, 118 p.

Bartholomay, R.C., 1990b, Mineralogical correlation of surficial sediment from area drainages with selected sedimentary interbeds at the Idaho National Engineering Laboratory, Idaho: U.S. Geological Survey Water-Resources Investigations Report 90-4147 (DOE/ID-22092), 18 p.

Benjamin, Lyn, Knobel, L.L., Hall, L.F., Cecil, L.D., and Green, J.R., 2004, Development of a local meteoric water line for southeastern Idaho, western Wyoming, and south-central Montana: U.S. Geological Survey Scientific Investigations Report 2004-5126 (DOE/ID-22191), 17 p.

Brenton, R.W., and Arnett, T.L., 1993, Methods of analysis by the U.S. Geological Survey National Water Quality Laboratory—Determination of dissolved organic carbon by UV-promoted persulfate oxidation and infrared spectrometry: U.S. Geological Survey Open-File Report 92-480, 12 p.

Brockway, C.E., and Robinson, C.W., 1988, Water resources data and management model for Beaver Creek, Camas Creek and the Mud Lake area of eastern Idaho: Moscow, University of Idaho, Idaho Water Resources Research Institute, variously paged.

Busenberg, Eurybiades, Weeks, E.W., Plummer, L.N., and Bartholomay, R.C., 1993, Age dating ground water by use of chlorofluorocarbons (CCL_3F and CCl_2F_2), and distribution of chlorofluorocarbons in the unsaturated zone, Snake River Plain aquifer, Idaho National Engineering Laboratory, Idaho: U.S. Geological Survey Water-Resources Investigations Report 93-4054 (DOE/ID-22107), 47 p.

Busenberg, Eurybiades, Plummer, L.N., and Bartholomay, R.C., 2001, Estimated age and source of the young fraction of ground water at the Idaho National Engineering and Environmental Laboratory: U.S. Geological Survey Water-Resources Investigations Report 01-4265 (DOE/ID-22177), 144 p.

Carkeet, Colleen, Rosentreter, J.J., Bartholomay, R.C., and Knobel, L.L., 2001, Geochemistry of the Big Lost River drainage basin, Idaho: U.S. Geological Survey Water-Resources Investigations Report 01-4031 (DOE/ID-22174), 31 p.

Carlson, Rick, Eliopulos, Gus, and Fox, Jessica, 2002, Ground water quality monitoring results of Mud Lake area in Jefferson County, Idaho: Idaho Department of Agriculture, Technical Results Summary no. 10, 4 p.

Childress, C.J.O., Foreman, W.T., Conner, B.F., and Maloney, T.J., 1999, New reporting procedures based on long-term method detection levels and some considerations for interpretations of water-quality data provided by the U.S. Geological Survey National Water Quality Laboratory: U.S. Geological Survey Open-File Report 99-193, 19 p. (Also available at http://pubs.er.usgs.gov/publication/ofr99193.)

Christiansen, R.L., 1982, Late Cenozoic volcanism of the Island Park area, eastern Idaho, *in* Bonnichsen, Bill, and Breckenridge, R.M., eds., Cenozoic geology of Idaho: Idaho Bureau of Mines and Geology Bulletin 26, p. 345–368.

Clark, G.M., 1994, Assessment of selected constituents in surface water of the upper Snake River basin, Idaho and western Wyoming, water years 1975–89: U.S. Geological Survey Water-Resources Investigations Report 93-4229, 49 p.

Clark, I.D., and Fritz, Peter, 1997, Environmental isotopes in hydrogeology: Boca Raton, Florida, Lewis Publishers, 328 p.

Conrad, M.E., and DePaolo, D.J., 2004, Carbon isotopic evidence for biodegradation of organic contaminants in the shallow vadose zone of the Radioactive Waste Management Complex: Vadose Zone Journal, v. 3, p. 143–153.

Coplen, T.B., Qi, Haiping, Révész, Kinga, Casciotti, Karen, and Hannon, J.E., 2012, Determination of the $\delta^{15}N$ of nitrate in water—RSIL lab code 2899, chap. 16 of Stable Isotope-Ratio Methods, sec. C of Révész, Kinga, and Coplen, Tyler B., eds., Methods of the Reston Stable Isotope Laboratory (slightly revised from version 1.0 released in 2007): U.S. Geological Survey Techniques and Methods, book 10, 35 p., available only online at http://pubs.usgs.gov/tm/2006/tm10c16/. (Supersedes version 1.0 released in 2007).

Crosthwaite, E.G., 1973, A progress report on results of test-drilling and ground-water investigations of the Snake River Plain aquifer, southeastern Idaho; Part 1, Mud Lake region 1969–70; Part 2, Observation wells south of Arco and west of Aberdeen: Idaho Department of Water Resources, Water Information Bulletin 32, 60 p.

Deutsch, W.J., Jenne, E.A., and Krupka, K.M., 1982, Solubility equilibria in basalt aquifers—The Columbia Plateau, eastern Washington, U.S.A.: Chemical Geology, v. 36, p. 15–34.

Doherty, D.J., McBroome, L.A., and Kuntz, M.A., 1979, Preliminary geological interpretation and lithologic log of the exploratory geothermal test well (INEL-1), Idaho National Laboratory, eastern Snake River Plain, Idaho: U.S. Geological Survey Open-File Report 79-1248, 9 p.

Drever, J.I., 1997, The geochemistry of natural waters: Upper Saddle River, New Jersey, Prentice Hall, 436 p.

Embree, G.F., McBroome, L.A., and Doherty, D.J., 1982, Preliminary stratigraphic framework of the Pliocene and Miocene rhyolite, eastern Snake River Plain, Idaho, *in* Bonnichsen, Bill, and Breckenridge, R.M., eds., Cenozoic geology of Idaho: Idaho Bureau of Mines and Geology Bulletin 26, p. 333–343.

Fishman, M.J., ed., 1993, Methods of analysis by the U.S. Geological Survey National Water Quality Laboratory—Determination of inorganic and organic constituents in water and fluvial sediments: U.S. Geological Survey Open-File Report 93-125, 217 p.

Fishman, M.J., and Friedman, L.C., 1989, Methods for determination of inorganic substances in water and fluvial sediments: U.S. Geological Survey Techniques of Water-Resources Investigations, book 5, chap. A1, 545 p.

Freeze, R.A., and Cherry, J.A., 1979, Groundwater: Englewood Cliffs, N.J., Prentice-Hall, 604 p.

Friedman, L.C., and Erdmann, D.E., 1982, Quality assurance practices for the chemical and biological analyses of water and fluvial sediments: U.S. Geological Survey Techniques of Water-Resources Investigations, book 5, chap. A6, 181 p. (Also available at http://pubs.er.usgs.gov/publication/twri05A6.)

Garabedian, S.P., 1992, Hydrology and digital simulation of the regional aquifer system, eastern Snake River Plain, Idaho: U.S. Geological Survey Professional Paper 1408-F, 102 p., 10 pl.

Garbarino, J.R., 1999, Methods of analysis by the U.S. Geological Survey National Water Quality Laboratory—Determination of dissolved arsenic, boron, lithium, selenium, strontium, thallium, and vanadium using inductively coupled plasma-mass spectrometry: U.S. Geological Survey Open-File Report 99-093, 31 p.

Garbarino, J.R., Kanagy, L.K., and Cree, M.E., 2006, Determination of elements in natural-water, biota, sediment and soil samples using collision/reaction cell inductively coupled plasma-mass spectrometry: U.S. Geological Survey Techniques and Methods, book 5, sec. B, chap. 1, 88 p.

Geslin, J.K., Link, P.K., Riesterer, J.W., Kuntz, M.A., and Fanning, C.M., 2002, Pliocene and Quaternary stratigraphic architecture and drainage systems of the Big Lost Trough, northeastern Snake River Plain, Idaho, *in* Link, P.K., and Mink, L.L., eds., Geology, Hydrogeology, and Environmental Remediation—Idaho National Engineering and Environmental Laboratory, Eastern Snake River Plain, Idaho: Geological Society of America Special Paper 353, p. 11–26.

Gianniny, G.L., Thackray, G.D., Kauffman, D.S., Forman, S.L., Sherbondy, M.J., and Findeisen, Delda, 2002, Late Quaternary highstands in the Mud Lake and Big Lost Trough subbasins of Lake Terreton, Idaho, *in* Link, P.K., and Mink, L.L., eds., Geology, Hydrogeology, and Environmental Remediation—Idaho National Engineering and Environmental Laboratory, Eastern Snake River Plain, Idaho: Geological Society of America Special Paper 353, p. 77–90.

Ginsbach, M.L., 2013, Geochemical evolution of groundwater in the Medicine Lodge Creek drainage basin, eastern Idaho: Pocatello, Idaho State University, M.S. thesis, 241 p.

Goodell, S.A., 1988, Water use on the Snake River Plain, Idaho and eastern Oregon: U.S. Geological Survey Professional Paper 1408-E, 51 p.

Hem, J.D., 1992, Study and interpretation of the chemical characteristics of natural water (3d ed.): U.S. Geological Survey Water-Supply Paper 2254, 263 p.

Hershey, R.L., Thomas, J.M., Rose, T.P., Paces, J.B., Farnham, I.M., and Benedict Jr., F.C., 2005, Evaluation of groundwater movement in the Frenchman Flat CAU using geochemical and isotopic analysis: U.S. Dept. of Energy report DOE/NV/13609-36, 65 p.

Idaho Department of Environmental Quality, 2005, Beaver-Camas Creek subbasin assessment and total maximum daily loads: Idaho Department of Environmental Quality, 223 p.

Idaho Department of Water Resources, 2012, Well Driller Reports: Idaho Department of Water Resources, accessed October 28, 2012, at http://www.idwr.idaho.gov/WaterManagement/WellInformation/DrillerReports/dr_default.htm.

Idaho Transportation Department, 2013, Winter maintenance—Anti-icing liquids: Idaho Transportation Department, accessed August 6, 2013, at http://itd.idaho.gov/ida-road/WinterMaint-MgCl.htm.

Iwahashi, G.S., 2010, Physical and compositional implications for the evolution of Spencer-High Point volcanic field, Idaho: Pocatello, Idaho State University, M.S. thesis, 165 p.

Johnson, G.S., Brockway, C.E., and Luttrell, S.P., 1984, Application of a numerical ground-water flow model to the Mud Lake area in southeastern Idaho: Moscow, University of Idaho, Idaho Water Resources Research Institute Technical Completion Report, Contract no. 14-08-0001-A-0016, 60 p.

Kirkham, V.R.D., 1927, A geologic reconnaissance of Clark and Jefferson and parts of Butte, Custer, Fremont, Lemhi, and Madison Counties, Idaho: Idaho Bureau of Mines and Geology, Pamphlet no. 19, 47 p.

Knobel, L.L., Bartholomay, R.C., and Orr, B.R., 1997, Preliminary delineation of natural geochemical reactions, Snake River Plain Aquifer System, Idaho National Engineering Laboratory and vicinity, Idaho: U.S. Geological Survey Water-Resources Investigations Report 1997-4093 (DOE/ID-22139), 52 p.

Knobel, L.L., Chapelle, F.H., and Meisler, Harold, 1998, Geochemistry of the Northern Atlantic Coastal Plain aquifer system: U.S. Geological Survey Professional Paper 1404-L, 57 p.

Knobel, L.L., Tucker, B.J., and Rousseau, J.P., 2008, Field methods and quality-assurance plan for quality-of-water activities, U.S. Geological Survey, Idaho National Laboratory, Idaho: U.S. Geological Survey Open-File Report 2008-1165 (DOE/ID-22206), 36 p.

Kuntz, M.A., 1992, Model-based perspective of basaltic volcanism, eastern Snake River Plain, Idaho, *in* Link, P.K., Kuntz, M.A., and Platt, L.B., eds., Regional Geology of Eastern Idaho and Western Wyoming: Geological Society of America Memoir 179, p. 289–304.

Kuntz, M.A., Covington, H.R., and Schorr, L.J., 1992, An overview of basaltic volcanism of the eastern Snake River Plain, Idaho, *in* Link, P.K., Kuntz, M.A., and Platt, L.B., eds., Regional Geology of Eastern Idaho and Western Wyoming: Geological Society of America Memoir 179, p. 227–257.

Kuntz, M.A., Skipp, Betty., and Lanphere, M.A., Scott, W.E., Pierce, K.L., Dalrymple, G.B., Champion, D.E., Embree, G.F., Page, W.R., Morgan, L.A., Smith, R.P., Hackett, W.R., and Rodgers, D.W., 1994, Geologic map of the Idaho National Engineering Laboratory and adjoining areas, eastern Idaho: U.S. Geological Survey Miscellaneous Investigations Series Map I-2330, scale 1:100,000.

Lanphere, M.A., Champion, D.E., Christiansen, R.L., Izett, G.A., and Obradovich, J.D., 2002, Revised ages for tuffs of the Yellowstone Plateau volcanic field—Assignment of the Huckleberry Ridge Tuff to a new geomagnetic polarity event: Geological Society of America Bulletin, v. 114, no. 5, p. 559–568.

Lasaga, A.C., Soler, J.M., Ganor, J., Burch, T.E., and Nagy, K.L., 1994, Chemical weathering rate laws and global geochemical cycles: Geochimica et Cosmochimica Acta, v. 58, p. 2,361–2,386.

Lindholm, G.F., and Goodell, S.A., 1986, Irrigated acreage and other land covers on the Snake River Plain, Idaho and eastern Oregon: U.S. Geological Survey Hydrologic Investigations Atlas HA-691, 1 pl., scale 1:500,000.

Lindholm, G.F., 1996, Summary of the Snake River Plain regional aquifer-system analysis in Idaho and eastern Oregon: U.S. Geological Survey Professional Paper, 59 p.

Luttrell, S.P., 1982, Ground-water flow characteristics in the Mud Lake area, southeastern Idaho: Moscow, University of Idaho, M.S. thesis, 69 p.

Mann, L.J., 1986, Hydraulic properties of rock units and chemical quality of water for INEL-1—A 10,365-foot deep test hole drilled at the Idaho National Engineering Laboratory, Idaho: U.S. Geological Survey Water-Resources Investigations Report 86-4020, 23 p.

Maupin, M.A., 1995, Water-quality assessment of the upper Snake River basin, Idaho and western Wyoming—Environmental setting, 1980–92: U.S. Geological Survey Water-Resources Investigations Report 94-4221, 35 p.

Mazor, Emanual, 1991, Applied chemical and isotopic groundwater hydrology: New York, Halstead Press, 256 p.

Mazurek, John, 2004, Genetic controls on basalt alteration within the eastern Snake River Plain aquifer system, Idaho: Pocatello, Idaho State University, M.S. thesis, 213 p.

McCurdy, D.E., Garbarino, J.R., and Mullin, A.H., 2008, Interpreting and reporting radiological water-quality data: U.S. Geological Survey Techniques and Methods, book 5, chap. B6, 33 p. (Also available at http://pubs.usgs.gov/tm/05b06.)

McLing, T.L., 1994, The pre-anthropogenic groundwater evolution at the Idaho National Engineering Laboratory, Idaho: Pocatello, Idaho State University, M.S. thesis, 62 p.

Morgan, L.A., 1992, Stratigraphic relations and paleomagnetic and geochemical correlations of ignimbrites of the Heise volcanic field, eastern Snake River Plain, eastern Idaho and Western Wyoming, *in* Link, P.K., Kuntz, M.A., and Platt, L.B., eds., Regional Geology of Eastern Idaho and Western Wyoming: Geological Society of America Memoir 179, p. 215–226.

Morgan, L.A., Doherty, D.J., and Leeman, W.P., 1984, Ignimbrites of the eastern Snake River Plain—Evidence for major caldera-forming eruptions: Journal of Geophysical Research, v. 89, no. B10, p. 8,665–8,678.

Morgan, L.A., and McIntosh, W.C., 2005, Timing and development of the Heise volcanic field, Snake River Plain, Idaho, western USA: Geological Society of America Bulletin, v. 117, no. 3/4, p. 288–306.

Mueller, D.K., 1998, Quality of nutrient data from streams and ground water sampled during 1993–95—National Water-Quality Assessment Program: U.S. Geological Survey Open-File Report 98-276, 25 p.

Mundorff, M.J., Crosthwaite, E.G., and Kilburn, Chabot, 1964, Ground water for irrigation in the Snake River basin in Idaho: U.S. Geological Survey Water-Supply Paper 1654, 224 p.

Nace, R.L., Deutsch, Morris, and Voegeli, P.T., 1956, Geography, geology, and water resources of the National Reactor Testing Station, Idaho—Part 2. Geography and geology: U.S. Geological Survey Open-File Report (IDO-22033), 225 p.

National Oceanic and Atmospheric Administration, 2012, Western Region Climate Center—S. Idaho: National Oceanic and Atmospheric Administration, accessed October 9, 2012, at http://www.wrcc.dri.edu/summary/Climsmsid.html.

Olmstead, F.H., 1962, Chemical and physical characteristics of ground water in the National Reactor Testing Station, Idaho: U.S. Atomic Energy Commission, Idaho Operations Office Publication, IDO-22043-USGS, 142 p.

Parkhurst, D.L., and Appelo, C.A.J., 2013, Description of input and examples for PHREEQC Version 3—A computer program for speciation, batch reaction, one-dimensional transport, and inverse geochemical calculations: U.S. Geological Survey Techniques and Methods, book 6, chap. A43, 497 p., available only at http://pubs.usgs.gov/tm/06/a43/.

Parliman, D.J., 1983, Reconnaissance of ground-water quality, eastern Snake River basin, Idaho: U.S. Geological Survey Water-Resources Investigations Report 82-4004, 99 p.

Patton, C. J., and Kryskalla, J. R., 2011, Colorimetric determination of nitrate plus nitrite in water by enzymatic reduction, automated discrete analyzer methods: U.S. Geological Survey Techniques and Methods, book 5, chap. B8.

Phillips, W.M., 2012, Eolian landforms and deposits of the eastern Snake River Plain, Idaho: Science Education Resource Center at Carleton College, accessed August 6, 2013, at http://serc.carleton.edu/38042.

Plummer, L.N., and Busenberg, Eurybiades, 1982, The solubilities of calcite, aragonite, and vaterite in CO_2—H_2O solutions between 0 and 90°C, and an evaluation of the aqueous model for the system $CaCO_3$—CO_2—H_2O: Geochimica et Cosmochimica Acta, v. 46, p. 1,011-1,040.

Pritt, J.W., and Raese, J.W., 1995, Quality assurance/quality control manual—National Water Quality Laboratory: U.S. Geological Survey Open-File Report 95-443, 35 p. (Also available at http://pubs.er.usgs.gov/publication/ofr95443.)

Ralston, D.R., and Chapman, S.L., 1969, Water-level changes in the Mud Lake area, Idaho, 1958–68: Idaho Department of Reclamation, Water Information Bulletin No. 7, 29 p.

Rattray, G.W., 2012, Evaluation of quality-control data collected by the U.S. Geological Survey for routine water-quality activities at the Idaho National Laboratory, Idaho, 1996 through 2001: U.S. Geological Survey Scientific Investigations Report 2012-5270 (DOE/ID-22222), 74 p.

Reed, M.F., and Bartholomay, R.C., 1994, Mineralogy of selected sedimentary interbeds at or near the Idaho National engineering Laboratory, Idaho: U.S. Geological Survey Open-File Report 94-374 (DOE/ID-22116), 19 p.

Rember, W.C., and Bennett, E.H., 1979, Geologic map of the Dubois quadrangle, Idaho: Idaho Department of Lands, Bureau of Mines and Geology, Geologic Map Series Dubois 2° Quadrangle.

Révész, Kinga, and Coplen, T.B., 2008a, Determination of the $\delta(^2H/^1H)$ of water—RSIL lab code 1574, chap. C1 of Révész, Kinga, and Coplen, T.B., eds., Methods of the Reston Stable Isotope Laboratory: U.S. Geological Survey Techniques and Methods 10–C1, 27 p., http://pubs.water.usgs.gov/tm10C1/.

Révész, Kinga, and Coplen, T.B., 2008b, Determination of the $\delta(^{18}O/^{16}O)$ of water—RSIL lab code 489, chap. C2 of Révész, Kinga, and Coplen, Tyler B., eds., Methods of the Reston Stable Isotope Laboratory: U.S. Geological Survey Techniques and Methods, 10–C2, 28 p., http://pubs.water.usgs.gov/tm10C2/.

Révész, Kinga, Qi, Haiping, and Coplen, T.B., 2012, Determination of the $\delta^{34}S$ of low-concentration sulfate in water—RSIL lab code 1949, chap. 8 of Stable Isotope-Ratio Methods, sec. C of Révész, Kinga, and Coplen, Tyler B., eds., Methods of the Reston Stable Isotope Laboratory (slightly revised from version 1.1 released in 2007): U.S. Geological Survey Techniques and Methods, book 10, 35 p., available only online at http://pubs.usgs.gov/tm/2006/tm10c8/. (Supersedes versions 1.0 and 1.1 released in 2006 and 2007, respectively.)

Rightmire, C.T., 1984, Description and hydrogeologic implications of cored sedimentary material from the 1975 drilling program at the Radioactive Waste Management Complex, Idaho: U.S. Geological Survey Water-Resources Investigations Report 84-4071 (DOE/ID-22067), 33 p.

Rightmire, C.T., and Lewis, B.D., 1987, Hydrogeology and geochemistry of the unsaturated zone, Radioactive Waste Management Complex, Idaho National Engineering Laboratory, Idaho: U.S. Geological Survey Water-Resources Investigations Report 87-4198 (DOE/ID-22073), 89 p.

Robertson, J.B., Schoen, R., and Barraclough, J.T., 1974, The influence of liquid waste disposal on the geochemistry of water at the National Reactor Testing Station, Idaho—1952–1970: U.S. Geological Survey Open-File Report (IDO-22053), 231 p.

Rupert, M.G., 1994, Analysis of data on nutrients and organic compounds in groundwater in the upper Snake River Basin, Idaho and Western Wyoming, 1980–91: U.S. Geological Survey Water-Resources Investigations Report 94-4135, 40 p.

Rupert, M.G., 1996, Major sources of nitrogen input and loss in the upper Snake River Basin, Idaho and Western Wyoming, 1990: U.S. Geological Survey Water-Resources Investigations Report 96-4008, 15 p.

Russell, I.C., 1902, Geology and water resources of the Snake River Plains of Idaho: U.S. Geological Survey Bulletin 199, 192 p., 25 pl.

Schramke, J.A., Murphy, E.M., and Wood, B.D., 1996, The use of geochemical mass-balance and mixing models to determine groundwater sources: Applied Geochemistry, v. 11, p. 523–539.

Sibson, R., 1981, A brief description of natural neighbor interpolation, *in* V. Barnett, ed., Interpolating Multivariate Data: New York, John Wiley and Sons, p. 21–36.

Singleton, G.L., Révész, Kinga, and Coplen, T.B., 2012, Determination of the $\delta^{13}C$ of dissolved inorganic carbon in water—RSIL lab code 1710, chap. 18 of Stable Isotope-Ratio Methods, sec. C of Révész, Kinga, and Coplen, T.B., eds., Methods of the Reston Stable Isotope Laboratory: U.S. Geological Survey Techniques and Methods book 10, 28 p., available only online at http://pubs.usgs.gov/tm/10c18/.

Solomon, D.K., and Cook, P.G., 2000, ^{3}H and ^{3}He, *in* Cook, P.G., Herczeg, A.L., eds., Environmental Tracers in Subsurface Hydrology: Boston, Kluwer Academic Publishers, p. 397–424.

Spinazola, J.M., 1994, Geohydrology and simulation of flow and water levels in the aquifer system in the Mud Lake area of the eastern Snake River Plain, eastern Idaho: U.S. Geological Survey Water-Resources Investigations Report 93-4227, 78 p.

Spinazola, J.M., Tungate, A.M., and Rogers, T.L., 1992, Geohydrologic and chemical data from wells in the Mud Lake area, eastern Idaho, 1988–91: U.S. Geological Survey Open-File Report 92-133, 92 p.

Stearns, H.T., Bryan, L.L., and Crandall, Lynn, 1939, Geology and water resources of the Mud Lake region, Idaho: U.S. Geological Survey Water-Supply Paper 818, 125 p.

Struzeski, T.M., DeGiacomo, W.J., and Zayhowski, E.J., 1996, Methods of analysis by the U.S. Geological Survey National Water Quality Laboratory—Determination of dissolved aluminum and boron in water by inductively coupled plasma-atomic emission spectrometry: U.S. Geological Survey Open-File Report 96-149, 17 p.

Swanson, S.A., Rosentreter, J.J., Bartholomay, R.C., and Knobel, L.L., 2002, Geochemistry of the Little Lost River drainage basin, Idaho: U.S. Geological Survey Water-Resources Investigations Report 02-4120 (DOE/ID-22179), 29 p.

Swanson, S.A., Rosentreter, J.J., Bartholomay, R.C., and Knobel, L.L., 2003, Geochemistry of the Birch Creek drainage basin, Idaho: U.S. Geological Survey Water-Resources Investigations Report 03-4272 (DOE/ID-22188), 36 p.

Thatcher, L.L., Janzer, V.J., and Edwards, K.W., 1977, Methods for determination of radioactive substances in water and fluvial sediments: U.S. Geological Survey Techniques of Water-Resources Investigations, book 5, chap. A5, 95 p.

Thomas, J.M., Benedict, Jr., F.C., Rose, T.P., Hershey, R.L., Paces, J.B., Peterman, Z.E., Farnham, I.M., Johannesson, K.H., Singh, A.K., Stetzenbach, K.J., Hudson, G.B., Kenneally, J.M., Eaton, G.F., and Smith, D.K., 2002, Geochemical and isotopic interpretations of groundwater flow in the Oasis Valley flow system, southern Nevada: U.S. Dept. of Energy report DOE/NV/11508-56, 102 p.

Thompson, Melissa, 2005, Beaver-Camas subbasin assessment and TMDL's: Idaho Department of Environmental Quality, 223 p.

Timme, P.J., 1995, National Water Quality Laboratory—1995 services catalog: U.S. Geological Survey Open-File Report 95-352, 120 p. (Also available at http://pubs.er.usgs.gov/publication/ofr95352.)

U.S. Department of Agriculture, 2009, 2007 Census of agriculture: Idaho State and County data, variously paged.

U.S. Department of Agriculture, 2012, Natural Resources Conservation Service, National Water and Climate Center: U.S. Department of Agriculture, accessed August 6, 2013 at http://www.wcc.nrcs.usda.gov/nwcc/site?sitenum=424&state=id.

U.S. Department of Agriculture, 2013, Range sheep production efficiency research: U.S. Department of Agriculture, accessed August 6, 2013, at http://www.ars.usda.gov/Main/docs.htm?docid=4311.

U.S. Geological Survey, 2005, Preliminary integrated geologic map databases for the United States – Western states—California, Nevada, Arizona, Washington, Oregon, Idaho, and Utah: U.S. Geological Survey, accessed March 15, 2013, at http://pubs.usgs.gov/of/2005/1305.

U.S. Geological Survey, 2007, 2001 national land cover data (2001 NLCD): U.S. Geological Survey, accessed August 6, 2013, at http://www.epa.gov/mrlc/nlcd-2001.html.

U.S. Geological Survey, 2010, Changes to the reporting convention and to data qualification approaches for selected analyte results reported by the National Water Quality Laboratory (NWQL): Office of Water Quality Technical Memorandum 2010.07, accessed August 6, 2013, at http://water.usgs.gov/admin/memo/QW/qw10.07.html.

U.S. Geological Survey, 2012a, USGS Inorganic Blind Sample Project (IBSP)—Monitoring and evaluating the National Water Quality Laboratory's Inorganic Analytical Data Quality: U.S. Geological Survey database, accessed August 6, 2012, at http://bqs.usgs.gov/ibsp/index.shtml.

U.S. Geological Survey, 2012b, USGS Organic Blind Sample Project: U.S. Geological Survey database, accessed August 6, 2013 at http://bqs.usgs.gov/obsp/rp.html.

U.S. Geological Survey, 2013a, National Water Quality Information System database: U.S. Geological Survey, accessed August 6, 2013 at http://waterdata.usgs.gov/nwis.

U.S. Geological Survey, 2013b, USGS DOTABLES: U.S. Geological Survey, accessed April 1, 2013, at http://water.usgs.gov/software/DOTABLES/.

U.S. Geological Survey, 2013c, The Reston Chlorofluorocarbon Laboratory: U.S. Geological Survey, accessed April 1, 2013, at http://water.usgs.gov/lab/.

U.S. Geological Survey, variously dated, National field manual for the collection of water-quality data: U.S. Geological Survey Techniques of Water-Resources Investigations, book 9, chaps. A1–A9. (Also available at http://pubs.er.usgs.gov/publication/twri09.)

Whitehead, R.L., 1992, Geohydrologic framework of the Snake River Plain regional aquifer system, Idaho and eastern Oregon: U.S. Geological Survey Professional Paper 1408-B, 32 p., 6 pl.

Witkind, I.J., 1975, Geology of a strip along the Centennial Fault, southwestern Montana and adjacent Idaho: U.S. Geological Survey Miscellaneous Investigations Map I-890, scale 1:62,500.

Witkind, I.J., 1980, Preliminary geologic map of the Centennial Mountains Wilderness Study Area, including the Centennial Mountains Instant Study Area (BLM), Beaverhead County, Montana, and Clark and Fremont Counties, Idaho: U.S. Geological Survey Open-File Report 80-922, 24 p.

Witkind, I.J., 1982, Geologic map of the Centennial Mountains Wilderness Study Area and contiguous areas, Idaho and Montana: U.S. Geological Survey Miscellaneous Investigations Map MF-1342-A, scale 1:50,000.

Wood, W.W, and Low, W.H., 1988, Solute geochemistry of the Snake River Plain regional aquifer system, Idaho and eastern Oregon: U.S. Geological Survey Professional Paper 1408-D, 79 p.

This page intentionally left blank.

Appendix A. U.S. Geological Survey Site Numbers

Table A1 is a cross reference for the report and U.S. Geological Survey (USGS) site numbers for water-quality samples. Table A2 lists the USGS site numbers for the wells with water-level measurements, and the dates of the measurements, used to create the water-table contours in figures 9 and 18.

Table A1. Cross reference of report and U.S. Geological Survey (USGS) site numbers for water-quality samples, Beaver and Camas Creek drainage basins, eastern Idaho.

Report site No.	USGS site No.
1	442615111442401
2	442017111495301
3	442847111534101
4	442335111532601
5	442051111540101
6	442056111541201
7	441740111540201
8	442756112011301
9	441614111593801
10	441756112055901
11	441209112055501
12	442456112125501
13	442053112101601
14	441442112114801
15	441222112142701
16	440524112095401
17	440553112170001
18	435846112145601
19	435358112161101
20	435241112185201
96	13108200
97	13108500
98	13113000
99	13114150

Table A2. U.S. Geological Survey (USGS) site numbers for wells with water-level measurements and dates of measurements that were used to create water-table contours in figures 9 and 18, Beaver and Camas Creek drainage basins, eastern Idaho.

USGS site No.	Water-level measurement date	USGS site No.	Water-level measurement date	USGS site No.	Water-level measurement date
422420111565801	07-15-57	435450112193601	04-15-89	435712112124101	04-12-89
441929111580001	09-28-66	435505112190201	04-15-89	435727112130001	04-12-89
441756112055901	01-15-67	435506112191701	04-15-89	435737112122301	04-12-89
441614111593801	02-14-69	435830112030301	04-15-89	435755112092001	04-12-89
441944112121401	12-12-70	435843112085501	04-15-89	435800112123101	04-12-89
442516111473301	09-10-75	435843112093201	04-15-89	435803112083301	04-12-89
441209112055501	05-06-80	435843112100801	04-15-89	435804112090201	04-12-89
441744111590601	05-06-80	435844112071501	04-15-89	435805112093301	04-12-89
440826112083601	07-07-88	435925112025301	04-15-89	435832112041201	04-12-89
441222112142701	11-04-88	435925112084701	04-15-89	435856112052901	04-12-89
441315112023701	11-05-88	435948112095701	04-15-89	440013112034301	04-12-89
440353112135701	03-15-89	435951112084701	04-15-89	440036112041601	04-12-89
440752111452901	03-15-89	435951112092101	04-15-89	440106112060701	04-12-89
435208112105101	03-28-89	440035112130501	04-15-89	440133112064201	04-12-89
435359112182501	03-28-89	440055112141601	04-15-89	440410112142801	04-12-89
435402112065001	03-28-89	440107112122101	04-15-89	440456112142901	04-12-89
435528112121201	03-28-89	440502112184601	04-15-89	440605112144501	04-12-89
435605112113601	03-28-89	440637112183401	04-15-89	440626112142901	04-12-89
435626112164304	03-28-89	435936112104101	04-16-89	440640112150901	04-12-89
435751112081001	03-28-89	435937112111701	04-16-89	435106112120401	04-18-89
435946112000501	03-28-89	435948112081201	04-16-89	435540112092901	04-18-89
440002112131801	03-28-89	440017112105301	04-16-89	435556112081701	04-18-89
440212112122501	03-28-89	435544112173001	04-17-89	435614112084801	04-18-89
440254112121001	03-28-89	435829112122201	04-17-89	435645112075501	04-18-89
440608112125001	03-28-89	435855112114601	04-17-89	435646112083001	04-18-89
435437112113901	04-10-89	435855112122201	04-17-89	435733112075701	04-18-89
435458112114601	04-10-89	435855112125801	04-17-89	435749112164001	04-18-89
435502112111001	04-10-89	440042112075701	04-17-89	435832112164501	04-18-89
435532112110201	04-10-89	440054112071701	04-17-89	435922111592601	04-18-89
435622112103301	04-10-89	440055112081001	04-17-89	435948111585101	04-18-89
435659112105201	04-10-89	435410112170903	04-11-89	435948111592601	04-18-89
440040112060101	04-10-89	435645112112401	04-11-89	435045112180901	04-19-89
440043112063801	04-10-89	435720112102001	04-11-89	435107112180001	04-19-89
440202112053101	04-10-89	435722112120201	04-11-89	435108112172601	04-19-89
441132112173301	04-10-89	435751112101401	04-11-89	435253112172701	04-19-89
435028112194801	04-11-89	440300112124101	04-11-89	435645112051001	04-19-89
435201112194901	04-11-89	440357112124001	04-11-89	435711112062301	04-19-89
435319112191701	04-11-89	440536112132401	04-11-89	435727112053501	04-19-89
435320112165301	04-11-89	440634112125401	04-11-89	435744112152801	04-19-89
435347112165301	04-11-89	440657112143101	04-11-89	435810112051301	04-19-89
435403112170501	04-11-89	440659112190601	04-11-89	435810112141101	04-19-89
435830112081001	04-14-89	440719112133901	04-11-89	435832112142101	04-19-89
435831112060401	04-14-89	440928112134201	04-11-89	435841112141801	04-19-89
435855112073501	04-14-89	441038112134201	04-11-89	435846112140001	04-19-89
440142112102801	04-14-89	441038112140701	04-11-89	435846112145601	04-19-89
440156112114901	04-14-89	435400112174101	04-12-89	435917112132001	04-19-89
440157112124601	04-14-89	435410112174801	04-12-89	435928112135401	04-19-89
440254112133601	04-14-89	435411112175101	04-12-89	441737112141601	04-19-89
440619112172301	04-14-89	435411112175801	04-12-89	442140112111601	04-19-89
440620112164101	04-14-89	435411112180101	04-12-89	435252112150301	04-20-89
435440112192002	04-15-89	435412112174701	04-12-89	435253112161201	04-20-89
435441112191901	04-15-89	435444112171001	04-12-89	435306112141401	04-20-89

Table A2. U.S. Geological Survey (USGS) site numbers for wells with water-level measurements and dates of measurements that were used to create water-table contours in figures 9 and 18, Beaver and Camas Creek drainage basins, eastern Idaho.—Continued

USGS site No.	Water-level measurement date	USGS site No.	Water-level measurement date
435317112132301	04-20-89	435420112184801	04-14-89
435340112113901	04-20-89	435422112190401	04-14-89
435345112123901	04-20-89	435454112185501	04-14-89
435352112161701	04-20-89	435506112185301	04-14-89
435357112150201	04-20-89	435725112084701	04-14-89
435358112161102	04-20-89	435759112075501	04-14-89
435422112144301	04-20-89	435829112073501	04-14-89
435436112135001	04-20-89	435830112063801	04-14-89
440710112150901	04-12-89	435457112140901	04-20-89
435016112182701	04-13-89	435459112131601	04-20-89
435042112182001	04-13-89	435511112125901	04-20-89
435346112105501	04-13-89	435625112123801	04-20-89
435347112173301	04-13-89	435707112064301	04-20-89
435352112171601	04-13-89	435740112141401	04-20-89
435405112174304	04-13-89	435748112135901	04-20-89
435409112120001	04-13-89	435803112162101	04-20-89
435409112174303	04-13-89	435828112153101	04-20-89
435411112171001	04-13-89	440841112133001	05-10-89
435418112175601	04-13-89	442047111561901	06-05-89
435422112120001	04-13-89	442054111472701	06-07-89
435425112180301	04-13-89	442227111455301	06-07-89
435440112175701	04-13-89	442242111481501	06-07-89
435445112174501	04-13-89	442247111495401	060-7-89
435446112173501	04-13-89	442343111474901	06-07-89
435525112093801	04-13-89	441852111441501	06-08-89
435628112092701	04-13-89	441921111522501	06-08-89
435656112093201	04-13-89	442002111513901	06-08-89
440405112151101	04-13-89	442116111515301	06-08-89
440438112151001	04-13-89	441745111401901	06-09-89
440451112154601	04-13-89	442010111414001	06-09-89
440553112162401	04-13-89	442029111400801	06-09-89
440553112170001	04-13-89	442121111421201	06-09-89
440554112154501	04-13-89	442250111423201	06-09-89
440606112104001	04-13-89	442312111432701	06-09-89
440626112154501	04-13-89	440831111513901	06-12-89
440657112154501	04-13-89	442335111532601	08-21-89
435108112185601	04-14-89	440839112003101	07-10-90
435123112163201	04-14-89	441740111540201	07-10-90
435140112155401	04-14-89	442847111534101	09-11-01
435200112164801	04-14-89	442053112101601	06-26-02
435408112184201	04-14-89		

Appendix B. Water-Quality Results from Water Samples Collected with a Bailer

Groundwater samples from sites 6 and 7 were collected with bailers. The wells were not purged prior to collection of these samples and the chemistry of these samples appears to be contaminated by exposure to the atmosphere. The chemical analyses for these samples are presented in tables B1–B5.

Table B1. Results of field measurements for temperature, pH, specific conductance, alkalinity, and dissolved oxygen and calculated partial pressure of carbon dioxide (log PCO_2) in water from sites 6 and 7, Beaver and Camas Creek drainage basins, eastern Idaho.

[Location of sites are shown in figure 2. **pH**: negative base-10 logarithm of hydrogen activity in moles per liter. **Carbon dioxide:** log PCO_2, base-10 logarithm of carbon dioxide partial pressure. **Abbreviations:** °C, degrees Celsius; µS/cm, microsiemens per centimeter at 25°C; mg/L, milligrams per liter, $CaCO_3$, calcium carbonate]

Site No.	Date sampled	Temperature (°C)	pH	Specific conductance (µS/cm)	Alkalinity (mg/L as $CaCO_3$)	Carbon dioxide (log PCO_2)	Dissolved oxygen	
							(mg/L)	(percent saturation)
6	08-16-2011	8.0	7.1	233	102	-2.10	7.7	82
7	08-15-2011	10.3	9.9	180	250	-1.89	10.4	117

Table B2. Concentrations of dissolved major ions and silica in water from sites 6 and 7 and the charge balance for each analysis, Beaver and Camas Creek drainage basins, eastern Idaho.

[Location of sites are shown in figure 2. Concentrations of dissolved major ions and silica are in milligrams per liter. **Charge balance:** Calculated from major ion concentrations and nitrate in milliequivalents per liter]

Site No.	Date sampled	Calcium	Magnesium	Potassium	Sodium	Bicarbonate	Chloride	Fluoride	Sulfate	Silica	Charge balance (percent)
6	08-16-2011	32	6.9	3.0	6.1	124	2.1	0.26	3.5	38	7.2
7	08-15-2011	16	0.2	5.9	6.5	305	6.3	0.21	12	0.3	-62.1

Table B3. Concentrations of dissolved nutrients and organic carbon in water from sites 6 and 7, Beaver and Camas Creek drainage basins, eastern Idaho.

[Location of sites are shown in figure 2. **Abbreviations**: mg/L, milligrams per liter; <, less than]

Site No.	Date sampled	Ammonia (mg/L as nitrogen)	Nitrite (mg/L as nitrogen)	Nitrite plus nitrate (mg/L as nitrogen)	Orthophosphate (mg/L as phosphorus)	Dissolved organic carbon (mg/L)
6	08-16-2011	0.02	0.002	0.03	0.08	0.93
7	08-15-2011	0.87	<0.001	0.02	<0.004	18.1

Table B4. Concentrations of selected trace elements in water from sites 6 and 7, Beaver and Camas Creek drainage basins, eastern Idaho.

[Location of sites are shown in figure 2. Concentrations of trace elements are in micrograms per liter. **Abbreviations**: <, less than]

Site No.	Date sampled	Aluminum	Barium	Boron	Chromium	Iron	Lead	Lithium	Manganese	Strontium	Zinc
6	08-16-2011	2.4	45	9.8	<0.06	24	0.52	19	115	77	66
7	08-15-2011	32	54	23	0.09	<3.2	4.7	20	0.30	129	86

Table B5. Measurements of the stable isotope ratios of hydrogen, oxygen, and carbon and the radiogenic isotope tritium in water from sites 6 and 7, Beaver and Camas Creek drainage basins, eastern Idaho.

[Location of sites are shown in figure 2. Stable isotope uncertainties are 2σ and tritium uncertainties are 1σ. **Abbreviations**: pCi/L, picocuries per liter; ±, plus or minus]

Site No.	Date sampled	Stable isotopes, permil			Tritium (pCi/L)
		Hydrogen ($\delta^{2}H\pm2$)	Oxygen ($\delta^{18}O\pm0.2$)	Carbon ($\delta^{13}C\pm0.2$)	
6	08-16-2011	-132.7	-17.46	-15.40	7.6±1.9
7	08-15-2011	-131.3	-17.45	[1]-13.89	19.5±2

[1]±3.5 per mil

Appendix C. Dissolved Gases

Samples for analysis of dissolved gases were collected from wells at sites 1, 3, 5, 8, 11, 12, 15, 18, and 20. The samples were analyzed at the USGS Chlorofluorocarbon Laboratory (CFC lab) in Reston, Va. Sample collection, analysis, and quality-assurance procedures for the CFC lab are described by the USGS (U.S. Geological Survey, 2013c). The results of analyses for dissolved gases are shown in table C1. Recharge temperatures were calculated using a recharge elevation equal to the land surface elevation of the well.

Table C1. Concentrations of dissolved gases in water from selected sites, calculated excess air, recharge elevations (that is, land-surface elevation of site), and calculated recharge temperature, Beaver and Camas Creek drainage basins, eastern Idaho.

[Location of sites are shown in figure 2. Excess air is in cubic centimeters per liter at estimated recharge temperature and pressure. Recharge elevation is in feet above National Geodetic Vertical Datum of 1929 (NGVD 29). ºC, degrees Celsius]

Site No.	Date sampled	Dissolved gases, in mg/L					Excess air	Recharge elevation	Recharge temperature (ºC)
		Nitrogen	Argon	Oxygen	Carbon dioxide	Methane			
1	08-16-2011	17.357	0.624	2.34	2.41	0	1.9	6,544	6.2
		17.626	0.628	2.70	2.69	0	2.2		
3	08-10-2011	19.935	0.726	7.68	13.98	0	2.0	6,630	0.1
		20.082	0.728	7.41	14.42	0	2.2		
5	08-15-2011	19.139	0.678	0.24	1.32	0.004	2.7	6,270	4.0
		19.062	0.674	0.26	1.37	0.004	2.7		
		19.016	0.676	0.25	1.31	0.004	2.6		
8	08-10-2011	15.294	0.582	4.81	18.08	0	0.1	6,681	6.5
		15.681	0.592	4.28	21.86	0	0.4		
11	08-09-2011	14.897	0.550	5.54	3.10	0	0.7	5,439	11.8
		15.096	0.554	5.71	3.11	0	1.0		
12	08-08-2011	29.627	0.895	0.31	3.12	0.010	11.7	6,370	0.0
		29.185	0.888	0.32	3.34	0.011	11.3		
		29.504	0.892	0.30	3.22	0.010	11.6		
15	08-09-2011	16.155	0.582	5.24	3.64	0	1.5	5,240	10.7
		16.188	0.582	5.34	3.62	0	1.7		
18	08-08-2011	16.482	0.599	5.53	3.69	0	1.3	4,805	9.9
		16.549	0.599	6.39	3.31	0	1.4		
		16.277	0.594	5.84	3.50	0	1.2		
20	08-09-2011	17.544	0.619	2.76	4.03	0	2.3	4,785	9.7
		17.564	0.618	2.71	3.98	0	2.4		
		17.472	0.617	3.49	3.39	0	2.4		

Publishing support provided by the U.S. Geological Survey
Publishing Network, Tacoma Publishing Service Center

For more information concerning the research in this report, contact the
Director, Idaho Water Science Center
U.S. Geological Survey
230 Collins Road
Boise, Idaho 83702
http://id.water.usgs.gov

ISSN 2328-0328 (online)
http://dx.doi.org/10.3133/sir20135226